Empirical and numerical approaches to predicting the thermal performance of green roofs

By Luke Gebert

A thesis submitted to Saint Mary's University, Halifax, Nova Scotia

in partial fulfillment of the requirements for the

Degree of Master of Science in Applied Science

© Luke Gebert, 2015

Halifax, Nova Scotia

Approved:	Dr. Jeremy Lundholm Supervisor
Approved:	Dr. Denis O'Carroll Supervisory Committee
Approved:	Dr. Mirwais Qaderi Supervisory Committee
Approved:	Dr. Andrew Coutts External Examiner
Date:	27th October, 2015

Abstract

Empirical and numerical approaches to predicting the thermal performance of green roofs

Luke Gebert

Green roofs are increasingly recognised as a sustainable option for reducing building energy demand. However, given the large investment required for their construction, accurate modelling methods are needed to predict their economic benefits for building owners and maximize their effectiveness. The representation of vegetation in the green roof energy balance model literature is reviewed to identify their limitations. It is concluded that an overemphasis on single source models, minimal validation periods and limited input data is likely burdening the robustness and applicability of these models. Using data collected in Calgary, Halifax and London, this study then aims to develop empirical models to offer another approach for predicting the thermal performance of green roofs. Significant multiple linear regression models highlight the importance of net radiation, air-to-surface temperature difference and humidity in predicting the substrate heat flux, with the green roof in the driest climate; Calgary, being the most effective.

Date: 27th October, 2015

Acknowledgements

I am very thankful to my supervisor Dr. Jeremy Lundholm who always provided me with excellent recommendations and guidance during my Master's Degree. As a principal investigator and member of my supervisory committee, I am also grateful for Dr. Denis O'Carroll's support with the green roof project and assistance with my thesis. Thank you to Dr. James Voogt as well for his suggestions and corrections for Chapter 2 of my thesis. I am also thankful for Dr. Mirwais Qaderi's and Dr. Andrew Coutts' contributions as a supervisory committee member and my external examiner, respectively.

As my thesis was part of a much larger project, I must express my deepest gratitude to the other staff and students of the RESTORE green roof group; Dr. Chris Smart, Dr. Clare Robinson, Dr. Maja Staniec, Patrick Breach, Dimuth Kurulula, Ginevra Perelli, Maria Sia and Stephanie Tran, for their collective technical support and expertise and data collection. I'm also very thankful to Mike Buckland-Nicks, Paige Fleet and Hughstin Grimshaw-Surette for collecting data for the RESTORE green roof project during the 2014 summer period (and also for Amy Heim's and Mike's summer 2013 contributions). A special thanks also to the members of the EPIC Lab for their support and feedback during my Master's Degree.

Lastly, I would like to thank my family and girlfriend Karra Christensen for their continual love and support.

Table of contents

Figures

Tables

Nomenclature

A	Advection heat flux (W m^{-2})
$A_{f,s}$	Area of fluid-solid interface (m^2)
C_f	Bulk transfer coefficient
C_p	Specific heat of air (J kg^{-1} K^{-1})
$C_{p,a}$	Specific heat of air at constant pressure (J kg^{-1} K^{-1})
CO_2	Ambient CO_2 concentration (ppm)
d	Zero plane displacement height (m)
$\frac{D_v}{D_q}$	Molecular diffusivity of gas *v* in air (mm^2 s^{-1})
e	Vapour pressure of air (kPa)
e_0	Windless exchange coefficient (2.0 W m^{-2})
e_s	Saturation vapour pressure (kPa)
$e_{s,plants}$	Vapour pressure of air in contact with plants (kPa)
ET	Evapotranspiration (kg m^{-2} s^{-1})

ET_0	Reference maximum evapotranspiration (kg m^{-2} s^{-1})
ET_{adv}	Advection enhanced evapotranspiration (kg m^{-2} s^{-1})
$f(u)$	Wind function (W m^{-2} kPa)
G	Ground/surface heat flux (W m^{-2})
Gr	Grashof number
h	Convective heat transfer coefficient (W m^{-2} K^{-1})
H	Sensible heat flux (W m^{-2})
$H_{f,cond}$	Conductive sensible heat flux (W m^{-2})
$H_{f,conv}$	Convective sensible heat flux (W m^{-2})
H_m	H at measurement height z (W m^{-2})
H_s	H at surface (W m^{-2})
k_0	Extinction coefficient
k_{air}	Thermal conductivity of air (W m^{-1} K^{-1})
k_c	Crop coefficient
k_{plant}	Thermal conductivity of plants (W m^{-1} K^{-1})
l	Latent heat of vaporization (J kg^{-1})
L	Latent heat flux (W m^{-2})
L_{ch}	Characteristic length (m)
LAI	Leaf area index (m^2 m^{-2})
LAI_{active}	Area index of active leaves (m^2 m^{-2})
LW	Longwave radiation (W m^{-2})
$LW_{f,g}$	Longwave radiation exchange between the foliage and substrate (W m^{-2})
M	Metabolic storage (W m^{-2})
n_{wilt}	Soil moisture value below which permanent wilting occurs (cm^3 cm^{-3})
n_{root}	Minimum value of soil moisture in the root zone (cm^3 cm^{-3})
Nu	Nusselt number
p	Atmospheric pressure (kPa)
P	Growing phase
Pr	Prandtl number
q	Specific humidity (g kg^{-1})
q_{af}	Mixing ratio of the air at the foliage interface (kg kg^{-1})
$q_{f,sat}$	Saturation mixing ratio at foliage temperature (kg kg^{-1})
r_a	Aerodynamic resistance (s m^{-1})
r_s	Stomatal resistance to mass transfer (s m^{-1})
r_{si}	Stomatal resistance of illuminated leaf (s m^{-1})
$r_{s,min}$	Minimum stomatal resistance (s m^{-1})
r''	Foliage surface wetness factor
R_n	Net radiative flux (W m^{-2})
Ra	Rayleigh number
Re	Reynolds number

S	Net thermal storage by plants & substrate (W m^{-2})
SW	Shortwave radiation (W m^{-2})
T_a	Temperature of within canopy air (°C)
$T_{a,c}$	Air temperature at the foliage (°C)
T_f	Foliage temperature (°C)
T_{plant}	Plant temperature (°C)
$T_{substrate}$	Temperature of substrate surface (°C)
u	Wind speed (m s^{-1})
u_z	Wind speed at height z (m s^{-1})
VPD	Vapour pressure deficit (kPa)
VPD_{canopy}	Vapour pressure deficit in the canopy (kPa)
VWC	Volumetric water content (cm^3 cm^{-3})
VWC_{fc}	VWC at field capacity (cm^3 cm^{-3})
VWC_{wp}	VWC at wilting point (cm^3 cm^{-3})
W_{af}	Wind speed at foliage (m s^{-1})
x	Downwind distance from edge (m)
z	Height above surface (m)
z_0	Roughness length (m)
z_h	Roughness length for heat (m)
z_m	Roughness length for momentum (m)
z_{mh}	Measurement height (m)

Greek letters

γ	Psychrometric constant (~0.059 kPa K^{-1})
Δ	Slope of the saturation vapour pressure vs temperature function (kPa $°C^{-1}$)
ΔH	Flux divergence of H (W m^{-2})
ΔT	Temperature difference between solid and fluid (°C)
ε_{plants}	Emissivity of the plants
$\varepsilon_{substrate}$	Emissivity of the substrate
κ	von Karman's constant (~0.4)
ρ_{af}	Density of air at foliage temperature (kg m^{-3})
ρ_f	Areal density of foliage (kg m^{-3})
σ	Stefan-Boltzmann constant ($5.67 \cdot 10^{-8}$ W m^{-2} K^{-4})
σ_f	Fractional vegetation coverage
τ_{IR}	Long-wave transmittance of the vegetative layer
ϕ	Porosity
φ_s	Solar radiation (W m^{-2})

Chapter 1: Introduction

The socio-economic activities of urban areas exert considerable pressure on natural resources and the environment. For instance, cities are estimated to account for more than 70% of the world's energy-related CO_2 emissions (Kort et al. 2012). Buildings are one of the main sites of energy use in urban areas. Population growth and improvements in building services have resulted in building energy demand increasing to the levels of the transportation and industry sectors (Pérez-Lombard et al. 2008). Buildings were responsible for approximately 32% of the world's energy demand in 2010, representing approximately 30% of energy-related CO_2 emissions and one-third of black carbon emissions (Lucon et al. 2014). Thermal energy demand comprises a large but temporally and spatially variable portion of the total energy demand for buildings.

Preventing heat stress and optimizing indoor thermal conditions to achieve acceptable standards of thermal comfort accounts for a large portion of the thermal energy demand. The human body responds to the thermal environment in a dynamic interaction that can lead to death if the body's response is inappropriate or if the energy levels are beyond the limits that are survivable. A person's response to the thermal environment determines the stress on their body as it uses its resources to maintain an optimum state and will therefore determine whether or not they are in thermal comfort (Parsons, 2014). Research has consistently shown that heat stress negatively impacts cognitive performance as stress forces an individual to allocate attentional resources to coping with the stress, reducing their capacity to process relevant information (Hancock et al. 2007).

In developed countries, improving thermal comfort with the use of space conditioning; heat, ventilation and air conditioning (HVAC) systems, accounts for around half of the energy demand for buildings and roughly 20% of the total energy use in the USA (Pérez-Lombard et al. 2008). At a global scale, it is estimated that over 60% of residential and around 50% of commercial building energy demand is for thermal purposes; with water heating and cooling being the dominant contributors for residential and commercial buildings, respectively (Ürge-Vorsatz et al. 2015).

1.1 Future stresses of thermal energy demand

The future thermal and energy performance of buildings is likely to be burdened by anthropogenic climate change (Li et al. 2012). Average global surface temperatures are anticipated to rise by 0.8-2.6 °C by 2050 and 2.5-7.8 °C by 2100 compared to pre-industrial levels as a result of continued greenhouse gas emissions and land use change. Rises in average temperatures are also likely to be accompanied by an increase in the frequency and intensity of heatwaves, with the IPCC Fifth Assessment report stating a 90% likelihood of significant increases occurring by the end of the 21st century (Collins et al. 2013).

These predictions are imposed on the existing urban heat island (UHI). The UHI refers to the higher temperatures commonly occurring in urban areas compared to their rural surroundings and is the most documented phenomenon of climate change. It results

from the following modifications to the energy balance associated with urban development (Landsberg, 1981; van der Zee et al. 1998; Akbari & Konopacki, 2005; Rizwan et al. 2008):

- Building materials, such as asphalt and concrete, store and re-radiate a greater amount of heat compared to natural environments
- Building materials also have a lower albedo than natural surfaces increasing the amount of energy that is absorbed
- Substituting vegetation with impervious surfaces reduces passive cooling via evapotranspiration
- Urban canyons increase heat absorption and decrease wind flow thus reducing heat losses by turbulent transfer
- Anthropogenic heat generation, including industrial and vehicular combustion, provides additional heat sources in urban areas
- Higher concentrations of greenhouse gases in urban areas due to more emission sources enhances the absorption of long-wave radiation by the urban atmosphere

Contemporary observations of the urban heat island intensity (UHII) have been in excess of 6 ºC (Hinkel et al. 2003). Higher urban temperatures result in greater energy consumption for cooling and peak electricity demand in cities (Akbari & Konopacki, 2004; Hirano & Fujita, 2012). Additionally, it has been predicted that the UHII in some cities

could rise to more than 10 ºC by 2100 (Wilby, 2008). This will have important implications for the health of urban populations and urban healthcare facilities as the effect of heat waves on human health is more pronounced in urban populations compared to their rural counterparts (Tan et al. 2007). Tan and colleagues observed that heat-related mortalities were generally much greater in the inner city areas of Shanghai, China compared to surrounding areas. This has been attributed to city inhabitants experiencing the thermal anomalies associated with heat waves for longer periods of time and at greater intensities than rural populations (Sheridan & Dolney 2003).

Future urban population growth is likely to further exacerbate energy demand concerns in urban areas. According to the 2014 United Nation population projections shown in Fig 1.1, the percentage of the world's population living in urban areas is expected to rise from 54% in 2014 to 66% by 2050. This represents an additional 2.5 billion people to the world's urban population by mid-century (UN, 2014).

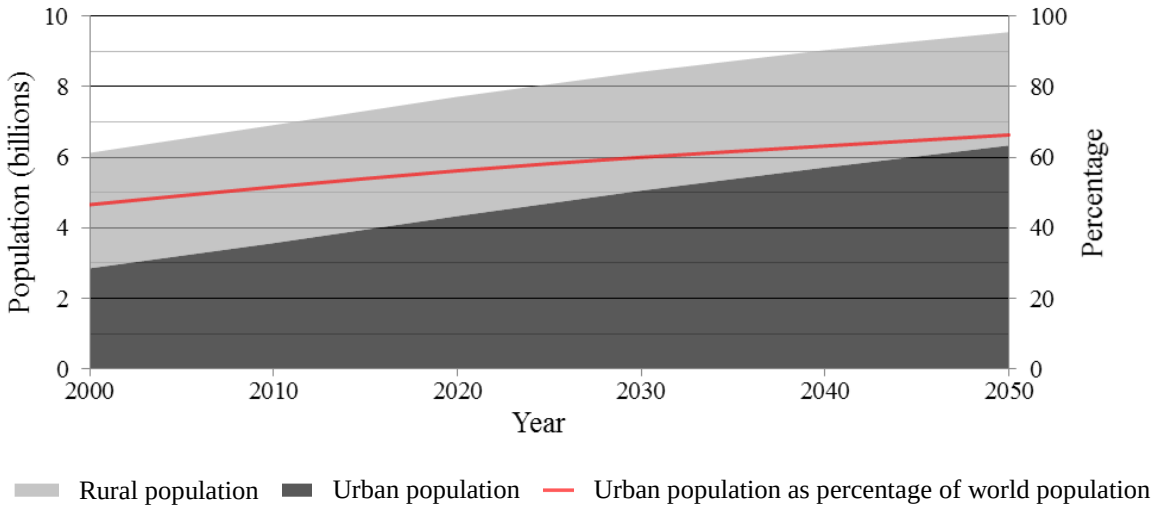

Fig 1.1 *UN projections of urban and rural populations* (UN, 2014)

Fig 1.2 combines these anticipated climate and population stressors using the mean surface air temperature projections for the mid-21st century and the predicted populations of the world's largest cities. As seen in this figure, large North American cities will likely face significant temperature increases by mid-century. These projections highlight the urgent need for energy conservation measures if buildings are to be more sustainable while simultaneously being able to provide comfortable thermal conditions in spite of rising average temperatures for an increasingly urbanized world. It is anticipated that if energy-efficient technologies are broadly applied to new and existing buildings, total energy use by buildings may stay constant or even decline by mid-century (Lucon et al. 2014).

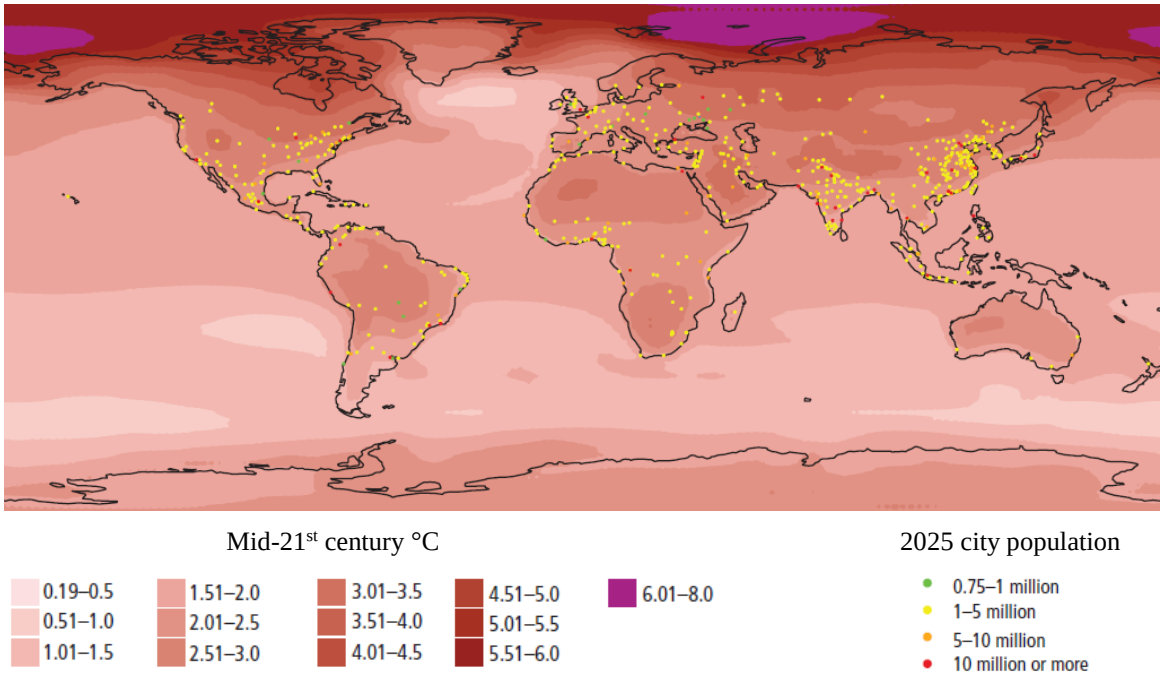

Fig 1.2 *Large cities (populations 750,000+) according to 2025 population projections and mid-21st century temperature increase according to an unchanged current GHG emission scenario* (Source: Revi et al. 2014)

1.2 Approaches to energy conservation

A variety of energy conservation measures exists to lower a building's energy demand for thermal purposes. The building envelope (i.e. walls, roofs, floors, doors and windows) will impact the energy demand for conditioning a building. Common approaches to improving the thermal performance of the existing building envelope include the addition of thermal insulation, installing more energy-efficient windows and simple and

inexpensive weatherstripping techniques to reduce air leakage into the building (Krarti, 2010).

These envelope conservation measures are particularly effective for residential buildings as their energy use is dominated by weather since heat gains and losses from direct heat conduction or from air infiltration or exfiltration through building surfaces accounts for a large portion of the buildings energy consumption (Krarti, 2010). However, for commercial buildings, which represent between 10 and 30% of total building sector thermal energy consumption in most regions (Lucon et al. 2014), improvements to the building envelope are often not cost-effective as modifications such as replacing windows and adding thermal insulation are usually considerably expensive (Krarti, 2010).

Another measure commonly recommended for conserving building thermal energy demand, typically for commercial buildings, is the modification of HVAC systems. There are numerous options for improving the energy efficiency of a HVAC system, including thermostat set-backs or set-ups during unoccupied periods, installing heat recovery systems if possible and retrofitting constant air volume systems with variable air volume systems when the existing HVAC system relies on constant volume fans to condition part or the entire building (Krarti, 2010). Through upgrades of HVAC equipment, and without changing the building envelope, commercial buildings have generally been able to achieve approximately a 25-50% reduction in space conditioning energy use (Harvey, 2013).

To complement these energy-efficient methods, green roofs, also known as vegetated or living roofs, offer a passive and more sustainable means to mitigating building thermal energy demand. These engineered roofing systems contain a growing medium (substrate) to support vegetation growth on man-made structures, most commonly rooftops. Green roofs impact building energy demands through their direct and indirect effects. The direct effect refers to green roofs altering the heat flow through a roof as a result of changing the surface temperature and increasing insulation levels. The indirect effect refers to green roofs altering the near surface air temperature which is assumed to increase the cooling capacity and energy efficiency of a HVAC system (Virk et al. 2015).

The support layers between the substrate and the roof structure varies but, as displayed in Fig 1.3, typically includes a root barrier to protect the roofing membrane from root penetration damage. Above the barrier, a drainage layer allows excess water not retained by the substrate to flow away from the roof and separating the substrate and drainage layer is a filter medium to prevent silt and particulate matter from blocking the drainage layer (Getter and Rowe, 2006).

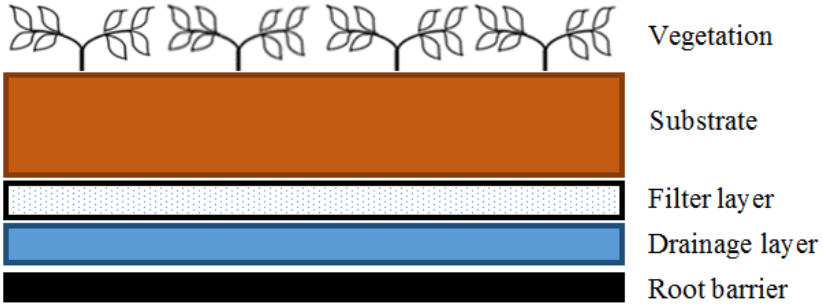

Fig 1.3 *Cross-section of a typical green roof*

Green roofs are typically categorised according to the depth of their growing medium, with intensive green roofs having deeper substrates of 15+ cm and extensive green roofs featuring shallower soils, typically between 5 and 15 cm. The deeper substrate of intensive green roofs can support a wider variety of plants, including shrubs and trees, than extensive green roofs offering enhanced ecosystem services over their shallower counterparts (Berndtsson et al. 2009; Razzaghmanesh & Beecham, 2014). However, the application of intensive green roofs is restricted due to their increased maintenance needs and weight, the latter limiting their establishment to buildings with a sufficient vertical load capacity. Given their lighter weight, extensive green roofs have a greater range of application.

Given the generally harsh environmental conditions plants are exposed to on green roofs, such as limited water availability due to shallow substrates, large temperature fluctuations, increased exposure to wind and solar radiation and nutrient deficient soils, appropriate plant species selection is vital to increase survival rates. Many perennial

succulents, particularly *Sedum* species which are the most commonly used plants on extensive green roofs, such as *Sedum acre* L. and *Sedum album* L., (Monterusso et al. 2005; Nagase & Dunnett, 2010), have proven to be ideal for extensive green roofs as they are physiologically adapted to withstand similar environmental conditions. Such adaptations include an increased water storage capacity and some species exhibiting the Crassulacean acid metabolism (CAM) photosynthetic pathway which involves stomata opening at night to fix carbon allowing the stomata to remain closed during the day when the vapour pressure deficit (VPD, kPa) is greater in order to minimize transpirational water loss (Reyes-García & Griffiths, 2009). The results of Butler and Orians (2011) also suggested that *Sedum* may expand the range of suitable plants for green roofs as they found *Sedum* spp. to have a facilitating effect on neighbouring species during times of summer water deficit.

Other commonly used low-maintenance plants that have been shown to be suitable in extensive green roof applications include grasses, such as *Festuca* L., and herbaceous perennials, like *Allium* L. and *Dianthus* L (Dunnett & Nolan, 2004; Snodgrass & Snodgrass, 2006). Given the importance of evapotranspiration to the cooling performance of green roofs and succulents water use efficiency minimizing their transpiration rates, non-succulents have generally been found to be more beneficial for cooling. In a study by Blanusa and colleagues (2013), the broad-leaved herbaceous perennial *Stachys byzantine* was found to cool the soil surface greater than other test species, including a *Sedum* mixture.

1.3 Thermal performance of green roofs

Through modification of the surface energy balance, relative to conventional roofs, green roofs reduce the amount of incoming solar radiation that enters the building through the roof membrane. In particular, the increase in heat dissipation through latent fluxes as well as an increase in albedo and thermal insulation are the main processes by which green roofs provide a thermal benefit to buildings. The specific energy benefits that a particular green roof provides depend on the local climate, time of year, design parameters and the building's characteristics. From existing studies performed on various types of buildings, the anticipated reduction in the annual energy load for a building installed with a green roof is between approximately 1% and 40% (Santamouris 2014).

Seasonal studies have shown that green roofs generally exhibited less fluctuation in surface temperatures and heat flux compared to conventional roofs (Eumorfopoulou & Aravantinos, 1998; Teemusk & Mander, 2009; Getter et al. 2011). In empirical studies, green roofs have been shown to significantly reduce heat flux in comparison to conventional roofs during summer periods as they minimize heat gains and maximize heat losses (Niachou et al. 2001; Santamouris et al. 2007; Getter et al. 2011; Theodosiou et al. 2014). Conversely, while research has suggested that the reduction of indoor heat loss in winter by green roofs is significantly less than the cooling effect in summer (Spolek, 2008;

Jim & Tsang, 2011; Jim, 2014), other studies have suggested that the thermal effect of green roofs is negligible during winter as the substrate is usually wet and therefore has a high thermal conductivity thus limiting its thermal insulation (Santamouris et al. 2007; Spala et al. 2008; Theodosiou et al. 2014). On the contrary, low soil moisture in drier climates may result in green roofs being less effective due to a reduction in latent heat loss (Coutts et al. 2013; Li et al. 2014).

Aside from the moisture content of the substrate, the substrate's depth is considered the most important design parameter for optimizing the thermal performance of a green roof as it largely defines its overall heat transfer coefficient; *U*-value. While research has suggested that green roof vegetation plays little role in the thermal performance of a green roof (Liu & Minor, 2005), other studies have emphasised the importance of plant species selection, with the optical properties of individual plants and increased species diversity correlated with a reduction in heat flux (Lundholm et al. 2010; Morau et al. 2012; Zhao et al. 2014).

Building characteristics, particularly insulation and building height, also greatly influence the energy contribution of green roofs. The energy benefit tends to be neutralised, particularly during summer, for well and moderately insulated buildings due to the lower thermal transmittance between the green roof and the interior space of the building (Nichaou et al. 2001; D'Orazio et al. 2012; Zinzi & Agnoli, 2012; Zhao et al. 2014). Nevertheless, green roofs are still practical for retrofitting non-insulated buildings. For

instance, in Tokyo and London, extensive retrofitting of urban buildings with improved insulation has begun in order to reduce energy requirements (Walker & Bellingham, 2011). Furthermore, in the case of Tokyo where the Philippine Sea plate subducts under the metropolitan region resulting in an increased earthquake risk (Sato et al. 2005), the existing seismic load capacity of buildings means their vertical load capacity, which plays an important role in the lateral-force-resisting system, is also enhanced due to the need for a high vertical load redistribution capacity (Taranath, 2004). This requirement of a high vertical load capacity means many Tokyo buildings can support green roof infrastructure. Additionally, in a modelling study undertaken using 2050 climate projections for London, Virk and colleagues (2014) found a simulated conditioned commercial building regularly exceeded thermal comfort limits without the presence of a retrofitted green roof. Therefore, in cities such as Tokyo and London where the widespread retrofitting of buildings' insulation has begun to minimize future energy use and adapt to climate change, green roofs are also a viable option for reducing building energy needs and improving thermal comfort.

When green roofs are installed on high rise buildings, the expected thermal benefits are very limited due to the dominance of heat transfer through the walls (Min et al. 2014). Additionally, for buildings in which the energy load is primarily due to the transfer of heat through the envelope, green roofs can contribute significantly to the reduction of heating and cooling loads. On the contrary, if a building's energy load is primarily governed by

ventilation gains or losses and/or internal or solar gains through walls and windows, green roofs are likely to have a limited energy contribution (Santamouris, 2014).

Cool or reflective roofs are another roofing approach to minimizing the influence meteorological conditions have on building energy demand. Cool roofs are characterized by roofing materials that have a high solar reflectance and high thermal emittance (Zinzi & Agnoli, 2012). This approach provides a cooling effect due to the greatly increased reflectance and emittance of radiation, with commercially available materials typically have a reflectance between 0.4 and an emissivity of 0.9 (Bretz & Akbari, 1997). Conventional roofs on the other hand typically have an albedo in the lower end of the range 0.05-0.25 (USEPA, 2005) while green roofs have an average albedo around 0.2 (Gaffin et al. 2009). For instance, comparing a white elastomeric coating that had an albedo greater than 0.72 with a black coating with an albedo of 0.08, Taha and colleagues (1992) found the surface temperature of cool roof was 45°C cooler.

While cool roofs have been found to reduce urban heat island intensity and surface temperatures more effectively than green roofs (Scherba et al. 2011; Mackey et al. 2012), research has varied as to whether or not green roofs are more effective for internal building comfort, given the very low *U*-value of cool roofs (Di Giuseppe & D'Orazio, 2015). A comparative simulation study by Sailor and colleagues (2011) found cool roofs provided more energy savings in warmer climates while green roofs were more beneficial in cooler climates. As an empirical example of cool roofs enhanced energy saving potential in

warmer climates, Coutts et al. (2013) found cool roofs to be more beneficial for the energy transfer into buildings when the soil moisture in the green roof system was low in Melbourne, Australia, a city with a Mediterranean climate characterized by extended periods of hot dry weather during the summer. However, in a review by Santamouris (2014) it was noted that the result of specific studies comparing the performance of green and cool roofs is case sensitive and they are greatly influenced by the characteristics of the particular roofing systems considered, such as the difference in their thermal capacitance and insulation properties. Additionally, weathering has been found to decrease the reflectance of cool roofs as a result of damage due to ultraviolet radiation, wind and acid rain, dust load, microbial growth and biomass accumulation, moisture penetration and condensation (Bretz & Akbari, 1997; Berdahl et al. 2002; Miller et al. 2002; Levinson et al. 2005; Cheng et al. 2011, 2012).

Besides the thermal benefits of green roofs, evidence suggests they can also offer a multitude of other benefits at a building and urban scale, an attribute cool roofs do not possess. As roofs tend to account for approximately 40-50% of the impermeable surface area in most developed cities (Stovin et al. 2012) and available free ground area in urban areas is often quite limited and of high economic value (Santamouris 2014), green roofs can greatly increase the amount of green space in heavily urbanized areas. By reintroducing vegetation into the urban environment, green roofs have been found to be effective in retaining and detaining stormwater to provide a decentralised stormwater management tool

(Hathaway, et al. 2008; Monterusso et al., 2002; Rowe, 2011; Schmidt, 2006), reducing air and stormwater pollution (Rowe, 2011), noise attenuation (Van Renterghem & Botteldooren, 2011), increasing fire resistance (Köhler, 2003), providing habitat and enhancing urban biodiversity (Brenneisen, 2003; Dunnett et al. 2008; Gedge & Kadas, 2005) carbon sequestration (Getter et al., 2009), agricultural production (Whittinghill et al. 2013) and increasing the lifespan of the roofing membrane (Porsche and Köhler 2003). On the other hand, cool roofs only offer the benefit of surface cooling which requires regular maintenance to be fully achieved. As green roofs vary so much in design and performance, Simmons and colleagues (2008) suggested that they must be designed according to specific goals rather than relying on assumed inherent attributes.

1.4 Predicting the thermal performance of green roofs

Given the monetary expense required to construct a green roof and the interconnected sensitivity of a green roof's energy performance to its design and climate, the accurate prediction of a green roof's energy conservation potential will likely increase the likelihood of a building owner investing in a green roof as well as increase the design's effectiveness if the installation of a green roof is deemed advantageous. Recent initial construction costs of standard green roofs in Canada have been reported as $\$130/m^2$-$\$165/m^2$ for extensive green roofs and starting at approximately $\$540/m^2$ for intensive

green roofs (Bianchini & Hewage, 2012a). Additionally, annual operation and maintenance costs have been estimated to be between $\$0.7/m^2$ and $\$13.5/m^2$ (Acks, 2006). However, considering these costs and the benefits of green roofs like those mentioned in Section 1.3, Bianchini and Hewage (2012b) estimated an average payback period in Canada of 10.4 years for extensive green roofs and 14 years for intensive green roofs, with green roofs expected to have a lifespan between 40 (Clark et al. 2008) and 55 years (Acks, 2006). Cost-benefit analyses like theirs rely heavily on the accurate prediction of the environmental benefits that green roofs can offer, including their thermal performance.

Mathematical models allow observations to be used to make predictions. They facilitate prognoses of how processes may operate in conditions other than those observed. Models also provide an opportunity for mechanistic insights to be gained through the organization of observations into explicit mathematical expressions. Models and observations are not perfect representations of real systems and therefore error must be accommodated for in both observations and models (Monson & Baldocchi, 2014). Mathematical models can be generated in one of two ways:

- *Empirical models*: Observations are organized using statistical correlations allowing unknown dependent variables to be predicted from known independent variables

- *Mechanistic (numerical) models*: Theoretical knowledge (process theory) is used to relate dependent variables to independent variables

Empirical models contain the implicit assumption that multivariate correlations are maintained in conditions other than those of the original observations. Mechanistic models on the other hand are often burdened by available theory with assumptions often having to be made to fill gaps in knowledge. Conventionally, mechanistic models are expected to be more accurate at predicting unobserved conditions as empirical models are based on limited observations that are not necessarily going to overlap with future states of the system. However, assumptions resulting from gaps in theory and uncertainties regarding appropriate input parameters for plants and substrates can result in as much, or more, error in mechanistic model predictions as empirical models (Monson & Baldocchi, 2014).

1.5 Direction of thesis

Given the importance of predicting the thermal performance of green roofs and the modelling techniques involved, this thesis will involve both empirical and mechanistic approaches to modelling the thermal behaviour of green roofs. Firstly, given the recent increase in published green roof energy models, Chapter 2 will provide a theoretical review substantiated by empirical evidence of the processes underpinning these existing

mechanistic models. Secondly, the development and application of an empirical model for green roof thermal performance will be discussed in Chapter 3. This model will involve green roof data collected from three identical sites in Canada; Calgary, Alberta; Halifax, Nova Scotia; and London, Ontario. Lastly, Chapter 4 will provide conclusions.

The research objectives are therefore summarised as:

(1) Critically review the representation of vegetation in the green roof energy model literature by combining existing theoretical and experimental data to provide general conclusions and suggestions for the refinement of numerical models

(2) Characterize substrate heat flux of green roofs located in different climates as well as develop and validate empirical green roof energy models for the prediction of substrate heat fluxes

References

Acks, K. (2006). A framework for cost-benefit analysis of green roofs: Initial estimates. In *Green roofs in the New York Metropolitan Region: Research report*. New York: Columbia University Center for Climate Research and NASA Goddard Institute for Space Studies.

Akbari, H., & Konopacki, S. (2004). Energy effects of heat-island reduction strategies in Toronto, Canada. *Energy and Buildings*, *29*, 191–210.

Akbari, H., & Konopacki, S. (2005). Calculating energy-saving potentials of heat-island reduction strategies. *Energy Policy*, *33*(6), 721-756.

Berdahl, P., Akbari, H., & Rose, L.S. (2002). Aging of reflective roofs: Soot deposition. *Applied Optics*, *41*, 2355–2360.

Berndtsson, J.C., Bengtsson, L., & Jinno, K. (2009). Runoff water quality from intensive and extensive vegetated roofs. *Ecological Engineering*, *35*(3), 369-380.

Bianchini, F., & Hewage, K. (2012a). How "green" are the green roofs? Lifecycle analysis of green roof materials. *Building and Environment*, *48*, 57-65.

Bianchini, F., & Hewage, K. (2012b). Probabilistic social cost-benefit analysis for green roofs: A lifecycle approach. *Building and Environment*, *58*, 152-162.

Blanusa, T., Monteiro, M.M.V., Fantozzi, F., Vysini, E., Li, Y., & Cameron, R.W. (2013). Alternatives to Sedum on green roofs: Can broad leaf perennial plants offer better 'cooling service'?. *Building and Environment*, *59*, 99-106.

Brenneisen, S. (2003, May). The benefits of biodiversity from green roofs: Key design consequences. In *Proceedings of the 1st North American Green Roof Conference* (pp. 323-329).

Bretz, S.E., & Akbari, H. (1997). Long-term performance of high-albedo roof coatings. *Energy and Buildings*, *25*, 159–167.

Butler, C., & Orians, C.M. (2011). Sedum cools soil and can improve neighboring plant performance during water deficit on a green roof. *Ecological Engineering*, *37*(11), 1796-1803.

Cheng, M.D., Miller, W., New, J., & Berdahl, P. (2012). Understanding the long-term effects of environmental exposure on roof reflectance in California. *Construction and Building Materials*, *26*(1), 516-526.

Cheng, M.D., Pfiffner, S.M., Miller, W.A., & Berdahl, P. (2011). Chemical and microbial effects of atmospheric particles on the performance of steep-slope roofing materials. *Building and Environment*, *46*(5), 999-1010.

Clark, C., Adriaens, P., & Talbot, F.B. (2008). Green roof valuation: A probabilistic economic analysis of environmental benefits. *Environmental Science & Technology*, *42*(6), 2155-2161.

Collins, M., Knutti, R., Arblaster, J., Dufresne, J.-L. , Fichefet, T., Friedlingstein, P., Gao, X., Gutowski, W.J., Johns, T., Krinner, G., Shongwe, M., Tebaldi, C., Weaver, A.J., & Wehner, M. (2013). Long-term climate change: Projections, commitments and irreversibility. In T.F. Stocker, D. Qin, G.-K. Plattner, M. Tignor, S.K. Allen, J. Boschung, A. Nauels, Y. Xia, V. Bex & P.M. Midgley (eds.), *Climate change 2013: The physical science basis*. Contribution of Working Group I to the Fifth Assessment Report of the Intergovernmental Panel on Climate Change. Cambridge & New York: Cambridge University Press.

Coutts, A.M., Daly, E., Beringer, J., & Tapper, N.J. (2013). Assessing practical measures to reduce urban heat: Green and cool roofs. *Building and Environment*, *70*, 266-276.

D'Orazio, M., Di Perna, C., & Di Giuseppe, E. (2012). Green roof yearly performance: A case study in a highly insulated building under temperate climate. *Energy and Buildings*, *55*, 439-451.

Di Giuseppe, E., & D'Orazio, M. (2015). Assessment of the effectiveness of cool and green roofs for the mitigation of the Heat Island effect and for the improvement of thermal comfort in Nearly Zero Energy Building. *Architectural Science Review*, *58*(2), 134-143.

Dunnett, N., Nagase, A., & Hallam, A. (2008). The dynamics of planted and colonising species on a green roof over six growing seasons 2001–2006: Influence of substrate depth. *Urban Ecosystem*, *11*, 373–384.

Dunnett, N., & Nolan, A. (2004). Effect of substrate depth and supplementary watering on the growth of nine herbaceous perennials in a semi-extensive green roof. *Acta Horticulturae*, *643*, 305-309.

Eumorfopoulou, E., & Aravantinos, D. (1998). The contribution of a planted roof to the thermal protection of buildings in Greece. *Energy and Buildings*, *27*(1), 29-36.

Gaffin, S.R., Khanbilvardi, R., & Rosenzweig, C. (2009). Development of a green roof environmental monitoring and meteorological network in New York City. *Sensors*, *9*(4), 2647-2660.

Gedge, D., & Kadas, G. (2005). Green roofs and biodiversity. *Biologist*, *52* (3), 161–169.

Getter, K.L., & Rowe, D.B. (2006). The role of extensive green roofs in sustainable development. *HortScience*, *41*(5), 1276-1285.

Getter, K.L., Rowe, D.B., Andresen, J.A., & Wichman, I.S. (2011). Seasonal heat flux properties of an extensive green roof in a Midwestern US climate. *Energy and Buildings*, *43*(12), 3548-3557.

Getter, K.L., Rowe, D.B., Robertson, G.P., Cregg, B.M., & Andresen, J.A. (2009). Carbon sequestration potential of extensive green roofs. *Environmental Science & Technology*, *43*, 7564–7570.

Hancock, P.A., Ross, J.M., & Szalma, J.L. (2007). A meta-analysis of performance response under thermal stressors. *Human Factors: The Journal of the Human Factors and Ergonomics Society*, *49*(5), 851-877.

Harvey, L.D. (2013). Recent advances in sustainable buildings: Review of the energy and cost performance of the state-of-the-art best practices from around the world. *Annual Review of Environment and Resources*, *38*, 281-309.

Hathaway, A.M., Hunt, W.F., & Jennings, G.D. (2008). A field study of green roof hydrologic and water quality performance . *Trans ASABE*, *51*, 37–44.

Hinkel, K.M., Nelson, F.E., Klene, A.E., & Bell, J.H. (2003). The urban heat island in winter at Barrow, Alaska. *International Journal of Climatology*, *23* (15), 1889-1905.

Hirano, Y., & Fujita, T. (2012). Evaluation of the impact of the urban heat island on Residential and commercial energy consumption in Tokyo. *Energy*, *37*(1), 371-383.

Jim, C.Y. (2014). Passive warming of indoor space induced by tropical green roof in winter. *Energy*, *68*, 272-282.

Jim, C.Y., & Tsang, S.W. (2011). Biophysical properties and thermal performance of an intensive green roof. *Building and Environment*, *46*(6), 1263-1274.

Krarti, M. (2010). *Energy audit of building systems: An engineering approach* (2nd ed.). Boca Raton: CRC Press.

Köhler, M. (2003, May). *Plant survival research and biodiversity: Lessons from Europe*. Presented at Greening Rooftops for Sustainable Communities (pp. 313–322), Chicago.

Kort, E.A., Frankenberg, C., Miller, C.E., & Oda, T. (2012). Space-based observations of megacity carbon dioxide. *Geophysical Research Letters*, *39*(17), L17806.

Landsberg, H.E. (1981). *The Urban Climate*. New York: Academic Press.

Levinson, R., Berdahl, P., Berhe, A.A., & Akbari, H. (2005). Effects of soiling and cleaning on the reflectance and solar heat gain of a light-colored roofing membrane. *Atmospheric Environment*, *39*(40), 7807-7824.

Li, D., Bou-Zeid, E., & Oppenheimer, M. (2014). The effectiveness of cool and green roofs as urban heat island mitigation strategies. *Environmental Research Letters*, *9*(5), 055002.

Li, D.H., Yang, L., & Lam, J.C. (2012). Impact of climate change on energy use in the built environment in different climate zones–a review. *Energy*, *42*(1), 103-112.

Liu, K., & Minor, J. (2005, May). *Performance evaluation of an extensive green roof*. Presented at Green rooftops for sustainable communities (pp. 1-11), Washington D.C.

Lucon O., Ürge-Vorsatz, D., Zain Ahmed, A., Akbari, H., Bertoldi, P., Cabeza, L.F., Eyre, N., Gadgil, A., Harvey, L.D.D., Jiang, Y., Liphoto, E., Mirasgedis, S., Murakami, S., Parikh, J., Pyke, C., & Vilariño, M.V. (2014). Buildings. In O. Edenhofer, R. Pichs-Madruga, Y. Sokona, E. Farahani, S. Kadner, K. Seyboth, A. Adler, I. Baum, S. Brunner, P. Eickemeier, B. Kriemann, J. Savolainen, S. Schlömer, C. von Stechow, T. Zwickel & J.C. Minx (eds.), *Climate change 2014: Mitigation of climate change* (pp. 671-738). Contribution of Working Group III to the Fifth Assessment Report of the Intergovernmental Panel on Climate Change. Cambridge & New York: Cambridge University Press.

Lundholm, J., MacIvor, J. S., MacDougall, Z., & Ranalli, M. (2010). Plant species and functional group combinations affect green roof ecosystem functions. *PLoS One*, *5*(3), e9677.

Mackey, C.W., Lee, X., & Smith, R.B. (2012). Remotely sensing the cooling effects of city scale efforts to reduce urban heat island. *Building and Environment*, *49*, 348-358.

Miller, W.A., Cheng, M-D., Pfiffner, S., & Byars, N. (2002). *The field performance of high-reflectance single-ply membranes exposed to three years of weathering in various U.S. climates*. Final Report to SPRI, Inc.

Min, H., Yoon, D., & Ju, S. (2014). Heating and cooling energy conservation effects by green roof systems in relation with building location, usage and number of floors. *KIEAE Journal*, *14*(2), 11-19.

Monson, R., & Baldocchi, D. (2014). *Terrestrial biosphere-atmosphere fluxes*. New York: Cambridge University Press.

Monterusso, M.A., Rowe, D.B., & Rugh, C.L. (2005). Establishment and persistence of Sedum spp. and native taxa for green roof applications. *HortScience, 40*(2), 391-396.

Monterusso, M.A., Rowe, D.B., Rugh, C.L., & Russell, D.K. (2002, August). Runoff water quantity and quality from green roof systems. In *XXVI International Horticultural Congress: Expanding Roles for Horticulture in Improving Human Well-Being and Life Quality 639* (pp. 369-376).

Morau, D., Libelle, T., & Garde, F. (2012). Performance evaluation of green roof for thermal protection of buildings in Reunion Island. *Energy Procedia*, *14*, 1008-1016.

Nagase, A., & Dunnett, N. (2010). Drought tolerance in different vegetation types for extensive green roofs: Effects of watering and diversity. *Landscape and Urban Planning*, *97*(4), 318-327.

Niachou, A., Papakonstantinou, K., Santamouris, M., Tsangrassoulis, A., & Mihalakakou, G. (2001). Analysis of the green roof thermal properties and investigation of its energy performance. *Energy and Buildings*, *33*(7), 719-729.

Parsons, K. (2014). *Human thermal environments: The effects of hot, moderate, and cold environments on human health, comfort, and performance* (3rd ed.). Boca Raton: CRC Press.

Pérez-Lombard, L., Ortiz, J., & Pout, C. (2008). A review on buildings energy consumption information. *Energy and Buildings*, *40*(3), 394-398.

Porsche, U., & Köhler, M. (2003, December). Life cycle costs of green roofs: A comparison of Germany, USA, and Brazil. In *Proceedings of the World Climate and Energy Event*. Retrieved from http://www.gruendach-mv. de/en/ri03_461_u_porsche.pdf

Razzaghmanesh, M., & Beecham, S. (2014). The hydrological behaviour of extensive and intensive green roofs in a dry climate. *Science of the Total Environment*, *499*, 284-296.

Revi, A., Satterthwaite, D.E., Aragón-Durand, F., Corfee-Morlot, J., Kiunsi, R.B.R., Pelling, M., Roberts, D.C., & Solecki, W. (2014). Urban areas. In C.B. Field, V.R. Barros, D.J. Dokken, K.J. Mach, M.D. Mastrandrea, T.E. Bilir, M. Chatterjee, K.L. Ebi, Y.O. Estrada, R.C. Genova, B. Girma, E.S. Kissel, A.N. Levy, S. MacCracken, P.R. Mastrandrea, & L.L.White (eds), *Climate change 2014: Impacts, adaptation, and vulnerability* (pp. 535-612). Contribution of Working Group II to the Fifth Assessment Report of the Intergovernmental Panel on Climate Change. Cambridge & New York: Cambridge University Press.

Reyes-García, C., & Griffiths, H. (2009). Ecophysiological studies of perennials of the Bromeliaceae in a dry forest: Strategies for survival. In E. De La Barrera & W.K. Smith (eds.), *Perspectives in biophysical plant ecophysiology: A tribute to Park S. Nobel* (pp. 121-152). Mexico City: UNAM.

Rizwan, A. M., Dennis, L. Y., & Chunho, L. I. U. (2008). A review on the generation, determination and mitigation of Urban Heat Island. *Journal of Environmental Sciences*, *20*(1), 120-128.

Rowe, D.B. (2011). Green roofs as a means of pollution abatement. *Environmental Pollution*, *159*, 2100–2110.

Sailor, D.J., Elley, T.B., & Gibson, M. (2011). Exploring the building energy impacts of green roof design decisions–a modeling study of buildings in four distinct climates. *Journal of Building Physics*, 1744259111420076.

Santamouris, M. (2014). Cooling the cities–a review of reflective and green roof mitigation technologies to fight heat island and improve comfort in urban environments. *Solar Energy*, *103*, 682-703.

Santamouris, M., Pavlou, C., Doukas, P., Mihalakakou, G., Synnefa, A., Hatzibiros, A., & Patargias, P. (2007). Investigating and analysing the energy and environmental performance of an experimental green roof system installed in a nursery school building in Athens, Greece. *Energy*, *32*(9), 1781-1788.

Sato, H., Hirata, N., Koketsu, K., Okaya, D., Abe, S., Kobayashi, R., Matsubara, M., Iwasaki, T., Ito, T., Ikawa, T., Kawanaka, T., Kasahara, K., & Harder, S. (2005). Earthquake source fault beneath Tokyo. *Science*, *309*(5733), 462-464.

Schmidt, M. (2006). The evapotranspiration of greened roofs and facades. In *Proceedings of the 4th Greening Rooftops for Sustainable Communities*.

Scherba, A., Sailor, D.J., Rosenstiel, T.N., & Wamser, C.C. (2011). Modeling impacts of roof reflectivity, integrated photovoltaic panels and green roof systems on sensible heat flux into the urban environment. *Building and Environment*, *46*(12), 2542-2551.

Sheridan, S.C., & Dolney, T.J. (2003). Heat, mortality, and level of urbanization: Measuring vulnerability across Ohio, US. *Climate Research*, *24*, 255-266.

Simmons, M.T., Gardiner, B., Windhager, S., & Tinsley, J. (2008). Green roofs are not created equal: The hydrologic and thermal performance of six different extensive green roofs and reflective and non-reflective roofs in a sub-tropical climate. *Urban Ecosystems*, *11*(4), 339-348.

Snodgrass, E.C., & Snodgrass, L.L. (2006). *Green roof plants: A resource and planting guide*. Portland: Timber Press.

Spala, A., Bagiorgas, H.S., Assimakopoulos, M.N., Kalavrouziotis, J., Matthopoulos, D., & Mihalakakou, G. (2008). On the green roof system. Selection, state of the art and energy potential investigation of a system installed in an office building in Athens, Greece. *Renewable Energy*, *33*(1), 173-177.

Spolek, G. (2008). Performance monitoring of three ecoroofs in Portland, Oregon. *Urban Ecosystems*, *11*(4), 349-359.

Stovin, V., Vesuviano, G., & Kasmin, H. (2012). The hydrological performance of a green roof test bed under UK climatic conditions. *Journal of Hydrology*, *414–415*, 148–161.

Taha, H., Sailor, D., & Akbari, H. (1992). *High-albedo materials for reducing building cooling energy use*. Lawrence Berkeley Laboratory Report 31721, Berkeley.

Tan, J., Zheng, Y., Song, G., Kalkstein, L., Kalkstein, A., & Tang, X. (2007). Heat wave impacts on mortality in Shanghai, 1998 and 2003. *International Journal of Biometeorology*, *51*, 193–200.

Taranath, B.S. (2004). *Wind and earthquake resistant buildings: Structural analysis and design*. Boca Raton: CRC press.

Teemusk, A., & Mander, Ü. (2009). Greenroof potential to reduce temperature fluctuations of a roof membrane: A case study from Estonia. *Building and Environment*, *44*(3), 643-650.

Theodosiou, T., Aravantinos, D., & Tsikaloudaki, K. (2014). Thermal behaviour of a green vs. a conventional roof under Mediterranean climate conditions. *International Journal of Sustainable Energy*, *33*(1), 227-241.

United States Environmental Protection Agency (2005). *Cool roofs*. Retrieved from http://www.epa.gov/heatisland/strategies/coolroofs.html/

United Nations, Department of Social and Economic Affairs (2014). *World urbanization. prospects: The 2014 revision, highlights*. Retrieved from http://esa.un.org/unpd/wup/Highlights/WUP2014-Highlights.pdf

Ürge-Vorsatz, D., Cabeza, L.F., Serrano, S., Barreneche, C., & Petrichenko, K. (2015). Heating and cooling energy trends and drivers in buildings. *Renewable and Sustainable Energy Reviews*, *41*, 85-98.

van der Zee, S.C., Hoek, G., Harssema, H., & Brunekreef, B. (1998). Characterization of particulate air pollution in urban and non-urban areas in the Nethderlands. *Atmospheric Environment, 32* (21), 3717-3729.

Van Renterghem, T., & Botteldooren, D. (2011). In-situ measurements of sound propagating over extensive green roofs. *Building and Environment*, *46* (3), 729–738.

Virk, G., Jansz, A., Mavrogianni, A., Mylona, A., Stocker, J., & Davies, M. (2014). The effectiveness of retrofitted green and cool roofs at reducing overheating in a naturally ventilated office in London: Direct and indirect effects in current and future climates. *Indoor and Built Environment*, *23*(3), 504-520.

Virk, G., Jansz, A., Mavrogianni, A., Mylona, A., Stocker, J., & Davies, M. (2015). Microclimatic effects of green and cool roofs in London and their impacts on energy use for a typical office building. *Energy and Buildings, 88,* 214-228.

Walker, L.R., & Bellingham, P. (2011). *Island environments in a changing world*. Cambridge: Cambridge University Press.

Whittinghill, L.J., Rowe, D.B., & Cregg, B.M. (2013). Evaluation of vegetable production on extensive green roofs. *Agroecology and Sustainable Food Systems*, *37*(4), 465-484.

Wilby, R.L. (2008). Constructing climate change scenarios of urban heat island intensity and air quality. *Environment and Planning B: Planning and Design*, 35, 902-919.

Zhao, M., Tabares-Velasco, P.C., Srebric, J., Komarneni, S., & Berghage, R. (2014). Effects of plant and substrate selection on thermal performance of green roofs during the summer. *Building and Environment, 78,* 199-211.

Zinzi, M., & Agnoli, S. (2012). Cool and green roofs. An energy and comfort comparison between passive cooling and mitigation urban heat island techniques for residential buildings in the Mediterranean region. *Energy and Buildings*, *55*, 66-76.

Chapter 2: The representation of vegetation in green roof energy balance models

Green roofs mitigate energy and hydrological perturbations resulting from urbanisation. As a roofing system that supports plant growth, green roofs are a means of reintroducing vegetation into urban environments by using otherwise vacant impervious surfaces. At the building scale, minimizing heat transfer between indoor and outdoor environments means green roofs can reduce demand on space conditioning (Niachou et al. 2001) which is estimated to account for approximately 20% of the total energy requirements in developed nations (Pérez-Lombard et al. 2008). At an urban climate-scale, the modified energy balance that results from the widespread transformation of dry impervious roof surfaces into a vegetated green roof surfaces directly affects the urban boundary layer (Takebayashi & Moriyama, 2007).

Quantifying the energy balance of green roofs can enumerate these thermal benefits and enable informed design decisions to maximize their effectiveness. Numerical simulation models use a series of equations involving assumptions that simplify thermal processes in order to model the thermal performance of green roofs. Numerous green roof energy balance models have been developed in recent years, with the more dynamic and detailed of these simulating the energy balance of green roofs. For that reason, this review will focus on the energy balance-based green roof models. Table 2.1 features a list of some of the green roof energy balance models that have been developed.

Table 2.1 *Examples of green roof energy balance-based models*

Model	Year	Evaluation study location	Plant(s) used*
Del Barrio	1998	None	
Theodosiou	2003	Thessaloniki, Greece	-
Kumar & Kaushik	2005	Yamuna Nagar, India	-
Lazzarin et al.	2005	Vincenza, Italy	*Sedum*
Alexandri & Jones	2007	Cardiff, UK	Grass
Takebayashi & Moriyama	2007	Kobe, Japan	Grass
Sailor	2008	Orlando, USA	-
Feng et al.	2010	Guangzhou, China	*Sedum lineare*
He & Jim	2010	Hong Kong	*Arachis pintoi, Duranta repens* & *Zoysia tenuifolia*
Ouldboukhitine et al.	2011	La Rochelle, France	*Sedum* & pampas grass
Djedjig et al.	2012	La Rochelle, France	*Sedum* & pampas grass
Morau et al.	2012	Le Tampon, Réunion	*Kalanchoe, Plectranthus* & *Sedum*
Tabares-Velasco & Srebric	2012	Environmental chamber & Chicago, USA[+]	*Delosperma nubigenum & Sedum spurium*

* species name featured if provided in the literature
- plant not mentioned
+ Tabares-Velasco et al. (2012)

These models commonly divide the green roof into two layers; vegetation and substrate layers, and calculate the temperatures of these layers for each time-step. They can

then be incorporated into existing building energy models to provide accurate predictions on the likely reduction in energy consumption resulting from the installation of a green roof. However, for energy simulations, vegetation introduces tremendous complexity due to its structural and physiological heterogeneity. Given the ecological literature for green roofs is limited in comparison to that of natural environments (Blank et al. 2013), modeling the energy balance of green roof environments often relies on the application of classical predictive equations and assumptions to estimate the effect of the vegetation layer. Recent reviews examine the effects of green roofs and other greening systems on building energy usage in general (Castleton et al., 2010; Raji et al., 2015), and environmental benefits of green roofs related to energy (Saadatian et al., 2013), but there has been no comprehensive review of numerical models used to describe green roof energy transfer. Given the importance of understanding plant characteristics for green roof modelling, the following review will focus solely on the vegetation layer of green roof energy balance models.

The aim of this review is to therefore examine green roof energy balance models. These models help us understand how energy is partitioned within the vegetation layer of a green roof. The review will highlight how these models have contributed to our understanding of green roofs and provide a critical analysis of their theoretical framework and overall effectiveness. This analysis will provide recommendations for the future development of these models and the empirical data required for their refinement and evaluation.

2.1 Energy balance of a green roof

The energy balance is the equilibrium that exists between the heat that enters and leaves the green roof system. As the first law of thermodynamics states that energy cannot be created or destroyed, only transformed; all of the energy should be accounted for in a system analysis (Jones, 2013). The energy balance for a green roof system can be written as (Jones 1992; Hillel, 1998):

$$R_n - H - L - G - \Delta S - \Delta M - \Delta A = 0 \quad (2.1)$$

R_n = net radiative flux (W m^{-2}) H = convective sensible heat flux (W m^{-2})
L = convective latent heat flux (W m^{-2}) G = surface conductive heat flux (W m^{-2})
S = net thermal storage by plants & substrate (W m^{-2})
M = metabolic storage (W m^{-2}) A = advection heat flux (W m^{-2})

Fig 2.1 conceptually represents these flux and storage terms in the layers of a green roof model. The radiant energy balance; the incoming and outgoing short- and long-wave radiation, is the net radiation. This sum of gains minus losses from the system means the net radiation represents the amount of radiant energy that the system absorbs. The net short-wave radiative flux involves the incoming direct and diffuse solar radiation and the outgoing reflected solar radiation. The net long-wave flux includes the incoming diffusive thermal radiation and minus the thermal radiation emitted (re-radiated) by the surface.

Given the emission of long-wave radiation from an object is hemispherical, long-wave radiation will also be exchanged between the vegetation and substrate layers of a green roof, as depicted by $LW_{f,g}$ in Fig 2.1. These radiative heat exchanges will be examined further in Section 2.2.1.

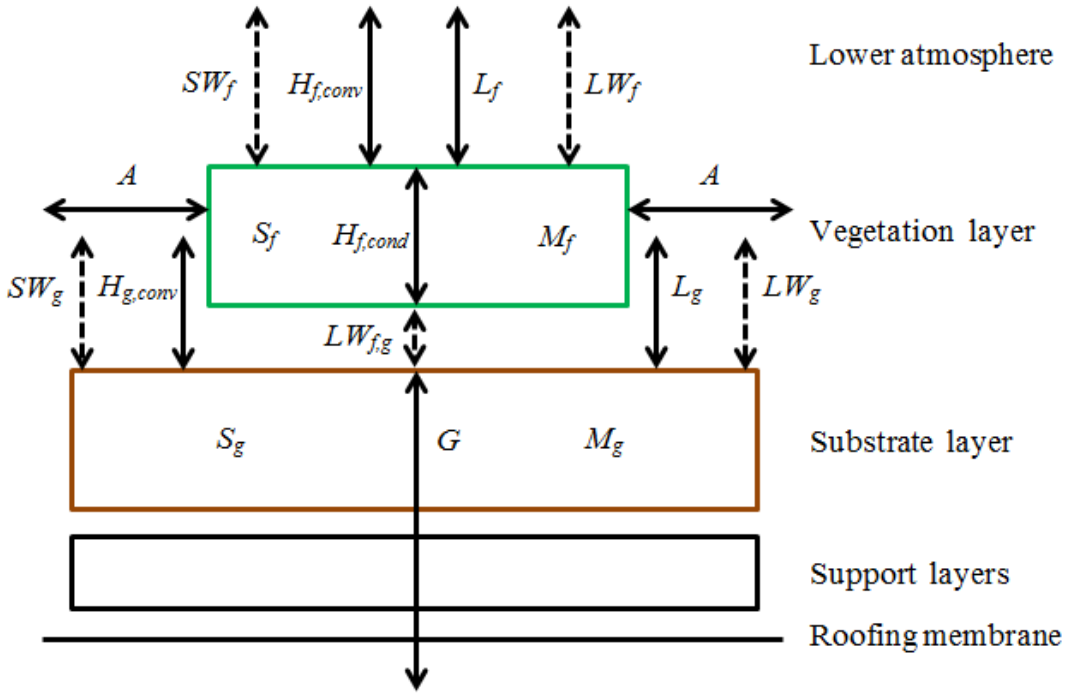

SW = short-wave radiation
LW = long-wave radiation
▬ ▬ ▪ = radiative heat flux
▬▬ = non-radiative heat flux
Subscripts:
f = foliage
g = ground
conv = convection
cond = conduction

Fig 2.1 *Conceptual diagram depicting the heat fluxes between and the energy storages within the layers of a green roof*

Under most conditions, the net radiation represents the total amount of energy available at the surface for non-radiative processes; sensible, latent and surface heat fluxes, as depicted in Fig 2.1. As these sensible and latent heat transfers between the vegetation, substrate and lower atmosphere occur between a solid surface and a fluid, they are convective processes, a mechanism that will be explained in greater detail later. Convective sensible heat fluxes occur when a temperature differential exists between the surface and the overlying fluid. If the temperature of a surface is greater than that of the overlying air, an outgoing convective sensible heat flux will warm the air. Conversely, there will be a cooling of the air and a convective sensible heat flux toward the surface when its temperature is less than that of the air. Latent heat fluxes involve energy changing the phase of a substance rather than its temperature. When evaporation and transpiration occur, the flow of energy as latent heat is away from the surface while during condensation the flow is towards the surface. The sensible and latent heat fluxes are closely coupled; when latent heat loss is reduced it will be compensated by an increase in sensible heat loss, and vice versa (Monson & Baldocchi, 2014). The sensible and latent heat fluxes for the vegetation layer will be further examined in Sections 2.2.2 and 2.2.3, respectively

Conversely, when a temperature gradient exists within a plant or the within canopy air column, a sensible heat transfer will occur by means of conduction. While thermal conduction through the substrate is an important component of green roof energy balance models, conduction within plants and the within-canopy air is commonly neglected in most

energy balance models (Monteith & Unsworth, 1990; Pielke, 2002), including those for green roofs (Alexandri & Jones, 2007; Sailor, 2008; Tabares-Velasco & Srebric, 2012). In this review, conductive heat fluxes in the vegetation layer are discussed in Section 2.2.2.

Additionally, besides heat fluxes, some of the available energy will be stored within the system temporarily. Due to the thermal capacity of the masses that compose the vegetation and substrate layers, each sub-system will store thermal energy. The storage of thermal energy by a mass will cause a change in its temperature. The heat storage in the system increases (warms) when the net radiation is larger than the sum of the other energy fluxes in Eq. 2.1 and the system cools when the net radiation is smaller than these fluxes. As both the vegetation and soil layers contain biological systems; flora and fauna, respectively, each sub-system also involves a metabolic storage of energy as a result of the biochemical reactions involved in metabolism (Shuttleworth, 2012). These storages of energy are small and often neglected in green roof energy balance models. Metabolic energy storage is examined in Section 2.2.4.

For particular applications of the surface energy balance it may be important to consider not only the surface transfers of sensible and latent heat, but also advective transfers. In the surface energy balance the convective sensible and latent heat fluxes are considered one dimensional (vertical direction only) and we assume the atmosphere is not significantly storing energy. Advection is the net horizontal transfer of heat, or other characteristics, across the volume that is defined for the energy balance of the system.

Where the surface is homogeneous and extensive we assume the horizontal flux at the upwind edge is equal to that at the downwind edge so that the net advective flux is then zero. Advection has not been considered in green roof energy models but it will be examined further in Section 2.2.5.

Besides the short-wave radiation not intercepted by vegetation, the partitioning and dissipation of energy within the vegetation layer just described largely determines the substrate surface temperature. Determining the surface temperature of the substrate is particularly important as the conduction of heat through the substrate layer will ultimately determine a green roof's influence on the thermal environment of the indoor space below.

2.1.1 Approaches to vegetation energy modelling

The presence of vegetation over a flat surface introduces several complications for energy modelling. Firstly, the ground surface can no longer be considered the most appropriate point for the surface energy balance as the radiative, latent and sensible heat fluxes vary spatially within the canopy. Secondly, the rate of thermal and metabolic storages and the latent heat exchange composed of condensation or evaporation at the vegetation surfaces as well as transpiration, the latter two collectively termed evapotranspiration, within the vegetation layer is difficult to measure and calculate (Arya, 2001). A canopy is therefore a complex system of sources and sinks of heat and mass, with

the spatial complexity and heterogeneity of the foliage and the turbulent air flow within and above the canopy resulting in the direction and magnitude of energy and mass fluxes constantly varying and ultimately being unpredictable on small scales (Del Barrio, 1998).

Most green roof energy balance models employ the simplifying assumption of horizontal homogeneity of heat fluxes within the vegetation canopy. This permits the use of one-dimensional models that consider the fluxes only in the vertical direction. This assumption has been justified in the literature on the basis that the vertical fluxes in the green roof vegetation layer are adequately greater than the horizontal divergence as the horizontal scale is small enough to render the divergence negligible (Del Barrio, 1998; Alexandri & Jones, 2007). However, on small scales advection is more likely because the surface types are less homogeneous at that scale.

A canopy is also vertically heterogeneous as a result of vertical gradients in leaf and air properties. This canopy structure can be represented as a single layer, dual layers or a continuum of layers. Simple single layer, or single source, models consider only one source of sensible and latent heat fluxes within the vegetation layer. They assume that the absorption and re-emission of scalars and momentum as well as the partitioning of energy into latent and sensible heat for the whole canopy can be accurately represented by a single theoretical plane; a single ‘leaf’. This representative leaf is scaled up to the canopy level using the dimensionless leaf area index (LAI), which refers to the single-side leaf area per unit of ground area. As the energy exchange between the atmosphere and an extensive,

homogenous dense canopy are fairly well understood, such a simplified approach can be considered valid (Kaimal & Finnigan, 1994; Shuttleworth, 2012).

In dual source models, two sources of heat and water vapour are represented. There can be transfers between the two layers as a coupled dual source model, commonly with a semi-transparent upper canopy layer (Lhomme et al. 1994). In a coupled dual source model, the component fluxes are additive (Lhomme & Chehbouni, 1999). In uncoupled dual source models, the two sources are considered separately without the interaction of fluxes from each source (Blyth & Harding, 1995). Unlike coupled dual source models, the component fluxes should be weighted by the respective area of each source in an uncoupled model (Lhomme & Chehbouni, 1999). The use of either a coupled or an uncoupled dual source model is generally a matter of scale, with small-scale heterogeneity more suitably represented as sparse vegetation in a coupled model and large-scale heterogeneity better represented by an uncoupled model (Lhomme & Chehbouni, 1999).

Multilayer models offer a more detailed representation of the energy and mass fluxes in a plant canopy by subdividing the canopy into homogenous horizontal layers. Each of these layers can be furthered divided into sunlit and shaded leaves and different leaf-angles. A detailed energy balance can be included to determine the profile of meteorological parameters within the canopy. Multilayer models are primarily used for research purposes, particularly as standard against which the performances of simpler models are compared (Landsberg & Sands, 2010).

While multilayer or multisource models offer the most representative depiction of within-canopy profiles, the green roof literature generally applies single source or 'big-leaf' models for the vegetation layer. The simplified big-leaf approach has the benefit over more complex multilayer models of not requiring detailed specifications of canopy structure and properties or a detailed consideration of the distribution of turbulence in the canopy air space. The need for detailed information generally limits the application of multilayer models to sites where this information is known (Shuttleworth, 2012). Del Barrio (1998) suggests within-canopy profiles available from multi-layer models also do not provide additional useful information on the thermal performance of green roofs. Moreover, when representing and modelling within-canopy parameters, it is more important to accurately determine the bulk aerodynamic and surface resistances between the canopy and the atmosphere than the detailed representation of within-canopy exchanges (Raupach and Finnigan, 1988).

Single layer models can take one of two forms - those derived from surface layer similarity and those that apply combination equations to the whole canopy. Both groups of models have been utilised in the green roof modelling literature. Surface layer similarity theory involves using logarithmic profiles within and above the canopy for velocity and scalars as well as bulk transfer formulas to characterize the canopy's capacity to absorb heat, water vapour and momentum. This approach considers the transfer of different scalars

and of momentum independently while combination equations on the other hand emphasize the relationship between sensible and latent heat fluxes (Kaimal & Finnigan, 1994).

Green roof energy balance models tend to apply sub-models originally intended as single source models, such as the Penman-Monteith (1965) model of evapotranspiration which will be discussed in Section 2.2.3, to both the vegetation and substrate layers in an uncoupled dual source configuration (Sailor, 2008). The fluxes of each layer can be simply distinguished by the fractional vegetation coverage. This parameter is an estimate of the proportion of an area that is covered by vegetation on the horizontal plane. Uncoupled models allow a simpler approach to dual source modelling that requires fewer assumptions than coupled dual source models such as the widely used expansion on the Penman-Monteith model; the Shuttleworth-Wallace model (1985).

2.2 Energy balance components

2.2.1 Radiative heat transfers

The law of conservation of energy means that when radiation interacts with the vegetation layer the total amount of energy that is absorbed, reflected and transmitted, as shown in Fig 2.2, is equal to the incident energy. The proportion of incident energy involved in each mechanism is represented in modelling by its respective coefficient; absorption (α),

reflection (ρ) and transmission (τ), such that $1 = \alpha + \rho + \tau$. The absorption of radiation increases the internal thermal energy of the vegetation while reflection and transmission have no net effect on the canopy layer.

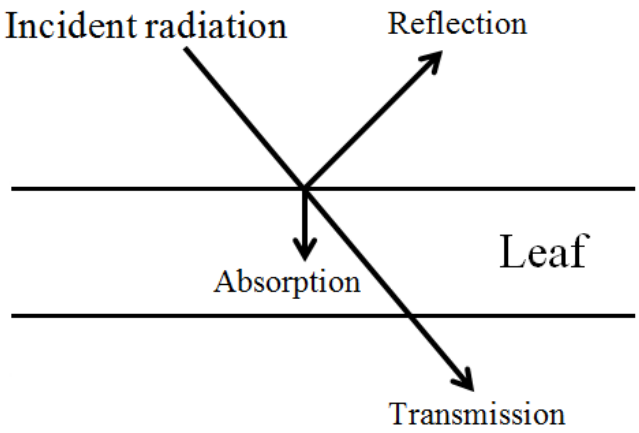

Fig 2.2 *The interaction of radiation at the leaf surface*

The ratio of absorption, reflection and transmission varies depending on the incident wavelength. As shown in Fig 2.3, leaves generally absorb the majority of incident ultraviolet (UV), photosynthetically active/visible (PAR/VIS) and mid-infrared radiation (MIR) while reflecting and transmitting the majority of energy in the near-infrared radiation region (NIR).

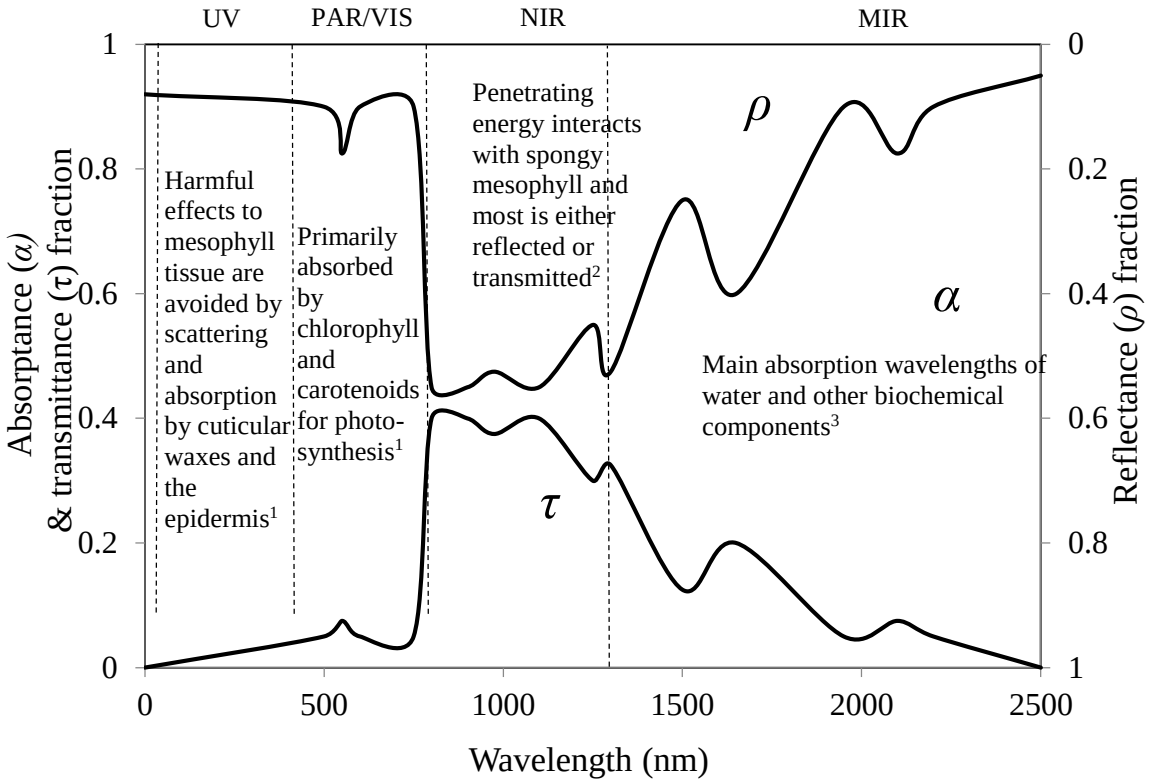

Fig 2.3 *Typical leaf absorption (α), reflection (ρ) and transmission (τ) spectra* (adapted from *Jones* & *Vaughan, 2010;* 1. Walter-Shea & Norman (1991); 2. Gausman (1977); 3. Verdebout et al. (1994))

Scaling these spectra up from a single leaf to a canopy level is complicated by the shading of leaves and multiple within-canopy reflections. The transmittance of a canopy is the sum of the unintercepted radiation and the radiation that is transmitted through or reflected downwards by leaves. Most common plant leaves have a solar transmittance of ~0.20 (Ross, 1975). However, for succulent plants like those commonly planted on green roofs, thick leaves result in higher absorptance and a very low or negligible transmittance

(Jones, 1983). Some green roof models have used Beer's Law (Eq. 2.2) to approximate transmittance (Del Barrio, 1998; Alexandri & Jones, 2007). This approach represents an exponential decrease of radiation through the canopy with larger LAI values decreasing transmittance and increasing shading. Jim & Tsang (2011) found that the transmittance and therefore extinction coefficient (k_0) was mostly dependent on LAI. Seasonally, their transmittance values varied from 0.17 in winter to 0.27 in summer. Aside from seasonal variations in LAI, this difference is also the result of the extinction coefficient in Beer's Law varying according to the solar angle. Leaf configuration also influences the extinction coefficient, with the larger k_0 values of a planophile canopy (horizontal leaf inclination) resulting in a greater absorptance than those of an erectophile canopy (vertical).

$$\tau = exp\ (-k_0\ \mathrm{LAI}) \tag{2.2}$$

Generalized values for the extinction coefficient can be found in the literature or calculated using expressions like Eq. 2.3 from Campbell (1986) used in Jim & Tsang (2011).

$$k_0 = \frac{\sqrt{x^2 + tan^2\psi}}{x + 1.774(x + 1.182)^{-0.733}} \tag{2.3}$$

x = ratio of averaged projected areas of canopy on horizontal and vertical surfaces, typically ranging from 0.6 to 2.5

As k_0 decreases, the canopy albedo is also reduced for each unit of *LAI*. Within-canopy reflectance means that the albedo of a canopy is smaller than the reflectance of the leaves of which it is composed (Del Barrio, 1998). Canopy albedo is an important component of the energy balance as it reduces the net radiation entering the system. Taller vegetation generally has a lower albedo as it facilitates greater within-canopy reflectance. Although the typical solar reflection coefficient for leaves is around 0.3 (Jones, 2013), for canopies below 1 m in height it is generally between 0.18 and 0.25 (Oke, 1987).

While spectral analyses are limited for green roofs, Zhao et al. (2014) measured the reflectivity of six species of *Sedum* and a *Sedum* mixture in a green roof study. While the spectral reflectivity of each *Sedum* condition resembled that shown in Fig 2.3 with respect to wavelength, the reflectivity varied between species at the same wavelength. Using the reflectance coefficients they obtained, Zhao and colleagues used the model of Tabares-Velasco & Srebric (2012) to simulate the thermal performance of green roof assemblies planted with *Sedum tomentosum* and the *Sedum* mix, which had the highest and lowest ρ values of 0.23 and 0.11, respectively. The results showed an average difference of 15.9-16.3% in the peak net radiation and 17.9-20.2% in the average net radiation between the two conditions when simulated in four cities. Given the difference in reflectivity observed within one genus and the influence this variation had on simulated net radiation, there is a need to measure the albedo of various green roof species to improve the predictive power of models for different plant species.

Multiple reflections within the canopy increase the canopy's absorption of radiation. The total absorptance for most common plant leaves has been reported to be between 0.4 and 0.6, with 0.5 commonly used for calculations (Nobel, 1983). However, Onmura et al. (2001) estimated from measurements an average absorptance of 0.77 for a green roof sample of grass. Furthermore, in a comparison of 30 species, *Sedum spectabile* Boreau was found to have the highest absorptance (Gausman & Allen, 1973). For *Sedum* and other succulent plants, absorptance is generally higher than non-succulents, reported between 0.59 and 0.83 (Gates et al. 1965), as a result of high leaf thickness and water content (Gausman & Allen, 1973). For green roof applications, Jim and Tsang (2011) recommended absorptance values of 0.8 and 0.2 for *PAR* and *NIR*, respectively.

The absorption, reflectance and transmission spectra vary temporally due to phenological changes associated with the solar zenith angle as well as the plant growth stage and environmental conditions. At a diurnal time-scale, the reflection coefficient has a pronounced U-shaped pattern with a minimum at solar noon coinciding with the minimum incidence angle as observed by Gaffin and colleagues (2009) for a green roof sample of *Sedum*. This phenomenon is observed in the reflection from vegetated surfaces as specular reflection occurs with the highest reflectivity occurring at large zenith angles. This is a result of vegetation having a non-Lambertian surface, with the roughness of the surface preventing diffuse reflection (Moene & van Dam, 2014). Despite this dynamic pattern

which is largely due to changes in the solar zenith angle, a constant reflection coefficient is commonly applied in green roof modelling.

While the solar angle will also vary albedo at a seasonal scale, leaf growth and senescence also affects the spectra throughout the year. As well as affecting the transmission of radiation through the canopy and the sensible and latent heat fluxes through changes in LAI, effects relating to the life cycle of leaves also change the canopy's absorption and reflection spectra throughout the year. These leaf optical properties are affected by factors such as the amount and distribution of pigments and water content which vary seasonally in response to environmental variations. For example, during leaf senescence, leaf reflectance and transmittance in the 400-700 nm region decreases with the appearance of tannins (brown pigments) while a decline in NIR reflectance results from the spongy mesophyll layer collapsing (Fourty et al. 1996).

Leaf senescence may also be stress-induced. During periods of stress, plants alter their physiology, morphology and development. These changes can affect the partitioning of incident energy at the leaf surface. Leaf reflectance is most commonly affected in the VIS spectral band for many common stressors and vascular plant species (Carter, 1993, 1994), due to the lowering of leaf chlorophyll concentrations because of metabolic disturbances (Knipling, 1970). Mori et al. (2009) compared the chlorophyll content of stressed and less-stressed leaves from four *Sedum* species grown on a green roof with chlorosis being observed in three of the species in stressed conditions. While acute stress

tends to affect the far-red spectrum (Carter & Knapp, 2001) it will likely have a negligible effect on the energy balance. However, continued stress and chlorophyll loss will progressively narrow the absorption spectrum of VIS (Gates, 1980). This is noteworthy as Nagase & Dunnett (2010) found in greenhouse conditions that eight species of forb and grass reached their permanent wilting point after two to three weeks without water in a green roof substrate, with similar results found in a green roof study (Bates et al. 2013). The availability of substrate moisture is considered to be the most limiting factor for plants in green roof ecosystems (Monterusso et al. 2005; Nagase & Dunnett, 2010) and may have consequences for the albedo of green roof species during dry periods.

Besides radiative exchanges between the sky and the vegetation layer, long-wave radiation exchanges should also be considered between the plant canopy and the substrate surface, as represented by $LW_{f,g}$ (W m^{-2}) in Fig 2.1. These exchanges are complex and difficult to calculate so are commonly neglected or simplified in green roof models using several assumptions, the most common of which is to represent the vegetation layer and substrate as two flat surfaces. A simplified approach is justified on the basis of extensive green roof plants having a low stature. Tabares-Velasco and Srebric (2012) compared three assumptions commonly used in the literature to calculate these exchanges and found they differed by less than 10%, or 4 W m^{-2}. They attributed the lack of variability between the three assumptions was likely due to the use of similar emissivity values for the canopy and substrate layers. They did not recommend representing the layers as two parallel surfaces

with different areas as it is relies on the sky view factor which requires LAI and plant height information. The sky view factor is defined as the geometric ratio between the radiation received by a surface from the sky and the radiation emitted from the entire hemispheric radiating environment (Watson & Johnson, 1987). On the contrary, the authors recommended assuming the layers can be represented as two infinite and parallel surfaces, shown in Eq. 2.4, as its simplicity does not compromise the accuracy of calculations and provided values in the middle of the other assumptions.

$$LW_{f,g} = (1 - \tau_{IR}) \frac{\sigma \left(T_{plants}^4 - T_{substrate}^4\right)}{\frac{1}{\varepsilon_{substrate}} + \frac{1}{\varepsilon_{plants}} - 1} \tag{2.4}$$

σ = Stefan-Boltzmann constant ($5.67 \cdot 10^{-8}$ W m^{-2} K^{-4})
τ_{IR} = long-wave transmittance of the vegetation layer
T_{plants} = plant temperature (°C)
$T_{substrate}$ = temperature of substrate surface (°C)
$\varepsilon_{substrate}$ = emissivity of the substrate ε_{plants} = emissivity of the plants

Foliage emissivity is defined as the ratio of energy radiated from the plant surface to that radiated from a black body. The emissivity of leaves as reported in the literature is around 0.96, ranging between 0.92 and 0.98 (Gates, 1980; Nobel, 1983). The emissivity of succulents has been found to be as high as 0.98 (Monteith & Unsworth, 2007) but grass emissivity ranges from 0.90-0.97 (Pielke, 2002). However, the emissivity of a canopy is greater than that of the leaves of which it is composed, often nearing 0.99 for dense canopies

due to the increased absoprtion that results from within-canopy reflectance (Campbell & Norman, 2012)

As noted by Feng et al. (2010), although the optical properties are the basic parameters of a green roof's energy balance, there is generally little knowledge regarding these properties amongst the species most commonly planted on green roofs. While a detailed representation of green roof vegetation's response to abiotic stress and seasonal variations in energy models is unrealistic, models of plant phenology exist for climate models. However, to verify these phenological models for green roof applications will require further research to quantify the variation in the spectral characteristics of these species during both healthy and stressed periods in order for green roof heat transfer models to be more dynamic in response to vegetation changes. Additionally, it appears that despite drought-tolerant species having a relatively low albedo compared to most plants, modelling suggests they can still play a significant role in reducing the surface heat flux through the substrate.

2.2.2 Sensible heat flux

When a temperature gradient exists within or between a solid and a fluid medium, a sensible heat flux will occur. While conduction refers to the transfer of heat across either a solid or fluid medium from particles with more energy to those with less, convection

refers to the transfer of heat between a surface and a moving fluid through the processes of conduction near the surface and bulk fluid motion above the surface (Bergman et al. 2011). Convection is the primary means of sensible heat transfer in the vegetation layer of a green roof and to the atmosphere above.

The rate of convective heat transfer, H_{conv} (W m^{-2}), between a flat surface and a fluid is given by Newton's law of cooling, shown in Eq. 2.5. A sensible heat flux, as seen in this equation, is proportional to the difference in temperature between the two bodies.

$$H_{conv} = h\, A_{fluid,solid}\, \Delta T \tag{2.5}$$

h = convective heat transfer coefficient (W m^{-2} K^{-1})
$A_{f,s}$ = area of fluid-solid interface (m^2)
ΔT = temperature difference between solid and fluid (°C)

A convective heat flux is commonly represented as the transfer of heat across a thin layer of fluid at the fluid-solid interface, known as the boundary layer. A heat flux occurs when this layer features a temperature gradient stemming from the bordering solid surface and fluid bulk having different temperatures. The temperatures of these two bodies are assumed to be uniform. The boundary layer acts as an insulating layer that provides resistance to the flow of heat between the solid and the fluid. The thickness of this boundary layer varies inversely to the heat transfer coefficient, thus conditions that result in a reduction in boundary layer thickness enhance convective heat transfer by increasing the transfer coefficient (Monson & Baldocchi, 2014).

The heat transfer coefficient is a proportionality factor that represents the convective heat flux per unit of temperature difference between the solid and the fluid. It depends on the physical properties as well as the motion and velocity of the fluid within the boundary layer and the geometry of the surface. It is also dependent on the nature of the convection, namely free (or natural) and forced convection. Free convection occurs when a temperature difference between a solid and a still fluid produces a density difference between the boundary layer and the bulk fluid. This creates a buoyancy force causing the boundary layer fluid to flow and transfer heat. Forced convection, on the other hand, involves an external force, such as wind, generating fluid motion. The flow velocities involved in forced convection are greater than those of free convection resulting in higher convective heat transfer coefficient in forced flow conditions. When both free and forced mechanisms act together to transfer heat, it is referred to as mixed convection (Shah & Sekulić, 2003).

Given the complexity of fluid movement, the value of the convective heat transfer coefficient is obtained using an empirical approach involving dimensionless numbers. These numbers are derived from correlational relationships that usually involve correlations with wind speed for forced convection and with a temperature difference for free convection (Defraeye et al 2013). Those used in the green roof literature are commonly derived or adapted from measurements on flat or rough rectangular plates. While an in-depth explanation of the convective heat transfer coefficient's approximation is beyond the

scope of this review, Table 2.2 provides a brief explanation of the dimensionless numbers commonly used in its estimation.

Table 2.2 *Definitions of dimensionless numbers used in the approximation of the convective heat transfer coefficient*

Number	**Definition**
Grashof (Gr)	Ratio of free convection buoyancy force to viscous force
Nusselt (Nu)	Ratio of convective and conductive heat transfer
Prandtl (Pr)	Ratio of the momentum and thermal diffusivities
Rayleigh (Ra)	Ratio of natural convective to diffusive transport
Reynolds (Re)	Ratio of the inertial and viscous forces

The green roof model of Tabares-Velasco and Srebric (2012) employed a modified form of Newton's law of cooling shown in Eq. 2.6. The LAI provides the area of the leaf-air interface at which convective heat transfer occurs. However, the calculation of non-dimensional models were originally developed from experiments involving flat surfaces. Therefore, when considering convective heat transfer from objects where geometrical similarity with flat surfaces cannot be assumed, such as from plant canopies, the calculation of non-dimensional models for free, mixed and forced convection must be modified. Rough surfaces enhance convective heat and mass transfer by increasing turbulence and the total contact area between the surface and the fluid. The addition of vegetation above a bare soil therefore increases the surface roughness, ultimately enhancing the turbulence and

increasing the surface area which subsequently increases convective heat loss (Ghiaasiaan, 2011). As Eq. 2.5 estimates the flux over a flat surface, Tabares-Velasco and Srebric (2012) included an enhancement factor (β) in Eq. 2.6 to account for the roughness of the plant canopy.

$$H_{f,conv} = \beta\, h\, \mathrm{LAI}\, (T_f - T_a) \tag{2.6}$$

T_f = foliage temperature (°C) T_a = temperature of within canopy air (°C)

As suggested by Schuepp (1993), the roughness coefficient (β) used by Tabares-Velasco & Srebirc (2012) was originally set to 1.5. However, the authors found that the Penman-Monteith equation for evapotranspiration, to be discussed in Section 2.2.3, underestimated the maximum evapotranspiration rate. They believed this may have been attributed to the use of the convective heat and mass transfer enhancement factor. Therefore, they later changed the enhancement factor to 3 for vegetated surfaces and 2.1 for non-vegetated surfaces (Tabares-Velasco et al. 2012) based on research by Clear et al. (2003) concerning convection on rooftops.

Additionally, based on previous green roof modelling research (Alexandri & Jones, 2007), Tabares-Velasco and Srebric (2012) proposed the incorporation of mixed convection to more accurately estimate the convective heat transfer coefficient. They included mixed convection by incorporating it into the Nusselt number, as shown in Eq.

2.7, to better detail the laminar-turbulent transition. This expression calculates the resistance to convection over a flat surface depending on the ratio of the Grashof number divided by the Reynolds number. The value of the Grashof number distinguishes between forced, mixed and free convection. For this approach, the influence of wind speed is included by use of the Reynolds number as it is linearly dependent on wind speed.

$$Nu = \begin{cases} 3 + 1.25 * 0.0253\, Re^{0.8} & Gr < 0.068\, Re^{2.2} & Forced\ convection \\ 2.53\,(\frac{Gr}{Re^{2.2}})^{\frac{1}{3}}(3 + 1.25 * 0.0253\, Re^{0.8})L^{\frac{1}{15}} & 0.068\, Re^{2.2} < Gr < 55.3\, Re^{\frac{5}{3}} & Mixed\ convection \\ 0.15\, Re^{\frac{1}{3}} & 55.3\, Re^{\frac{5}{3}} < Gr & Free\ convection \end{cases} \quad (2.7)$$

Aside from the dimensionless model of convection, several correlational models have been specifically developed for vegetated surfaces using empirical and semi-empirical methods. The semi-empirical approaches, which are the most widely used in the green roof literature, involve modifying Newton's law of cooling by including plant characteristics and employing the logarithmic wind profile for the estimation of aerodynamic resistance. Conversely, the empirical methods involve defining correlations between heat transfer and scalar parameters or the convective heat transfer coefficient based on an extensive amount of experimental work.

The most commonly applied semi-empirical convection models in the green roof energy literature are Eq. 2.8 and 2.9. These similar models use a resistance network to estimate the transfer of heat across the boundary layer. This approach is analogous to

Ohm's law for an electrical circuit; the heat transfer rate (current) is proportional to the temperature difference (voltage) and inversely proportional to the thermal resistance. Eq. 2.8 is used in the green roof models of Del Barrio (1998), Kumar & Kaushik (2005), Alexandri & Jones (2007) and Djedjig et al. (2012), while Eq. 2.9; a multiplicative model from Deardorff (1978), is used in Sailor (2008) and Ouldboukhitine et al. (2011).

$$H_{f,conv} = LAI \frac{\rho af \; cp,a}{r_a}(T_f - T_a) \tag{2.8}$$

$$H_{f,conv} = 1.1 \; LAI \; \rho_{af} \; C_{p,a} \; C_f \; u_w \; (T_a - T_f) \tag{2.9}$$

r_a = aerodynamic resistance (s m^{-1})
ρ_{af} = density of air at foliage temperature (kg m^{-3})
$C_{p,a}$ = specific heat of air at constant pressure (J kg^{-1} K^{-1})
C_f = bulk transfer coefficient u_w = within-canopy wind speed (m s^{-1})

As LAI only accounts for the surface of the leaves, Deardorff (1978) included a scale factor of 1.1 in Eq. 2.9 to approximate the heat transfer from the stems, twigs and limbs of the plant which exchange sensible heat but do not transpire. As featured in the FASST low vegetation model (Frankenstein & Koenig, 2004), Ouldboukhitine and colleagues (2011) added a windless exchange coefficient, e_0 (2.0 W m^{-2}), to Eq. 2.9. This prevents a decoupling of the plant surface from the atmosphere under extremely stable conditions when the wind speed at the air-foliage interface, u_w, approaches zero as convection will still occur under these conditions. The dimensionless heat transfer

coefficient C_f in Eq. 2.9 takes into account both sides of the leaves and is inversely proportional to the within-canopy wind speed. However, Eq. 2.9 has been criticised for requiring a lot of parameters that are not easily accessed without on-site measurements (Ayata et al. 2011).

While these models are related, the parameterization of aerodynamic or external resistance to heat transfer is a key component which importantly separates green roof energy models' estimation of convective heat transfer. The transfer of heat and mass by diffusion from the canopy to the atmosphere is regulated by an aerodynamic resistance. The magnitude of this diffusion resistance depends largely on wind speed, with high resistance occurring in still or slow winds (Mansfield, 1973). A lower resistance occurs with higher wind speeds as the greater air movement continuously replenishes the air close to the boundary layer, thus maintaining a steep gradient to drive diffusion (Jones, 2014). Aerodynamic resistance arises as a consequence of the frictional drag exerted by a surface, in this case the foliage, with wind speed increasing logarithmically above flat, extensive uniform surfaces (Hanan, 1997). Aerodynamic resistance therefore links the characteristics of the foliage surface and the turbulence that drives the transfer of sensible heat away or towards the surface (Pitman, 2003).

However, there is an insufficient understanding of physical atmospheric processes to derive laws from first principles in order to quantify these transfers. Consequently, surface layer modelling commonly utilizes theories of similarity which are based on the

consistency and repeatability of boundary layer observations for particular assumptions to be justified and empirical relationships derived. The green roof models of Sailor (2008), Ouldboukhitine et al. (2011) and Djedjig et al. (2012) apply Monin-Obukhov similarity theory (MOST, Monin & Obukhov, 1954) formulations to estimate aerodynamic resistance. MOST relates surface layer turbulent fluxes of momentum, sensible heat and moisture to mean vertical gradients of wind, temperature and water vapour, respectively (Brutsaert, 1982; Garratt, 1992; Arya, 2001). Eq. 2.10 provides a MOST-derived estimation of the aerodynamic resistance to heat commonly used in green roof models. As this expression indicates, aerodynamic resistance is inversely related to the log of the surface roughness length which is an aerodynamic measure of roughness defined as the height at which the neutral wind profile will extrapolate to a wind speed of zero. The roughness lengths are approximated as a fraction of the height of the plants, but their specification can be very difficult. Nevertheless, at a given wind speed, taller vegetation has a lower aerodynamic resistance, facilitating a greater turbulent transfer of convective heat away from the canopy surface (Hungate & Koch, 2014). Expressions for the featured parameters in Eq. 2.10 can be found in Ayata et al. (2011) and Djedjig et al. (2012).

$$r_a = \frac{In\left[\frac{(z-d)}{z_m}\right] In\left[\frac{(z-d)}{z_h}\right]}{\kappa^2 u_z} \tag{2.10}$$

d = zero plane displacement height (m)
z_m = roughness length for momentum (m)
z_h = roughness length for heat (m)
κ = von Karman's constant (~0.4)
u_z = wind speed at height z (m s^{-1})

However, the logarithmic wind profile assumed in Eq. 2.10 is only valid in neutral and near-neutral atmospheric conditions. In non-neutral conditions, both thermal and mechanical turbulence occurs unless the wind speed is zero or is constant with height. In unstable conditions, vertical motion resulting from turbulence is enhanced while it is dampened in stable conditions. This leads to distortions of the logarithmic wind profile method in non-neutral conditions (Rohli & Vega, 2013). Some green roof models combine Eq. 2.10 with stability functions to account for these buoyancy effects (Sailor, 2008). However, Djedjig and colleagues (2012) suggested that the effects of buoyancy could be assumed negligible for green roof applications and applied a simpler form of Eq. 2.10. They justified this assumption with the premise that the minimal leaf-air temperature differential and the generally high wind speed compared to the average size of the leaves limits the influence of buoyancy on the wind profile.

An alternative approach is to use a correlational model to estimate aerodynamic resistance. Del Barrio (1998) used Eq. 2.11 for a green roof simulation. The equation was originally developed by Stahghellini (1987) from an extensive data set collected from greenhouse tomato plants.

$$r_a = \frac{a{L_{ch}}^m}{(L_{ch}\,(T_f - T_a) + b\,u^2)^n} \tag{2.11}$$

L_{ch} = characteristic length (m) a = 1174
b = 207 m = 0.5
n = 0.25

Stahghellini (1987) found that for increasing wind speeds, particularly those above 0.2 m s^{-1}, the consequence of error in the aerodynamic resistance diminishes, which is beneficial given the high wind speeds commonly associated with rooftop environments (Dunnett & Kingsbury 2004). However, it should be noted that the coefficients derived for Eq. 2.11 may not be applicable for species other than tomato plants and for the air flow conditions commonly found on rooftops.

Early green roof studies used a linear relationship with wind speed to calculate the convective heat transfer coefficient (Nayak et al. 1982; Cappelli et al. 1998). Feng and colleagues (2010) employed a correlational model of convective heat flux, wind speed and the leaf-air temperature differential to estimate convection on a green roof. Alexandri and Jones (2007) compared the accuracy of a linear relationship between the convective heat transfer coefficient, as used in Eq. 2.5, and wind speed, u (m s^{-1}), shown in Eq. 2.12, with the semi-empirical logarithmic wind profile method in Eq. 2.8 for calculating the convective heat transfer.

$$h = \begin{matrix} 5.6 + 18.6\,u & u < 5\ m\ s^{-1} \\ 7.2\,u^{0.78} & 5\ m\ s^{-1} < u < 30\ m\ s^{-1} \end{matrix} \qquad (2.12)$$

They found that calculated above-canopy air temperatures using the log wind profile method averaged 0.3 °C in error with a maximum error of 1.3 °C during the day compared to measured temperatures. Meanwhile, the correlational method averaged 1.0 °C

in error with a maximum of 2.4 °C. However, the largest difference between the measured and calculated data from both equations used by Alexandri & Jones (2007) occurred at the warmest air temperatures, which is what motivated Tabares-Velasco and Srebric (2012) to include mixed convection in the Nusselt number formulation of Eq. 2.7.

For a comparison between different methods, Ayata and colleagues (2011) measured the sensible heat flux of a *Delosperma nubigenum* green roof sample for both free and forced convection regimes using a laboratory apparatus based on the overall energy balance. They compared this data with calculated values from a modified form of Newton's law of cooling (Eq. 2.5) with dimensionless analysis deriving the convective heat transfer coefficient, the semi-empirical logarithmic wind profile method of Eq. 2.8 and the empirical McAdams' method for estimating the convective heat transfer coefficient (McAdams, 1954, Eq. 2.13). The McAdams' method had not previously been used for green roof applications but is recommended when forced convection is the dominant form of convection and the leaf sizes are relatively small. Assuming conditions on each side of a thin leaf are similar, the McAdams derived coefficient is used in Newton's cooling law with a factor of 2 in order to account for both sides of the leaves. The measured and calculated results showed fairly good agreement for each method, as shown by the root mean square error (RMSE) and r^2 values displayed in Table 2.3, although the McAdams' method provided only moderate accuracy for forced convection conditions.

$$h = 5.9 + 4.1\, u\, \frac{511+294}{511+T_a} \quad (2.13)$$

Table 2.3 *Root mean square error and r squared values between calculated and energy balance residuals* (Source: Ayata et al. 2011)

	Forced convection		Free convection	
Method	RMSE (W m^{-2})	r^2	RMSE (W m^{-2})	r^2
Modified Newton's law	18	0.73	23	0.71
Logarithmic wind profile	19	0.72	61	0.78
McAdams' method	30	0.52	13	0.87
Ayata et al.	11	0.81	6.60	0.90

During their comparison of existing models, Ayata and colleagues (2011) observed a strong relationship between the soil volumetric water content (VWC) and the convective heat flux, noting it was even greater than the correlation between the temperature differential and convection. As the soil moisture decreased exponentially over several days, the latent heat flux also decreased exponentially while convection increased at a similar rate. As will be discussed further in Section 2.2.3, lower soil moisture reduces transpiration and the evaporative cooling it provides to the surface of leaves, thus increasing leaf temperatures, the leaf-air temperature differential and ultimately the convective heat flux. Ayata and colleagues suggested that a robust model of convective heat transfer for green roofs must therefore incorporate the volumetric water content of the substrate, as shown in Eq. 2.14, with measures of its accuracy shown in Table 2.3. This model needs to be tested

with on-site experimental studies to better understand its performance. In particular, for wind speeds greater than 3 m s^{-1} and for temperature differences greater than 7 °C, values for the exponent *n* need to be further investigated.

$$H_{f,conv} = \begin{cases} \sigma_f \text{ LAI h } \left(\frac{e^u}{(11\,u\,VWC)^2}\right)\left(T_f - T_a\right)^n & Forced\ convection \\ \sigma_f \text{ LAI h } \left(\frac{VWC}{u}e^{3\,VWC}\right)\left(T_f - T_a\right) & Free\ convection \end{cases} \quad (2.14)$$

σ_f = vegetation fractional coverage
n = exponent dependent on flow regime (0 to 1)

The results of this study and the model proposed highlight the difficulties faced when using conventional methods to estimate not only the convective heat transfer on green roofs, but vegetation in general. Green roofs have additional parameters that affect convection, such as the fractional vegetation coverage. This is an important consideration as the convective models discussed rely on correlations developed in conditions that may differ greatly from those experienced on a green roof. Empirically-derived relationships contain the implicit assumption that multivariate correlations are maintained in conditions other than those of the original observations. As convection is affected by a variety of environmental, and in the case of leaves, physiological factors, this reduces the likelihood of overlap between green roof and non-green roof environments.

For instance, green roof parameters differ greatly from those of the rectangular plates from which the dimensionless numbers are generally derived. Defraeye et al. (2013)

noted that for convective exchanges at the leaf surface, the boundary conditions for the plates differ from those of real leaves as a result of leaves not having uniform surface temperature. Although the incoming heat flux may be quasi constant across the surface, depending on leaf orientation, it is not balanced by convection alone as conduction and the emission of long-wave radiation also contribute to non-uniformity. However, the impact of these different thermal boundary conditions on the dimensionless numbers is considered limited for leaves (Schuepp, 1993).

Additionally, for the dimensionless numbers, the flat plate correlations are different from leaf surfaces as a result of different flow patterns. The flow of air along a leaf and its degree of turbulence will be markedly different to that of a flat plate due to leaf inclination and edge effects (Defraeye et al. 2013). There are flat rectangular leaf models for dimensionless numbers (Chen et al. 1988; Monteith & Unsworth, 1990) however leaves have some degree of curvature and when considered at a canopy level by means of the LAI, the vegetation layer is not analogous to a flat surface. Tabares-Velasco and Srebric (2012) did attempt to account for this difference between leaves and plates by means of the empirically-derived enhancement factor in Eq. 2.6, although amendments were required highlighting the difficulty in quantifying the differences due to the geometry of the canopy surface.

The structure of vegetation, as well as fractional vegetation coverage, also limits the suitability of MOST in the estimation of aerodynamic resistance. These properties

violate the assumption of a horizontally homogenous turbulence field. Panin and colleagues (1998) found that horizontal inhomogeneity resulted in the underestimation of turbulent fluxes in terrains of varying heterogeneity. The authors noted that it has generally been assumed that the MOST approach is still applicable for individual positions of an inhomogeneous terrain. Nevertheless, scintillometry studies by Lagouarde et al. (1996) and Chebouni et al. (1999) over an area consisting of two adjacent and contrasting vegetated surfaces indicated that the violation of MOST was small. Huo and colleagues (2015) showed that MOST functions can be accurately adjusted for heterogeneous surfaces using a coefficient that specifies the degree of heterogeneity.

The location of a green roof on a rooftop also complicates the use of MOST as it modifies the wind field. MOST only considers the wind flow over a flat surface but this condition is not analogues to a rooftop. Buildings disturb the wind environment of urban areas and, depending on the geometry of the urban landscape, particularly the height to width ratio between two buildings, can produce complicated patterns of wind flow that will violate the assumptions of MOST (Oke, 1987).

While the convective model developed by Ayata and colleagues (2011) is an important step forward in the estimation of green roof heat convection, results obtained from experiments are generally very case specific. In particular, canopy differences such as leaf orientations, surface roughness, turbulence conditions, stomatal distribution and morphologies like leaf shape and thickness means the ability of a model to accurately

predict the convective heat flux of canopy from which it was not derived may be compromised. Furthermore, correlations are often expressed as a function of different characteristic lengths and wind speeds (Defraeye et al. 2013).

Although conduction is involved in the convection process, as noted earlier, the conduction of heat within the vegetation layer is generally considered negligible. However, Tabares-Velasco and Srebric (2012) included the thermal conductivity of the vegetation layer in their model with Eq. 2.15. The conduction of heat in vegetation layer depends on the ability of plants and within-canopy air to conduct heat; their thermal conductivity (k_{plant} and k_{air}, respectively, W m^{-1} K^{-1}), and the porosity of the layer (ϕ). Thermal conductivity varies according to the material's moisture content, pressure and temperature (Thirumaleshwar, 2009).

$$H_{f,cond} = \phi\, k_{air} + (1-\phi) k_{plant} \tag{2.15}$$

The thermal conductivity of plants is fairly low, averaging around 0.54 W m^{-1} K^{-1} for the stem of herbaceous plants (Kirkham, 2014) and around 0.24-0.50 W m^{-1} K^{-1} for leaves (Nobel, 2009). These coefficients are slightly less than that of water which is to be expected given plant biomass is generally composed of water, air and organic polymers, all of which have low conductivity. Due to the high leaf water content of succulents, Tabares-Velasco and Srebric (2012) selected a thermal conductivity value of 0.50 W m^{-1} K^{-1} for

their *Delosperma nubigenum* and *Sedum spurium* green roof samples. The thermal conductivity of the within-canopy air in the vegetation layer will be even lower, generally in the range of 0.024-0.027 W m^{-1} K^{-1} (Thirumaleshwar, 2009). From LAI and plant height measurements, they estimated a porosity of 0.85. The temperature differential driving conductive heat transfer in green roof plants and the within-canopy air can be expected to be quite minimal given the small stature of canopies like those on extensive green roofs which minimizes conduction in the layer.

The inappropriateness of conductivity formulae that assume uniform temperatures for plant structures, such as leaves, has been raised as measurements have shown inhomogeneous temperature distributions (Vogel, 1970, 1981). The leaf temperature over the thickness of a leaf is usually considered quasi-constant, with little or no temperature gradient given the thickness is typically less than 5 mm for *Sedum* species (Teeri et al. 1981). Conversely, in the lateral direction, distinctive temperature gradients are apparent as a result of low thermal conductivity (Jayalakshmy and Philip, 2010).

The validation of sensible heat conduction estimates within the canopy layer is difficult given practical limitations similar to those encountered in the quantification of convection. Accurate temperature measurements for the top and bottom of the canopy air profile and the plant biomass are required for a comprehensive validation of conduction estimates. Temperatures also will be horizontally heterogeneous throughout the green roof canopy, further complicating attempts to accurately quantify conduction.

The inability of the convective sensible heat flux to be directly quantified limits the precision of its expression in energy balance models as models are compared to likely erroneous empirical data. Nevertheless, comparisons between models like those in Ayata et al. (2011) are valuable in determining the best approach for estimating convective heat transfer. Given the high wind velocities commonly present in rooftop environments, validating models across a greater range of wind speeds would also be beneficial. Regarding the overall heat transfer of green roof assemblies, models have detailed the important role the sensible heat flux plays in heat dissipation, particularly when soil moisture is low.

2.2.3 Latent heat flux

The latent heat flux that results in passive cooling involves soil and wet-canopy evaporation and plant transpiration, collectively termed evapotranspiration (ET, kg m^{-2} s^{-1}). A considerable amount of energy is required for water to change from a liquid to vapour and when this change occurs, energy is absorbed from the evaporating surface without a change in temperature occurring. Whereas sensible heat transfers are driven by a temperature gradient, the driving force of ET is the vapour pressure differential between saturated plants and the relatively drier surrounding air; the vapor pressure deficit (VPD). Latent heat's contribution to the energy balance is almost always negative as heat absorbed

by a plant is converted to an increase in the kinetic energy of water molecules in latent heat transfers, with sufficient energy causing vaporization. The flux can be positive when water condenses on a leaf (Monson & Baldocchi, 2014), although this is generally not considered in green roof models.

The direct role of plants in the ET process; transpiration, involves the evaporation of water from the air-liquid interfaces along pores in the cell walls of epidermal, mesophyll and guard cells which diffuses out of the leaf through stomata that are opened to absorb CO_2 during photosynthesis (Nobel, 2009). In green roof modelling, as in most plant models, the air beneath the stomata is assumed to be saturated (Alexandri & Jones, 2007). Ouldboukhitine and colleagues (2014) aimed to quantify green roof transpiration rates and the thermal resistance of green roof arrays by comparing ET and evaporation in vegetated and bare modules, respectively. The thermal resistance of the trays without plants were measured as ~0.8 m^2 K W^{-1} while the thermal resistance of the trays containing *Lolium perenne* were ~0.92 m^2 K W^{-1} and ~1.27 m^2 K W^{-1} for *Vinca major*. Transpiration accounted for approximately 13% of the additional thermal resistance of *Lolium perenne* and 37% for *Vinca major*. While these results show the benefits of plant transpiration for heat dissipation, they also highlight the difference in transpiration rates between species.

Green roof models have tended to apply methods of ET estimation developed for agricultural applications. There is limited validation of these techniques against direct measurements of green roof ET (Marasco et al. 2014). The green roof energy balance

literature has generally employed one of two single source models for estimating the latent heat flux of ET from the canopy layer, meaning they only consider one source of latent heat flux. These models involve a resistance network similar to those for sensible heat (Eqs. 2.8 and 2.9). The following ET model from Deardorff (1978) has been used in energy balance models that adapted the FASST low vegetation model (Frankenstein & Koenig, 2004) for green roof applications (Sailor, 2008; Ouldboukhitine et al. 2011).

$$L_f = LAI\, \rho_{af}\, C_f\, l\, W_{af}\, r'' \,(q_{af} - q_{f,sat}) \tag{2.16}$$

l = latent heat of vaporization (J kg^{-1}) r'' = foliage surface wetness
q_{af} = mixing ratio of the air at the foliage interface
$q_{f,sat}$ = saturation mixing ratio at foliage temperature

Like the sensible heat flux, the diffusion of water vapour from the leaf surface encounters resistance in the boundary layer to its outward movement into the atmosphere. Deardorff (1978) represented this resistance by the foliage surface wetness factor, which is the ratio of aerodynamic resistance to the total resistance, as displayed in Eq. 2.17. While the roughness lengths for both heat and moisture are both much less than the momentum roughness length due to the additional resistance to molecular diffusion for heat and moisture exchange, both are assumed to have the same value.

$$r'' = \frac{r_a}{r_a + r_s} \tag{2.17}$$

r_s = stomatal resistance to mass transfer (s m^{-1})

The other model of ET commonly applied in the green roof modelling literature is the widely used Penman-Monteith model (1965), shown in Eq. 2.18. For this approach, Monteith modified the original Penman equation (1948) to incorporate the effects of water stress on vegetation with the addition of stomatal resistance. Variations of this model have been used in the green roof models of Del Barrio (1998), Kamur and Kaushik (2005), Alexandri & Jones (2007), Djedjig et al. (2012), Morau et al. (2012) and Tabares-Velasco & Srebric (2012).

$$L_f = LAI \frac{\rho_{af} C_p}{\gamma(r_s+r_a)} (e_{s,plants} - e) \quad (2.18)$$

C_p = specific heat of air (J kg^{-1} K^{-1}) γ = psychrometric constant (~0.059 kPa K^{-1})
$e_{s,plants}$ = vapour pressure of air in contact with plants (kPa)
e = vapour pressure of air (kPa)

Ouldboukhitine and colleagues (2012) compared the estimated ET as calculated using the Penman-Monteith model with measured ET from green roof samples of a *Sedum* and a grass. The measurements showed the grass had a higher ET rate than the *Sedum* and after 3 days approximately double the amount of water had evapotranspired from the grass than had evaporated from a non-vegetated substrate. The daily ET rate for the grass, measured as 2.53 mm, was underestimated using the Penman-Monteith equation (1.66 mm/day), with the authors determining a correction factor of 1.37 to correct the model. However, this correction factor may only be applicable to the species and conditions used in the study.

Conversely, Djedjig et al. (2012) found the Penman-Monteith equation provided accurate modelling of substrate surface temperatures and water content changes following a heavy rain event for *Sedum* and pampas grass assemblies. Their simulations found that following a long period of no precipitation when the substrate water content was below 10% of its maximum capacity, ET was greatly reduced and nearly all of the absorbed radiation by the vegetation was dissipated as sensible heat ($T_f > T_a$). However, they found the energy balance differed with higher substrate water contents, with ET becoming the primary flux when the leaf temperature neared the air temperature as transpiration rates increased to passively cool the leaves. Djedjig and colleagues were able to link the reduction in the green roof's surface temperature to the water availability in the substrate by comparing substrate surface temperatures for different substrate saturation ratios. The results showed surface temperature differed by approximately 25 °C between dry and saturated substrates due to the effect of transpiration. Sensible heat was reduced with increased soil water content because the increase in transpiration reduced the temperature difference between the air and the leaves (Ayata et al. 2011).

Like the Deardorff (1978) approach, the Penman-Monteith model features a sub-model for canopy stomatal resistance. The degree of accuracy of the Penman-Monteith model has been shown to be largely dependent on the estimation of canopy resistance (Vogel et al. 1995). Stomatal resistance, the reciprocal of stomatal conductance, refers to the stomatal response to internal and external stressors that limit the diffusion of water

vapour from the intercellular openings between guard cells (stomata) on the surface of leaves. Sub-models of stomatal resistance generally assume that these intercellular spaces contain saturated air, as previously mentioned.

Stomatal regulation involves a balance between controlling water loss by preventing the loss of this saturated air while maintaining adequate rates of photosynthesis and evaporative cooling (Hall et al. 1976). Succulents, such as *Sedum*, contain tissue that serves to store utilizable water during periods of low soil moisture content (von Willert et al. 1992). They exhibit high stomatal resistance in response to high atmospheric demand (high VPD) during dry soil conditions. This is a means of retaining temporary storages of water as transpiration has an inverse linear relationship with stomatal resistance (Lambers et al. 2008). Green roof modelling of succulents has shown that stomatal resistance largely controls the latent heat flux, with aerodynamic resistance playing a very minor role (Tabares-Velasco & Srebric, 2012). Conversely, aerodynamic resistance to water vapour diffusion has a more significant effect on the transpiration of plants such as grasses, which have a comparatively lower stomatal resistance.

It is particularly difficult to simulate stomatal behaviour due to numerous factors such as both long- and short-distance chemical and hydraulic signalling being involved in stomatal response to environmental changes (Jones, 2013). Stomatal regulation has been empirically shown at the leaf scale to be sensitive to a number of environmental factors (Jarvis & Morison, 1981; Avissar et al. 1985). The green roof model literature tends to

employ variations of the Jarvis-Stewart model (Jarvis, 1976; Stewart, 1988) which parameterizes the effect that particular environmental factors have on stomatal behaviour (Del Barrio, 1998; Sailor, 2008; Djedjig et al. 2012; Tabares-Velasco & Srebric, 2012). Shown in Eq. 2.19, this approach expresses stomatal resistance as a species-specific minimum resistance (i.e. stomatal resistance under optimal conditions, $r_{s,min}$, s m) multiplied by a series of independent stress functions represented in Eq. 2.19 by $f_n(x)$, where x is the parameter that affects stomatal resistance. This regression model represents a meteorological approach to soil-vegetation-atmosphere transfer (SVAT) parameterization of stomatal response rather than a physiological approach which involves the CO_2 assimilation rate (Leuning, 1995).

$$r_s = \frac{r_{s,min}}{LAI} f_1(\varphi_s) f_2(T_f) f_3(VWC) f_4\ (VPD) f_5\ (CO_2) \tag{2.19}$$

φ_s = solar radiation (W m^{-2}) CO_2 = ambient CO_2 concentration (ppm)

The green roof models vary in which functions are included in their expression of stomatal resistance. For instance, Del Barrio (1998) did not include f_3, Sailor (2008) considered neither f_2 nor f_5 and Tabares-Velasco & Srebric (2012) did not include f_5.

Several expressions of each of these functions exist, with each one commonly formulated in controlled environments for a particular species determined by the statistical analysis of a wide range of measurements (Lhomme et al. 1998). Many are formulated for pine or rainforests which are not comparable to green roof ecosystems. For this reason,

Tabares-Velasco & Srebric (2012) evaluated various functions to find the most accurate for their green roof samples of *Delosperma nubigenum* and *Sedum spurium*. They found the following four function equations were most congruent with their measured data, with $f_5\ (CO_2)$ excluded from their comparisons.

$f_1(\varphi_s)$ represents the impact that variations in solar radiation (φ_s,W m^{-2}) , have on stomatal resistance. The irradiance at which maximum stomatal aperture is reached is difficult to quantify given this characteristic varies not only between species but also by radiation environment. For example, the stomata of shaded leaves will open at lower light levels than those of sun-adapted leaves, which could result in significant differences with higher LAI (Jones, 2013). It is generally expressed using an exponential or a hyperbolic function (Lhomme et al. 1998), with Tabares-Velasco & Srebric (2012) finding an exponential model from Avissar & Pielke (1991), developed using a tobacco plant, to provide the most accurate output when compared to measured evapotranspiration rates. Djedjig et al. (2012) also employed Eq. 2.20 in their green roof model.

$$f_1(\varphi_s) = 1 + exp^{-0.034(SW-3.5)} \tag{2.20}$$

SW = short-wave radiation (W m^{-2})

$f_2(T_f)$ characterizes the role that foliage temperature has on transpiration. Stomata generally open in response to increasing leaf temperature until an optimum temperature is reached, although a change in temperature will nearly always be accompanied by a change

in leaf-air VPD so the two functions are closely related (Campbell & Norman, 1998). The relationship between stomatal resistance and temperature can be modelled using an exponential or a power function. Tabares-Velasco & Srebric (2012) found a power function they adapted from Noilhan & Planton (1989) had the best fit with measured data. The value of 35 °C in Eq. 2.21 represents the optimum temperature for maximum stomatal aperture, although this value is species-specific and generally ranges from 20-35 °C but is typically around 30 °C (Willmer & Fricker, 1996).

$$f_2(T_f) = \frac{1}{1-0.0016(35-T_f)^2} \tag{2.21}$$

$f_3(VWC)$ represents the role that soil moisture has on stomatal resistance. Tabares-Velasco & Srebric (2011) found that substrate water content was the dominant factor determining evapotranspiration rates in their green roof study, although radiation was affected in their study by the limitations of their artificial light source. They adapted a previous model (Jacquemin & Noilhan, 1990) to incorporate measurements of *Delosperma nubigenum* and *Sedum spurium* under numerous environmental conditions (Eq. 2.22). Stomatal regulation is generally insensitive to water availability until plants have depleted a particular amount of plant-available soil water; 0.7 VWC_{fc}in Eq. 2.22. Below this value, an abrupt increase in stomatal resistance occurs as hydraulic conductivity decreases. Eventually, plant stomata close in response to water stress (Chapin et al. 2012).

$$f_3(VWC) = \begin{cases} 1 & VWC > 0.7\,VWC_{fc} \\ \frac{0.7\,VWC_{fc} - VWC_{wp}}{VWC - VWC_{wp}} & VWC_{wp} < VWC < 0.7\,VWC_{fc} \\ 1000 & VWC_{wp} > VWC \end{cases} \quad (2.22)$$

VWC_{fc}= VWC at field capacity
VWC_{wp}= VWC at wilting point

$f_4\ (VPD)$ represents the influence of VPD on stomatal resistance. In general, stomatal resistance increases with increasing VPD to avoid a decline in plant water potential (Saliendra et al. 1995). This relationship can be simulated using either a linear or logarithmic function (Jones, 1992). Tabares-Velasco & Srebric (2012) suggested a logarithmic function from Oren et al. (1999) and Ogle & Reynolds (2002) for desert plants as drought-tolerant species have been found to exhibit less strict regulation of water potential during higher VPD conditions (Oren et al. 1999).

$$f_4\ (VPD) = \frac{1}{1 - 0.41\ In\ (e_{s,plants} - e)} \quad (2.23)$$

Comparing the stomatal sub-functions in Eqs. 2.20 to 2.23, Tabares-Velasco & Srebric (2012) found $f_4\ (VPD)$ was the most sensitive to environmental changes as the vapour pressure differential depends on both air and leaf temperature as well as atmospheric humidity.

Stomata are also generally sensitive to the CO_2 mole fraction in intercellular spaces, with intercellular CO_2 concentration negatively correlated to stomatal aperture. Sensitivity

to ambient CO_2 concentrations is species and environment dependent, with C_4 species being most sensitive (Willmer & Fricker, 1996). However, it is not uncommon for the influence of CO_2 to be omitted from the Jarvis-Stewart stomatal resistance model given ambient CO_2 concentration varies little during diurnal periods when the available energy is greatest (Lhomme et al. 1998). However, Del Barrio (1998) included $f_5\ (CO_2)$ using an equation formulated by Stanghellini (1987) from tomato plant data.

$$f_5\,(CO_2) = 1 + 6.08 \times 10^{-7}(CO_2 - 200)^2 \tag{2.24}$$

Alexandri & Jones (2007) compared a multiplicative Jarvis-type model (Baldocchi et al. 1987; Wesely, 1989, Eq. 2.25) of stomatal resistance, originally developed to model the deposition of trace gases, and an additive model of variable resistances (Deardorff, 1978, Eq. 2.26) to porometer measurements of ET. The stomatal resistance values for the green roof sample of grass (species not specified) ranged between approximately 250-600 s m^{-1}.

$$r_s = r_{min}\left[1 + \left(\frac{200}{\varphi_s + 0.1}\right)^2\right]\frac{400}{T_{a.c}(313.15 - T_{a,c})}\frac{D_v}{D_q} \quad (2.25)$$

$$r_s = \frac{r_l}{0.5\ LAI}\left[\frac{\varphi_{s,max}}{0.03\ \varphi_{s,max} + \varphi_s} + P + \left(\frac{n_{wilt}}{n_{root}}\right)^2\right] \quad (2.26)$$

$T_{a.c}$ = air temperature at the foliage (ranges from 273.15-313.15 K, outside of which stomatal resistance is assumed infinite (Jacobson, 1999))
$\frac{D_v}{D_q}$ = the ratio of the molecular diffusion of water vapour to that of gas q ($mm^2\ s^{-1}$)
P = growing phase (function of the time of year, $P = 0$ during the growing season)
n_{wilt} = soil moisture value below which permanent wilting occurs
n_{root} = minimum value of soil moisture in the root zone

Alexandri & Jones (2007) found the additive model had better convergence with the measured data than the multiplicative approach. The additive equation provided estimates within the 10% error band of the porometer for both diurnal and nocturnal resistances. Conversely, the multiplicative equation underestimated diurnal resistances and nocturnal resistances became infinite as $I = 0$ which the authors suggested makes this approach problematic for modelling. While inclusion of the growing phase parameter may explain the better accuracy of Eq. 2.26, the multiplicative model does not include a function pertaining to water stress which likely affected its accuracy. Additionally, the validation study period of 5 days did not facilitate an extensive evaluation of either method. It is also important to note for models that use the wilting point (ex. Deardorff, 1978), due to their capacity to store water and minimize water loss, *Sedum* species have been found to survive months without rain (Snodgrass & Snodgrass, 2006). Jarrett et al. (2006) noted that this makes it difficult to define their permanent wilting point. Rana & Katerji (2000)

recommended using a multiplicative model approach for more accurate estimations of stomatal resistance.

The Jarvis-Stewart model and its variations have been criticized for their multiplicative approach. By multiplying concomitant effects any synergistic interactions between the environmental functions and the plant are not considered (Gerosa et al. 2012). Another concern that has been expressed is the exclusion of physiological influences on stomatal resistance. For instance, leaf age and morphology have been found to affect stomatal resistance (Field, 1987; Schulze et al. 1987). Stomatal resistance is also affected by other environmental factors not considered by the functions of the Jarvis-Stewart model, such as air pollutants which may be particularly relevant to green roof vegetation given urban areas tend to exhibit elevated concentrations of pollutants such as SO_2 and O_3 (Robinson et al. 1998; Mayer, 1999). While it is currently difficult to apply more mechanistic approaches to stomatal modelling due to limited physiological data for green roof species, considering functions like the growing phase, which was featured in the Deardorff (1978) model, in multiplicative models may ameliorate the performance of green roof models.

Besides representative stomatal resistance sub-models, the accuracy of the Penman-Monteith is also dependent on the minimum stomatal resistance value. For green roof studies, limited empirical investigations mean authors commonly use values obtained from the literature. For instance, some green roof models have assumed minimum stomatal

resistance varies from 50 to 300 s m^{-1} (Del Barrio, 1998; Sailor, 2008). However, Jones (1992) noted that for succulent plants, stomatal resistances vary from 450-1000 s m^{-1} and 225-1125 s m^{-1} for desert plants. Alexandri & Jones (2007) measured stomatal resistance values between 250-600 s m^{-1} for a green roof sample of grass. Furthermore, the stomatal behaviour of species and plant types on green roofs may not be comparable to their counterparts in natural environments given the restrictions commonly placed on plants by green roof ecosystems. A green roof study by Starry and colleagues (2014) found that stomatal resistance ranged from a minimum of 6.59 and 16.18 s m^{-1} for *Sedum album* and *Sedum kamtschaticum*, respectively, during well-watered conditions to more than 1000 s m^{-1} for both species during dry conditions. This considerable change in stomatal resistance presents a challenge to the models currently employed for green roof applications. It also highlights the need for empirical data for green roof species to determine minimum stomatal resistance values and the range of values expected in response to environmental perturbations.

Stomatal resistance models require an upscaling from single leaf stomatal resistance to the whole canopy bulk stomatal resistance. Given the available energy needed for evapotranspiration varies throughout a plant canopy, vertical heterogeneity should be accounted for in single source models. This was crudely accounted for in Alexandri & Jones (2007) by assuming that approximately half of the canopy is illuminated and actively contributing to heat and vapour transfer with Eq. 2.27 from Allen et al. (1998).

$$r_s = \frac{r_{si}}{LAI_{active}} \quad (2.27)$$

r_{si} = stomatal resistance of illuminated leaf (s m^{-1})
LAI_{active} = 0.5 LAI

Another approach for estimating evapotranspiration that has been used in green roof modelling (Lazzarin et al. 2005) is the crop coefficient model originally proposed by Jensen (1969). This model is most commonly used in agricultural applications to estimate the water use of squared kilometres of crop fields. The effect of climate on plant water requirements is represented by the reference maximum evapotranspiration (ET_0, kg m^{-2} s^{-1}) and the effect of the plant by the crop coefficient (K_c), which is the ratio of the measured ET and ET_0 (Hiscock & Bense, 2014), as shown in Eq. 2.28. The crop coefficient is therefore a scaling factor that distinguishes the plant from the reference vegetation.

$$ET = K_c ET_0 \quad (2.28)$$

The reference ET can be measured or estimated but it must be subjected to the same weather conditions as the plant whose evapotranspiration is being estimated. The approach used in Lazzarin and colleagues (2005) defines the ET_0 value from a hypothetical grass that is actively growing and well-watered which they estimated according to the Penman

combination equation (1956), shown in Eq. 2.29. This method assumes that evapotranspiration is a function of net radiation, saturation deficit and wind speed.

$$ET_0 = \frac{\Delta R_n + \gamma f(u)(e_{s,plants} - e)}{\Delta + \gamma} \quad (2.29)$$

Δ = slope of the saturation vapour pressure vs temperature function (kPa °C^{-1})
f(u) = wind function (W m^{-2} kPa)

The wind function is a linear regression adjustment intended to account for the differences in ET regulation between estimated and observed ET_0 for grass grown in the UK. It is therefore necessary to adapt the wind function to each site to correctly apply the Penman formula (Rana & Katerji, 2000). It has been modified several times with numerous linear relationships existing that vary according to geographical location and plant type (Jensen et al. 1990). Lazzarin et al. (2005) applied the following estimation for the wind function.

$$f(u) = 0.26\ (1 + 0.54u) \quad (2.30)$$

Validated using a green roof assembly planted with *Sedum*, the results of the simulation of Lazzarin and colleagues (2005) provided accurate predictions of measured ET rates in well-watered conditions but the estimations showed a weak correlation with measured data during water-stressed conditions. Their crop coefficient varied from as high

as 0.51 during periods without water stress to below zero during dry periods. A possible explanation for the inconsistent accuracy of this model was the use of the Penman model for the reference ET. Additionally, ET was only measured as the residual of the energy terms rather than a direct measurement. Using linear regressions like the wind function does not take into account the variability in canopy properties (Rana & Katerji, 2000).

Other green roof studies have obtained mixed levels of accuracy in ET estimations using variations of the Penman-Monteith (1965) equation to estimate *Sedum* reference ET for the crop coefficient method (DiGiovanni et al. 2012; Sherrard & Jacobs, 2011; Marasco et al. 2014). With the use of a constant crop coefficient value of 0.53 and a short study period that was late in the growing season, Sherrard & Jacobs (2012) noted the accuracy of their hydrological model would have likely suffered from an underestimated crop coefficient during the mid-summer period. Cumulatively, DiGiovanni and colleagues (2011) found the British Meteorological Office Rainfall and Evaporation Calculation System (NRCC) version of the Penman-Monteith equation overestimated ET by 15% while the ASCE Standardized Reference Evapotranspiration Equation (Allen et al. 2005) version of the Penman-Monteith model overestimated ET by 80%. Conversely, Marasaco et al. (2014) found the ASCE equation provided a more accurate estimation of chamber ET measurements than an energy balance model. Although the results of the ASCE approach were generally similar to the measured ET, they found it overestimated the lowest ET values during winter months and underestimated peak ET values during the summer

months. Nevertheless, the advantage of using reference ET and crop coefficients to estimate ET is that plant and local climate effects are considered separately and it provides a standardized method allowing values to be compared across sites. Sherrard & Jacobs (2012) recommended longer study periods to refine crop coefficients according to seasonal changes and also assess the effects of plant species, soil types and depths.

However, single source models treat the surface as a uniform layer. As such, scale is an important consideration when using single source evapotranspiration models. Combination equations, such as the Penman-Monteith model, are intended for closed canopies where advective effects, discussed in Section 2.2.5, can be neglected. These models are most suitable for canopies 1 km^2 or greater (Rose & Sharma, 1984) when near equilibrium conditions with constant one-dimensional transfer occur in a well-developed boundary layer (Dunin, 1991). For smaller canopies, such as green roofs, isolation exposure, i.e. increased wind and radiation loading, will likely minimize the effectiveness of these models (Rose & Sharma, 1984). Other relevant factors being equal, green roof canopies will likely exhibit different rates of evapotranspiration to agricultural crop communities typically used to develop evapotranspiration models. Additionally, green roof plants and substrates also differ from the agricultural crops and further work is therefore required to refine these models to more accurately reflect the processes occurring within green roof systems (Stovin et al. 2013). Models of evapotranspiration exist for isolated

stands that may be more suitable for green roofs and these will be discussed further in Section 2.2.5.

Given latent heat is the primary means of heat dissipation for green roofs in wet conditions (Lazzarin et al. 2005; Tabares-Velasco & Srebric, 2011), its accurate representation is paramount to the performance of energy models. As discussed, there are numerous approaches in the literature for calculating the latent heat flux, with each one requiring parameters that are species-specific. This poses a challenge to green roof modelling as it depends on a considerable quantity of empirical data in order for these models to be adequately versatile. While the aim of some studies has been to find the existing model that most accurately estimates green roof latent heat fluxes (Tabares-Velasco & Srebric, 2012), others have modified such models to better correlate with green roof empirical data (Tabares-Velasco & Srebric, 2011; Ouldboukhitine et al. 2012). However, green roofs may require further refinement of single source models or the application of more complex models in order to accurately and robustly calculate latent heat fluxes due to their unique conditions and plant species.

2.2.4 Energy storages – thermal and metabolic

While most of the incoming energy that reaches the plants' surfaces will be re-radiated back into atmosphere or dissipated through sensible and latent heat fluxes, some

of the energy will be stored within the vegetation layer. Of this stored energy, that which increases/decreases the internal heat energy (temperature) of the plants and within-canopy air is referred to as thermal energy storage whereas the energy involved in the physiological processes of the plants is referred to as metabolic energy storage.

The specific heat of foliage is fairly high for a solid material, with Jayalakshmy and Philip (2010) finding fresh leaves from various species ranging from 1287 to 2267 J kg^{-1} K^{-1} and 1514 and 5174 J kg^{-1} K^{-1} for dry leaves. However, little heat can be stored in the canopy layer of a green roof due to the limited air and biomass. This means temperature within the canopy can change relatively fast in response to cooling or heating mechanisms. Feng et al. (2010) used the following calculation of heat content in a solid of *Sedum lineare* on a green roof. They estimated that the thermal energy storage only accounted for 0.1% of the net radiation. This is a likely estimate given only large plant structures such as trunks can store considerable amounts of energy (Nobel, 2009). This model can also be used to quantify the storage of energy by the within-canopy air, which comprises majority of the canopy layer's volume but has a much lower energy density.

$$S_f = \rho_f Cplants \frac{\Delta T_f}{\Delta t} \tag{2.31}$$

ρ_f = areal density of foliage (kg m^{-3}) $Cplants$ = specific heat of plants (J kg^{-1} K^{-1})
Δt = time interval (s)

Feng and colleagues (2010) also estimated the metabolic storage of their green roof by means of the photosynthetic rate. Photosynthesis is the process by which plants convert radiative energy into chemical energy for growth, reproduction and maintenance. Although metabolic storage is only estimated to account for approximately 1-2% of the net radiation in vegetated environments (Gates, 1980), Feng and colleagues (2010) estimated that the net photosynthesis of the *Sedum lineare* accounted for 9.5% of the net radiation. Although a large mass of active vegetation in low light could have a metabolic storage accounting for ~5% of the net radiation (Hillel, 1998), these circumstances are not applicable to an extensive green roof. Feng and colleagues (2010) did not verify this estimate with empirical data and they likely overestimated its contribution due to erroneous parameterizations of minimalistic equations that considered solar radiation as the sole factor determining net photosynthesis rates. This approach ignored the complex interaction of plant and other environmental variables that affect net photosynthesis such as soil moisture content, leaf age and morphology and ambient CO_2 concentrations (Mohr & Schopfer, 1995). In contrast, Starry and colleagues (2014) measured relatively low net photosynthetic rates of *Sedum album* and *Sedum kamtschaticum* on green roofs even during periods of high soil volumetric water content (VWC). Nevertheless, it is recommended that future studies examine net photosynthesis within the context of the energy balance to assess the findings of Feng et al. (2010).

Regarding the relationship between the thermal and metabolic storages, the harsh environment green roofs often present for plants limits their net storage of energy. Stresses that commonly occur on green roofs, such as water stress due to shallow substrates, elevated temperatures and high radiative heat flux intensities, soil nutrient deficiencies and desiccation and physical damage due to high wind speeds (Dunnett and Kingsbury, 2004), mean green roofs are suboptimal environments for plants. These stresses, either singularly or collectively, will result in lower photosynthetic rates compared to non-stressed counterparts (Chapin, 1991). Lower rates of photosynthesis lead to lower growth rates, and therefore less thermal mass, as less energy is apportioned to producing biomass. Additionally, any damage suffered due to the aforementioned stresses, such as photodamage to the photosynthetic apparatus resulting from excessive radiative heat exposure, requires a greater allocation of photosynthetic products to the maintenance of plant tissue rather than contributing to the growth of the plant. Therefore, the harsh environment of green roofs ultimately limits both the thermal and metabolic energy storage of the vegetation layer by reducing growth.

As green roofs are commonly planted with succulents which have relatively high water content for plants, the canopy layer is likely to have a high thermal storage per unit mass for a vegetated system. However, succulents are also likely to have a comparatively lower metabolic storage compared to most plant types and coupled with the minimal mass of the low stature vegetation on green roofs, the combined storage of energy by the plants

on a green roof likely comprises only a small portion of the net radiation. Nevertheless, further quantification of the thermal and metabolic storage on green roofs will provide energy balance closure (ie. Eq. 2.1 equals zero) which is particularly important given sensible heat convection is commonly quantified as the residual.

2.2.5 Advection heat flux

The assumption of a closed system with solar radiation as the system's only external energy input means the one-dimensional approach commonly used in green roof modelling ignores the energy exchanged by advection. Horizontal transfer of energy, for instance, can represent a significant net gain or loss for the canopy system, with advection potentially causing local turbulent fluxes to vary considerably on a green roof. Advection stems from air flow over changing surfaces; variations in surface roughness, such as between a green roof and surrounding concrete. This causes a change in surface momentum flux which affects the wind field as well as changes in the surface availability of scalars, including heat and moisture (Kaimal & Finnigan, 1994).

Previous research has found that the local and micro-advection of warmer, drier air from upstream built-up areas can enhance the evapotranspiration flux from urban vegetation. This effect arises from increased sensible heat and surface-to-air humidity gradient, ultimately leading to an increase in the latent heat flux and a decrease in the

sensible heat flux if the radiative energy remains constant (Kaimal & Finnigan, 1994). With the presence of advection, the latent heat flux can even exceed the net radiation due to the additional energy for evapotranspiration supplied by the sensible heat flux (Oke, 1979).

Referred to as the ‘clothesline effect’, this phenomenon occurs in small isolated vegetation areas or along the upwind edge of a vegetation canopy that is surrounded by a surface of lower roughness, such as concrete. The air above the surface surrounding a green roof is likely to be higher in sensible heat compared to the air above a green roof, which is higher in latent heat because there is more water available at the surface. Evapotranspiration from the green roof will be enhanced when wind transports the drier, warmer urban air over a green roof. Importantly for advective enhancement in green roof systems is the often lack of obstacles to radiation and wind surrounding a green roof.

Spronken-Smith and colleagues (2000) found the evapotranspiration from an irrigated suburban park was greatest at its upwind edge with an exponential decline in rates over a fetch of approximately 20 m; the leading-edge or fetch effect. The total evapotranspiration from the park was over 3 times greater than that of the surrounding suburban area and 1.3 times greater than an irrigated rural grass site. This effect was caused by the advection of sensible heat towards the park as the neighbouring dry paved area was consistently 1-2 °C higher. Additionally, this advected air was drier given the lower water availability over the paved surface which increased the humidity driving force for evapotranspiration over the park. The magnitude of this observed clothesline effect varies

depending on the height of the vegetation. For a 100 m^2 area, grass will have an evapotranspiration rate approximately 10% higher than the reference evapotranspiration rate while trees will have an evapotranspiration rate around 30% greater than the reference evapotranspiration (Doorenbos and Pruitt, 1984). Estimations of the horizontal extent of the clothesline effect have varied from less than 20 m at a grass site (Rider et al. 1967) to over 200 m at a cotton site (Rijks, 1971).

Even at fetch distances sufficiently large enough for edge effects to be negligible, evapotranspiration can still be enhanced compared to the potential rate; the 'oasis effect'. In this instance, the enhancement of evapotranspiration is the result of warmer urban air subsiding over the cooler park due to mass divergence. This additional downward flux of sensible heat further enhances evaporation. While the oasis effect has been estimated to occur at a minimum area of approximately 1000 m^2 for an irrigated grassed area (Doorenbos and Pruitt, 1984), micro-oasis effects can occur over much smaller areas (Jones, 2014).

While many green roofs may not be sufficiently large enough for a significant oasis effect to occur, advection by means of the clothesline effect will likely result in significant differences (heterogeneity) in the latent heat flux. As evidence of this on a micro-scale, Hagishima et al. (2007) measured the evapotranspiration from homogenous potted *Camellia* plants on a concrete slab arranged in three different horizontal densities. Within the densest canopy, composed of 169 plants separated by 0.5 m, the evapotranspiration rate

for plants on the leading edge was around 1.3 times the evapotranspiration rate of the plants located in the centre of the canopy. Furthermore, their results suggested the importance of horizontal biomass density on latent heat flux, with the evapotranspiration rate of the low density canopy being 1.5 times greater than that of the high density canopy. As a result of landscaping choices, varying canopy densities may exist on a green roof, further increasing the horizontal heterogeneity of the latent heat flux. Hagishima and colleagues recommended the parameterization of surface water availability in evapotranspiration models for urban vegetation.

Additionally, the effects of advection on the latent heat flux may cause additional stress to green roof plants, thereby further modifying the surface energy balance. Using the Soil Water Atmosphere and Plant (SWAP) model to simulate the water balance of a green roof, Metselaar (2012) accounted for a possible clothesline effect by increasing the reference evapotranspiration rate by 25%. Results showed that the possible advective enhancement of evapotranspiration could lower the median pressure head and increase drought stress, particularly for mineral substrates. Metselaar noted that even for identical green roof designs, the location of a rooftop can have a profound effect on the evapotranspiration as each roof has distinctive conditions.

Limited empirical knowledge of advection in urban environments stems from the considerable effort involved in making field measurements. These measurements require the deployment of multiple flux towers involving the duplication of expensive equipment.

As such, micrometeorological studies have tended to quantify advection by mathematical simulations rather than experiments (Kaimal & Finnigan, 1994). A considerable limitation for the development of these analytical models of wind fields though is the lack of empirical data against which to compare them (Finnigan, 2005). Urban research has tended to ignore local- and micro-scale heat and moisture advection based on the theoretical assumption of its negligibility due to horizontal homogeneity (Lietzke et al. 2015). From an energy modelling perspective, assuming the effect of advection on the energy balance is negligible avoids an uncertain and complex task but is likely to result in erroneous predictions.

In order to approximate the flux divergence resulting from advection, a method from Alfieri et al. (2012) adapted from Prueger et al. (1996) is shown in Eq. 2.32. In this advection-diffusion model, the evapotranspiration resulting from the contribution of advection (ET_{adv}, kg m^{-2} s^{-1}) is estimated using the depletion of sensible heat content in the air above the green roof.

$$-ET_{adv} = \Delta H = H_s - H_m = \rho C_{p,a} \int_{z_0}^{z_{mh}} u(z) \frac{\partial T_a(z)}{\partial x} \partial z \quad (2.32)$$

ΔH = flux divergence of H (W m^{-2})
H_s = H at surface (W m^{-2})
H_m = H at measurement height z (W m^{-2})
z_{mh} = measurement height (m)
z_0 = roughness length (m)
z = height above surface (m)
x= downwind distance from edge (m)

Aside from using partial differential equations to approximate advective enhancement of the latent heat flux, empirical methods, such as the lysimetry study of

Hagishima et al. (2007), could provide further insight into the effects of advection on green roofs. With measurements under multiple wind conditions, these empirical methods could lead to more accurate enhancement factors than the rough estimation used by Metselaar (2012) for use in green roof energy balance modelling.

Given the significant advective fluxes observed in empirical studies, its neglect will likely limit the accuracy of green roof energy balance models. As wind velocities are generally high on rooftops as a result of the high surface roughness of urban areas and vertical wind shear, the transport of heat and moisture by bulk fluid motion is likely to be non-negligible. While models of evapotranspiration enhancement by advection will likely alleviate current oversights, further research is required to improve these methods for green roof systems. The fact that buildings modify airflow so that it does not behave as if it was over a flat open surface requires addressing as it may greatly affect the energy balance of green roofs.

2.3 Discussion of green roof energy modelling approaches

As shown in this review, green roof models rely on several assumptions regarding the partitioning of energy above and within the plant canopy. Unlike multilayer modelling which can use direct leaf-scale measurements, the big-leaf models used for modelling the vegetation layer require canopy-scale parameters that cannot be measured directly. This is

because the microclimate variables that drive fluxes of heat and mass occur as gradients within the canopy. These gradients lead to differences in the temperature, vapour pressures and latent and sensible heat fluxes between individual leaves. These differences are the result of varied leaf inclinations, orientations and shading within the canopy (Avissar, 1993). Assuming the canopy fluxes are linearly coupled to the average of these environmental drivers, big-leaf models use mean values to represent these gradients. This assumption introduces the risk of non-linear averaging errors occurring due to the possibility of a heterogeneous distribution of a driving variable and a non-linear response to that driver (Monson & Baldocchi, 2014). These non-linear averaging errors are a common reason for the overestimation of ET by big-leaf models (Landsberg & Sands, 2011).

Given the low stature of extensive green roof plants, particularly *Sedum*, the limited within-canopy profiles of microclimate parameters means they are unlikely to have an expansive range of values that would benefit from the use of a multilayer model. A simpler and more suitable approach for such canopies may be two-leaf single source models that differentiate between sunlit and shaded leaves (Wang & Leuning, 1998; Dai et al. 2004). Although requiring more parameters than big-leaf models, two-leaf modelling provides a better representation of the within-canopy microclimate and the response to these drivers. The results of Dai and colleagues (2004) showed their two-leaf model performed better than a similar big-leaf model. Leuning et al. (1998) found their two-leaf model (Wang &

Leuning, 1998) provided simulations that were fairly congruent with a data-intensive multilayer model (Leuning et al. 1995). Overestimations of latent heat fluxes and underestimations of sensible heat fluxes were typically <5%. However, further refinements regarding the calculation of canopy photosynthesis by Wang (2000) to the Wang & Leuning model (1998) reduced discrepancies between the two-leaf model and the multi-layered model (Leuning et al. 1995) to <3%. Incorporating two-leaf rather than big-leaf modelling approaches into green roof models may therefore provide more accurate and robust predictions by better representing the within-canopy profile.

Coupled dual source models may also provide robust simulations of the vegetation and substrate layers. As mentioned in Section 2.1.1, small-scale heterogeneity is more suitably represented in a coupled model (Lhomme & Chehbouni, 1999) which may be more realistic for green roofs, especially those with multiple plant species and/or those without total vegetation cover. Single source models are generally derived for horizontally homogenous vegetation, possibly limiting their suitability for green roofs. The interaction of fluxes between the vegetation and substrate may be more suitable for extensive green roofs given the low stature of the plants increasing the impact of fluxes between the plants and the substrate.

Aside from the number of layers included in green roof models, another concern regarding existing green roof models is their nominal and deterministic treatment of parameter values. Sensitivity analyses have highlighted the significant impact that

parametrization of plant properties such as LAI and albedo can have on the energy performance of green roofs. However, due to the variation in vegetation properties both spatially and temporally and the unavoidable deviation from designated parameter values during and after the construction of green roofs means these values will change. Due to this inherent deviation, Liu (2014) noted that the energy performance of green roofs cannot be predicted deterministically but rather probabilistically. Consequently, Liu undertook a parametric uncertainty analysis to examine the range of building energy prediction outcomes using EnergyPlus software. This involved treating the values of the most significant green roof parameters as random variables with prescribed probability distributions. Simulation results showed that uncertainty at the parameter level can result in significant variations at the building energy level. The dispersion of energy saving values was almost linearly proportional to key green roof parameters over a relatively large range. For a reliable assessment of the long-term cost-effectiveness of a green roof installation, nominal parametric values will therefore likely limit the accuracy of these assessments regarding building energy savings. However, future research needs to acquire information regarding the probabilistic distribution of key parameters as currently the confidence level of achieving target energy savings is ultimately unknown, undermining the quality of green roof life cycle assessments.

2.4 Conclusion

Numerous studies have attempted to model the energy balance of green roofs. Given the overwhelming complexity of the heat storages and fluxes within the vegetation layer, these researchers have adopted various assumptions in order to provide estimates of the green roof systems' thermal performance. However, given the limited number of empirical studies concerning the energy fluxes and storages within green roof systems, these assumptions are based on information taken from ground environments that may not be easily transferred to vegetation on rooftops. Green roof vegetation may differ greatly from that of the vegetation at ground level given differences in physiology and advection that may affect each component of the energy balance.

Therefore, the use of single source models, which use averaged values either based on the limited number of green roof studies or from ground-level measurements from the literature, may be oversimplifying heat transfers in the vegetation layer. Comparisons with more complex modelling approaches, such as two-leaf models, is required to determine whether or not more accurate representations of green roof vegetation yield more precise estimates of green roofs' thermal performance. Additionally, there is a considerable amount of diversity amongst plant species regarding growth, phenology, physiology and optical properties. For the validation and application of these numerical models, further research

concerning the diversity of these properties is needed in order for these models to be purposeful.

However, as explained during this review, the vegetation layer and thermal performance of a green roof is greatly affected by the rooftop's climate. Empirical green roof studies have had the limitation thus far of only representing a single climate. Each numerical model's validation study has involved monitoring only one green roof. This may have limited the climate regions to which the minimal number of green roof models that have been developed are appropriate. The study featured in the following chapter therefore will provide important information for the validation of these models and provide an unprecedented level of insight into the relationship between the thermal performance of green roofs and climate.

References

Alexandri, E., & Jones, P. (2007). Developing a one-dimensional heat and mass transfer algorithm for describing the effect of green roofs on the built environment: Comparison with experimental results. *Building and Environment*, *42*(8), 2835-2849.

Alfieri, J.G., Kustas, W.P., Prueger, J.H., Hipps, L.E., Evett, S.R., Basara, J.B., Neale, C.M.U., French, A.N., Colaizzi, P., Agam, N., Cosh, M.H., Chavez, J.L., & Howell, T.A. (2012). On the discrepancy between eddy covariance and lysimetry-based surface flux measurements under strongly advective conditions. *Advances in Water Resources*, *50*, 62-78.

Allen, R.G., Pereira, L.S., Raes, D., & Smith, M. (1998). Crop evapotranspiration – Guidelines for computing crop water requirements. *FAO irrigation and drainage paper 56*. Rome: FAO.

Allen, R.G., Walter, I.A., Elliot, R., Howell, T., Itenfisu, D., & Jensen, M. (2005). *The ASCE standardized reference evapotranspiration equation*. Reston: ASCE-EWRI.

Arya, S.P. (2001). *Introduction to micrometeorology* (2nd ed.). San Diego: Academic Press.

Avissar, R. (1993). Observations of leaf stomatal conductance at the canopy scale: An atmospheric modeling perspective. *Boundary-Layer Meteorology*, *64*(1-2), 127-148.

Avissar, R., Avissar, P., Mahrer, Y., & Bravdo, B.A. (1985). A model to simulate response of plant stomata to environmental conditions. *Agricultural and Forest Meteorology*, *34*(1), 21-29.

Avissar, R., & Pielke, R.A. (1991). The impact of plant stomatal control on mesoscale atmospheric circulations. *Agricultural and Forest Meteorology*, *54*(2), 353-372.

Ayata, T., Tabares-Velasco, P.C., & Srebric, J. (2011). An investigation of sensible heat fluxes at a green roof in a laboratory setup. *Building and Environment*, *46*(9), 1851-1861.

Baldocchi, D.D., Hicks, B.B., & Camara, P. (1987). A canopy stomatal resistance model for gaseous deposition to vegetated surfaces. *Atmospheric Environment*, *21*(1), 91-101.

Bates, A.J., Sadler, J.P., & Mackay, R. (2013). Vegetation development over four years on two green roofs in the UK. *Urban Forestry & Urban Greening*, *12*(1), 98-108.

Bergman, T.L., Lavine, A.S, Incropera, F.P., & DeWitt, D.P. (2011). *Fundamentals of heat and mass transfer* (7th ed). Hoboken: John Wiley & Sons.

Blank, L., Vasl, A., Levy, S., Grant, G., Kadas, G., Dafni, A., & Blaustein, L. (2013). Directions in green roof research: A bibliometric study. *Building and Environment*, *66*, 23-28.

Blyth, E.M., & Harding, R.J. (1995). Application of aggregation models to surface heat flux from the Sahelian tiger bush. *Agricultural and Forest Meteorology*, *72*, 213-235.

Brutsaert, W.H. (1982). *Evaporation into the atmosphere*. Dordrecht: D. Reidel Publishing.

Campbell, G.S. (1986). Extinction coefficients for radiation in plant canopies calculated using an ellipsoidal inclination angle distribution. *Agricultural and Forest Meteorology*, *36*(4), 317-321.

Campbell, G.S., & Norman, J.M. (1998). *An introduction to environmental biophysics* (2nd ed.). New York: Springer.

Cappelli, M., Cianfrini, C., & Corcicone, M. (1998). Effects of vegetation roof on indoor temperatures. *Heat Environment*, *16*(2), 85-90.

Carter, G.A. (1993). Responses of leaf spectral reflectance to plant stress. *American Journal of Botany*, *80*(3), 239-243.

Carter, G.A. (1994). Ratios of leaf reflectances in narrow wavebands as indicators of plant stress. *International Journal of Remote Sensing*, *15*(3), 697-703.

Carter, G.A., & Knapp, A.K. (2001). Leaf optical properties in higher plants: linking spectral characteristics to stress and chlorophyll concentration. *American Journal of Botany*, *88*(4), 677-684.

Castleton, H. F., Stovin, V., Beck, S. B. M., & Davison, J. B. (2010). Green roofs: Building energy savings and the potential for retrofit. *Energy and Buildings*, *42*(10), 1582-1591.

Chapin, F.S., III (1991). Integrated responses of plants to stress. *BioScience*, 29-36.

Chapin, F.S., III, Matson, P.A., & Vitousek, P. (2012). *Principles of terrestrial ecosystem ecology* (2nd ed.). New York: Springer.

Chehbouni, A., Kerr, Y.H., Watts, C., Hartogensis, O., Goodrich, D., Scott, R., Schieldge, J., Lee, K., Shuttleworth, W.J., Dedieu, G., & De Bruin, H.A.R. (1999). Estimation of area-average sensible heat flux using a large-aperture scintillometer during the Semi-Arid Land-Surface-Atmosphere (SALSA) Experiment. *Water Resources Research*, *35*(8), 2505-2511.

Chen, J.M., Ibbetson, A., & Milford, J.R. (1988). Boundary-layer resistances of artificial leaves in turbulent air: I. Leaves parallel to the mean flow. *Boundary-Layer Meteorology*, *45*(1-2), 137-156.

Clear, R.D., Gartland, L., & Winkelmann, F.C. (2003). An empirical correlation for the outside convective air-film coefficient for horizontal roofs. *Energy and Buildings*, *35*(8), 797-811.

Dai, Y., Dickinson, R.E., & Wang, Y.P. (2004). A two-big-leaf model for canopy temperature, photosynthesis, and stomatal conductance. *Journal of Climate*, *17*(12), 2281-2299.

Deardorff, J.W. (1978). Efficient prediction of ground surface temperature and moisture, with inclusion of a layer of vegetation. *Journal of Geophysical Research*, *83*(C4), 1889-1903.

Defraeye, T., Verboven, P., Ho, Q.T., & Nicolai, B. (2013). Convective heat and mass exchange predictions at leaf surfaces: Applications, methods and perspectives. *Computers and Electronics in Agriculture*, *96*, 180-201.

Del Barrio, E.P. (1998). Analysis of the green roofs cooling potential in buildings. *Energy and Buildings*, *27*(2), 179-193.

DiGiovanni, K., Montalto, F., Gaffin, S., & Rosenzweig, C. (2012). Applicability of classical predictive equations for the estimation of evapotranspiration from urban green spaces: Green roof results. *Journal of Hydrologic Engineering*, *18*(1), 99-107.

Djedjig, R., Ouldboukhitine, S.E., Belarbi, R., & Bozonnet, E. (2012). Development and validation of a coupled heat and mass transfer model for green roofs. *International Communications in Heat and Mass Transfer*, *39*(6), 752-761.

Doorenbos, I., & Pruitt, W.O. (1984). Crop water requirements. *Irrigation and Drainage Paper No. 24*. Rome: FAO.

Dunin, F.X. (1991). Extrapolation of 'point' measurements of evaporation: Some issues of scale. *Vegetatio, 91*(1-2), 39-47.

Dunnett, N., & Kingsbury, N. (2004). *Planting green roofs and living walls*. Portland: Timber Press.

Feng, C., Meng, Q., & Zhang, Y. (2010). Theoretical and experimental analysis of the energy balance of extensive green roofs. *Energy and Buildings*, *42*(6), 959-965.

Field, C. (1987). Leaf-age effects on stomatal conductance. In E. Zeiger, G.D. Farquhar & I.R. Cowan (ed.), *Stomatal function* (pp. 367-84). Stanford: Stanford University Press.

Finnigan, J. (2005). Advection and modeling. In X. Lee, W.J. Massman & B. Law (eds.), *Handbook of micrometeorology: A guide for surface flux measurement and analysis* (pp. 209–244). Dordrecht: Kluwer Academic Publishers.

Fourty, T., Baret, F., Jacquemoud, S., Schmuck, G., & Verdebout, J. (1996). Leaf optical properties with explicit description of its biochemical composition: Direct and inverse problems. *Remote Sensing of Environment*, *56*(2), 104-117.

Frankenstein, S., & Koenig, G. (2004). *FASST Vegetation Models* (TR-04-25). Hanover: U.S. Army Engineer Research and Development Center.

Gaffin, S.R., Khanbilvardi, R., & Rosenzweig, C. (2009). Development of a green roof environmental monitoring and meteorological network in New York City. *Sensors*, *9*(4), 2647-2660.

Garratt, J.R. (1992). *The atmospheric boundary layer*. Cambridge: Cambridge University Press.

Gates, D.M. (1980). *Biophysical ecology*. New York: Springer-Verlag.

Gates, D.M., Keegan, H.J., Schleter, J.C., & Weidner, V.R. (1965). Spectral properties of plants. *Applied Optics*, *4*(1), 11-20.

Gausman, H.W. (1977). Reflectance of leaf components. *Remote Sensing of Environment*, *6*(1), 1-9.

Gausman, H.W., & Allen, W.A. (1973). Optical parameters of leaves of 30 plant species. *Plant Physiology*, *52*(1), 57-62.

Gerosa, G., Mereu, S., Finco, A., Marzuoli, R., & Cuore, S. (2012). Stomatal conductance modeling to estimate the evapotranspiration of natural and agricultural ecosystems. In A. Irmak (ed.), *Evapotranspiration – remote sensing and modeling* (pp. 403-420). Rijeka: InTech.

Ghiaasiaan, S.M. (2011). *Convective heat and mass transfer*. New York: Cambridge University Press.

Hagishima, A., Narita, K.I., & Tanimoto, J. (2007). Field experiment on transpiration From isolated urban plants. *Hydrological Processes*, *21*(9), 1217-1222.

Hall, A.E., Schulze, E.D., & Lange, O.L. (1976). Current perspectives of steady-state stomatal responses to environment. In O.L Lange, L. Kappen & E.D. Schulze (ed.), *Water and plant life* (pp. 169-188). Berlin: Springer-Verlag.

Hanan, J.J. (1997). *Greenhouses: Advanced technology for protected horticulture*. Boca Raton: CRC Press.

He, H., & Jim, C.Y. (2010). Simulation of thermodynamic transmission in green roof ecosystem. *Ecological Modelling*, *221*(24), 2949-2958.

Hillel, D. (1998). *Environmental soil physics: Fundamentals, applications, and environmental considerations*. San Diego: Academic Press.

Hiscock, K., & Bense, V. (2014). *Hydrogeology: Principles and practice* (2nd ed). Chichester: John Wiley & Sons.

Hungate, B.A., & Koch, G.W. (2014). 'Biospheric impacts and feedbacks'. In G.R. North, J.A. Pyle, & F. Zhang (ed.), *Encyclopedia of atmospheric sciences, volumes 1-6* (2nd ed., pp.132-140). London: Academic Press.

Huo, Q., Cai, X., Kang, L., Zhang, H., & Song, Y. (2015). Effects of surface source/sink distributions on the flux–gradient similarity in the unstable surface layer. *Theoretical and Applied Climatology*, *119*(1-2), 313-322.

Jacobson, M.Z. (1999). *Fundamentals of atmospheric modeling*. Cambridge: Cambridge University Press.

Jacquemin, B., & Noilhan, J. (1990). Sensitivity study and validation of a land surface parameterization using the HAPEX-MOBILHY data set. *Boundary-Layer Meteorology*, *52*(1-2), 93-134.

Jarrett, A.R., Hunt, W.F., & Berghage, R.D. (2006, July). *Annual and individual-storm green roof stormwater response models*. Presented at the SABE Annual International Meeting, Portland.

Jarvis, P.G. (1976). The interpretation of the variations in leaf water potential and stomatal conductance found in canopies in the field. *Philosophical Transactions of the Royal Society of London. B, Biological Sciences*, *273*(927), 593-610.

Jarvis, P.G., & Morison J.I.L. (1981). The control of transpiration and photosynthesis by stomata. In P.G. Jarvis & T.A. Mansfield (eds.), *Stomatal physiology*. Cambridge: Cambridge University Press.

Jayalakshmy, M.S., & Philip, J. (2010). Thermophysical properties of plant leaves and their influence on the environment temperature. *International Journal of Thermophysics*, *31*(11-12), 2295-2304.

Jensen, M.E. (1969). Scheduling irrigation with computers. *Journal of Soil and Water Conservation*, *24*(5), 193-195.

Jensen, M.E., Burman, R.D., & Allen, R.G. (1990). Evapotranspiration and irrigation water requirements. *Manual No. 70*. Reston: American Society of Civil Engineers.

Jim, C.Y., & Tsang, S.W. (2011). Ecological energetics of tropical intensive green roof. *Energy and Buildings*, *43*(10), 2696-2704.

Jones, J.A.A. (2014). *Global hydrology: Processes, resources and environmental management*. New York: Routledge.

Jones, H.G. (1983). *Plants and microclimate: A quantitative approach to environmental plant physiology*. Cambridge: Cambridge University Press.

Jones, H.G. (1992). *Plants and microclimate: A quantitative approach to environmental plant physiology* (2nd ed.). Cambridge: Cambridge University Press.

Jones, H.G. (2013). *Plants and microclimate: A quantitative approach to environmental plant physiology* (3rd ed.). Cambridge: Cambridge University Press.

Jones, H.G., & Vaughan, R.A. (2010). *Remote sensing of vegetation: Principles, techniques, and applications*. Oxford: Oxford University Press.

Kaimal, J.C., & Finnigan, J.J. (1994). *Atmospheric boundary layer flows: Their structure and measurement*. New York: Oxford University Press.

Kirkham, M.B. (2014). *Principles of soil and plant water relations* (2nd ed.). Amsterdam: Academic Press.

Knipling, E.B. (1970). Physical and physiological basis for the reflectance of visible and near-infrared radiation from vegetation. *Remote Sensing of Environment, 1*(3), 155-159.

Kumar, R., & Kaushik, S.C. (2005). Performance evaluation of green roof and shading for thermal protection of buildings. *Building and Environment, 40*(11), 1505-1511.

Lagouarde, J.-P., McAneney, K.J., & Green, E.F. (1996). Scintillometer measurements of sensible heat flux over heterogeneous surfaces. In J.B. Stewart, E.T. Engman, R.A. Feddes, & Y. Kerr (ed.), *Scaling up in hydrology using remote sensing* (pp. 147–160). Chichester: Wiley.

Lambers, H., Chapin III, F.S., & Pons, T.L. (2008). *Plant physiological ecology* (2nd ed.). New York: Springer.

Landsberg, J.J., & Sands, P. (2011). *Physiological ecology of forest production: Principles, processes and models*. Amsterdam: Academic Press.

Lazzarin, R.M., Castellotti, F., & Busato, F. (2005). Experimental measurements and numerical modelling of a green roof. *Energy and Buildings, 37*(12), 1260-1267.

Leuning, R. (1995). A critical appraisal of a combined stomatal-photosynthesis model for C_3 plants. *Plant, Cell & Environment, 18*(4), 339-355.

Leuning, R., Dunin, F.X., & Wang, Y.P. (1998). A two-leaf model for canopy conductance, photosynthesis and partitioning of available energy II: Comparison with measurements. *Agricultural and Forest Meteorology, 91*(1), 113-125.

Leuning, R., Kelliher, F.M., de Pury, D.G.G., & Schulze, E.D. (1995). Leaf nitrogen, photosynthesis, conductance and transpiration: Scaling from leaves to canopies. *Plant, Cell & Environment, 18*(10), 1183-1200.

Lhomme, J.P., & Chehbouni, A. (1999). Comments on dual-source vegetation–atmosphere transfer models. *Agricultural and Forest Meteorology, 94*(3), 269-273.

Lhomme, J.P., Elguero, E., Chehbouni, A., & Boulet, G. (1998). Stomatal control of transpiration: Examination of Monteith's formulation of canopy resistance. *Water Resources Research, 34*(9), 2301-2308.

Lhomme, J.P., Monteny, B., & Amadou, M. (1994). Estimating sensible heat flux from radiometric temperature over sparse millet. *Agricultural and Forest Meteorology, 68*(1), 77-91.

Lietzke, B., Vogt, R., Young, D.T., & Grimmond, C.S.B. (2014). Physical fluxes in the urban environment. In N. Chrysoulakis, E.A. de Castro & E.J. Moors (eds.), *Understanding urban metabolism: A tool for urban planning* (pp. 29-44). New York: Routledge.

Liu, M.M. (2014). Probabilistic prediction of green roof energy performance under parameter uncertainty. *Energy, 77,* 667-674.

Mansfield, T.A. (1973). The role of stomata in determining the responses of plants to air pollutants. *Current Advances in Plant Science, 2*, 11-20.

Marasco, D.E., Hunter, B.N., Culligan, P.J., Gaffin, S.R., & McGillis, W.R. (2014). Quantifying evapotranspiration from urban green roofs: A comparison of chamber measurements with commonly used predictive methods. *Environmental Science & Technology*, *48*(17), 10273-10281.

Mayer, H. (1999). Air pollution in cities. *Atmospheric Environment*, *33*(24), 4029-4037.

McAdams, W.H. (1954). *Heat transmission* (3rd ed). New York: McGraw-Hill.

Metselaar, K. (2012). Water retention and evapotranspiration of green roofs and possible natural vegetation types. *Resources, Conservation and Recycling*, *64*, 49-55.

Moene, A.F., & van Dam, J.C. (2014). *Transport in the atmosphere-vegetation-soil continuum*. New York: Cambridge University Press.

Mohr, H., & Schopfer, P. (1995). *Plant physiology*. Berlin: Springer-Verlag.

Monin, A.S., & Obukhov, A. (1954). Basic laws of turbulent mixing in the surface layer of the atmosphere. *Trudy Geofizicheskogo Instituta, Akademiya Nauk SSSR*, 163-187.

Monson, R., & Baldocchi, D. (2014). *Terrestrial biosphere-atmosphere fluxes*. Cambridge: Cambridge University Press.

Monteith, J.L. (1965). Evaporation and environment. *Symposia of the Society for Experimental Biology*, *19*, 205-234.

Monteith, J.L., & Unsworth, M.H. (1990). *Principles of environmental physics* (2nd ed.). London: Edward and Arnold.

Monteith, J.L., & Unsworth, M.H. (2007). *Principles of environmental physics* (3rd ed.). London: Academic Press.

Monterusso, M.A., Rowe, D.B., & Rugh, C.L. (2005). Establishment and persistence of Sedum spp. and native taxa for green roof applications. *HortScience*, *40*(2), 391-396.

Morau, D., Tiana, R.H., & Ludovic, A.A. (2012). Simple model for the theoretical survey of the green roof thermal behavior. *Journal of Technology Innovations in Renewable Energy*, *1*(2), 92-102.

Mori, I.C., Utsugi, S., Tanakamaru, S., Tani, A., Enomoto, T., & Katsuhara, M. (2009). Biomarkers of green roof vegetation: Anthocyanin and chlorophyll as stress marker pigments for plant stresses of roof environments. *Journal of Environmental Engineering and Management*, *19*(1), 21-27.

Nagase, A., & Dunnett, N. (2010). Drought tolerance in different vegetation types for extensive green roofs: Effects of watering and diversity. *Landscape and Urban Planning*, *97*(4), 318-327.

Nayak, J.K., Srivastava, A., Singh, U., & Sodha, M.S. (1982). The relative performance of different approaches to the passive cooling of roofs. *Building and Environment*, *17*(2), 145-161.

Niachou, A., Papakonstantinou, K., Santamouris, M., Tsangrassoulis, A., & Mihalakakou, G. (2001). Analysis of the green roof thermal properties and investigation of its energy performance. *Energy and Buildings*, *33*(7), 719-729.

Nobel, P.S. (1983). *Biophysical plant physiology and ecology*. San Francisco: W.H. Freeman and Company.

Nobel, P.S. (2009). *Physicochemical and environmental plant physiology* (4th ed.). San Diego: Academic Press.

Noilhan, J., & Planton, S. (1989). A simple parameterization of land surface processes for meteorological models. *Monthly Weather Review*, *117*(3), 536-549.

Ogle, K., & Reynolds, J.F. (2002). Desert dogma revisited: Coupling of stomatal conductance and photosynthesis in the desert shrub, Larrea tridentata. *Plant, Cell & Environment*, *25*(7), 909-921.

Oke, T.R. (1979). Advectively-assisted evapotranspiration from irrigated urban vegetation. *Boundary-Layer Meteorology*, *17*(2), 167-173.

Oke, T.R. (1987). *Boundary layer climates* (2nd ed.). London: Methuen.

Onmura, S., Matsumoto, M., & Hokoi, S. (2001). Study on evaporative cooling effect of roof lawn gardens. *Energy and Buildings*, *33*(7), 653-666.

Oren, R., Sperry, J.S., Katul, G.G., Pataki, D.E., Ewers, B.E., Phillips, N., & Schäfer, K.V.R. (1999). Survey and synthesis of intra-and interspecific variation in stomatal sensitivity to vapour pressure deficit. *Plant, Cell & Environment*, *22*(12), 1515-1526.

Ouldboukhitine, S.E., Belarbi, R., & Djedjig, R. (2012). Characterization of green roof components: measurements of thermal and hydrological properties. *Building and Environment*, *56*, 78-85.

Ouldboukhitine, S.E., Belarbi, R., Jaffal, I., & Trabelsi, A. (2011). Assessment of green roof thermal behavior: a coupled heat and mass transfer model. *Building and Environment*, *46*(12), 2624-2631.

Ouldboukhitine, S.E., Spolek, G., & Belarbi, R. (2014). Impact of plants transpiration, grey and clean water irrigation on the thermal resistance of green roofs. *Ecological Engineering*, *67*, 60-66.

Panin, G.N., Tetzlaff, G., & Raabe, A. (1998). Inhomogeneity of the land surface and problems in the parameterization of surface fluxes in natural conditions. *Theoretical and Applied Climatology*, *60*(1-4), 163-178.

Penman, H.L. (1948). Natural evaporation from open water, bare soil and grass. *Proceedings of the Royal Society of London. Series A. Mathematical and Physical Sciences*, *193*(1032), 120-145.

Penman, H.L. (1956). Estimating evaporation. *Transactions of the American Geophysical Union*, *37*, 43-50.

Pérez-Lombard, L., Ortiz, J., & Pout, C. (2008). A review on buildings energy consumption information. *Energy and Buildings*, *40*(3), 394-398.

Pielke, R.A. (2002). *Mesoscale meteorological modeling* (2nd ed.). New York: Academic Press.

Pitman, A.J. (2003). The evolution of, and revolution in, land surface schemes designed for climate models. *International Journal of Climatology*, *23*(5), 479-510.

Prueger, J.H., Hipps, L.E., & Cooper, D.I. (1996). Evaporation and the development of the local boundary layer over an irrigated surface in an arid region. *Agricultural and Forest Meteorology, 78*, 223–237.

Raji, B., Tenpierik, M. J., & van den Dobbelsteen, A. (2015). The impact of greening systems on building energy performance: A literature review. *Renewable and Sustainable Energy Reviews, 45*, 610-623.

Rana, G., & Katerji, N. (2000). Measurement and estimation of actual evapotranspiration in the field under Mediterranean climate: a review. *European Journal of Agronomy*, *13*(2), 125-153.

Raupach, M.R., & Finnigan, J.J. (1988). 'Single-layer models of evaporation from plant canopies are incorrect but useful, whereas multilayer models are correct but useless': Discuss. *Australian Journal of Plant Physiology*, *15*(6), 705-716.

Rider, N.E., Philip, J.R., & Bradley, E.F. (1963). The horizontal transport of heat and moisture - a micrometeorological study. *Quarterly Journal of the Royal Meteorological Society*, *89*(382), 507-531.

Rijks, D.A. (1971). Water use by irrigated cotton in Sudan III. Bowen ratios and advective energy. *Journal of Applied Ecology*, *8*(3), 643-663.

Robinson, M.F., Heath, J., & Mansfield, T.A. (1998). Disturbances in stomatal behaviour caused by air pollutants. *Journal of Experimental Botany, 49*, 461-469.

Rohli, R.V., & Vega, A.J. (2013). *Climatology* (3rd ed). Sudbury: Jones & Bartlett Publishers.

Rose, C.W., & Sharma, M.L. (1984). Summary and recommendations of the workshop on "evapotranspiration from plant communities". *Agricultural Water Management*, *8*(1), 325-342.

Ross, J. (1975). Radiative transfer in plant communities. In J.L. Monteith (ed.), *Vegetation and the atmosphere, vol. 1: Principles* (pp. 13-55). London: Academic Press.

Saadatian, O., Sopian, K., Salleh, E., Lim, C. H., Riffat, S., Saadatian, E., Toudeshki, A., & Sulaiman, M. Y. (2013). A review of energy aspects of green roofs. *Renewable and Sustainable Energy Reviews*, 23, 155-168.

Sailor, D.J. (2008). A green roof model for building energy simulation programs. *Energy and Buildings*, *40*(8), 1466-1478.

Saliendra, N.Z., Sperry, J.S., & Comstock, J.P. (1995). Influence of leaf water status on stomatal response to humidity, hydraulic conductance, and soil drought in *Betulao occidentalis*. *Planta, 196*(2), 357-366.

Schulze, E.-D., Turner, N.C., Gollan, T., & Shackel, K.A. (1987). Stomatal response to air humidity and soil drought. In E. Zeiger, G.D. Farquhar & I.R. Cowan (ed.), *Stomatal function* (pp. 311-322). Stanford: Stanford University Press.

Schuepp, P.H. (1993). Tansley review no. 59: Leaf boundary layers. *New Phytologist*, 477-507.

Shah, R.K., & Sekulić, D.P. (2003). *Fundamentals of heat exchanger design*. Hoboken: John Wiley & Sons.

Sherrard Jr, J.A., & Jacobs, J.M. (2011). Vegetated roof water-balance model: Experimental and model results. *Journal of Hydrologic Engineering*, *17*(8), 858-868.

Shuttleworth, W.J. (2012). *Terrestrial hydrometeorology*. Hoboken: John Wiley & Sons.

Shuttleworth, W.J., & Wallace, J.S. (1985). Evaporation from sparse crops – an energy combination theory. *Quarterly Journal of the Royal Meteorological Society*, *111*, 839–855.

Snodgrass, E.C., & Snodgrass, L.L. (2006). *Green roof plants: A resource and planting guide*. Portland: Timber Press.

Spronken-Smith, R.A., Oke, T.R., & Lowry, W.P. (2000). Advection and the surface energy balance across an irrigated urban park. *International Journal of Climatology*, *20*(9), 1033-1047.

Stanghellini, C. (1987). *Transpiration of greenhouse crops: An aid to climate management*. Unpublished doctoral dissertation, Wageningen University, Wageningen.

Starry, O., Lea-Cox, J.D., Kim, J., & van Iersel, M.W. (2014). Photosynthesis and water use by two Sedum species in green roof substrate. *Environmental and Experimental Botany*, *107*, 105-112.

Stewart, J.B. (1988). Modelling surface conductance of pine forest. *Agricultural and Forest Meteorology, 43*(1), 19-35.

Stovin, V., Poë, S., & Berretta, C. (2013). A modelling study of long term green roof retention performance. *Journal of Environmental Management, 131,* 206-215.

Tabares-Velasco, P.C., & Srebric, J. (2011). Experimental quantification of heat and mass transfer process through vegetated roof samples in a new laboratory setup. *International Journal of Heat and Mass Transfer, 54*(25), 5149-5162.

Tabares-Velasco, P.C., & Srebric, J. (2012). A heat transfer model for assessment of plant based roofing systems in summer conditions. *Building and Environment, 49*, 310-323.

Tabares-Velasco, P.C., Zhao, M., Peterson, N., Srebric, J., & Berghage, R. (2012). Validation of predictive heat and mass transfer green roof model with extensive green roof field data. *Ecological Engineering, 47,* 165-173.

Takebayashi, H., & Moriyama, M. (2007). Surface heat budget on green roof and high reflection roof for mitigation of urban heat island. *Building and Environment, 42*(8), 2971-2979.

Teeri, J.A., Tonsor, S.J., & Turner, M. (1981). Leaf thickness and carbon isotope composition in the *Crassulaceae*. *Oecologia, 50*(3), 367-369.

Theodosiou, T.G. (2003). Summer period analysis of the performance of a planted roof as a passive cooling technique. *Energy and Buildings, 35*(9), 909-917.

Thirumaleshwar, M. (2009). *Fundamentals of heat and mass transfer*. Delhi: Dorling Kindersley.

Van Mechelen, C., Dutoit, T., Kattge, J., & Hermy, M. (2014). Plant trait analysis delivers an extensive list of potential green roof species for Mediterranean France. *Ecological Engineering, 67,* 48-59.

Verdebout, J., Jacquemoud, S., & Schmuck, G. (1994). Optical properties of leaves: Modelling and experimental studies. In J. Hill & J. Mégier (ed.), *Imaging spectrometry - A tool for environmental observations* (pp. 169-191). Dordrecht: Kluwer Academic.

Vogel, C.A., Baldocchi, D.D., Luhar, A.K., & Rao, K.S. (1995). A comparison of a hierarchy of models for determining energy balance components over vegetation canopies. *Journal of Applied Meteorology*, *34*(10), 2182-2196.

Vogel, S. (1970). Convective cooling at low airspeeds and the shape of broad Ieaves. *Journal of Experimental Botany*, *21*, 91-101.

von Willert, D.J., Eller, B.M., Werger, M.J.A., Brinckmann, E., & Ihlenfeldt, H.-D. (1992). *Life strategies of succulents in deserts, with special reference to the Namib Desert*. Cambridge: Cambridge University Press.

Walter-Shea, E.A., & Norman, J.M. (1991). Leaf optical properties. In R.B. Myneni & J. Ross (ed.), *Photon-vegetation interactions: Application in plant physiology and optical remote sensing* (pp. 229-251). New York: Springer-Verlag.

Wang, Y.P. (2000). A refinement to the two-leaf model for calculating canopy photosynthesis. *Agricultural and Forest Meteorology*, *101*(2), 143-150.

Wang, Y.P., & Leuning, R. (1998). A two-leaf model for canopy conductance, photosynthesis and partitioning of available energy I: Model description and comparison with a multi-layered model. *Agricultural and Forest Meteorology*, *91*(1), 89-111.

Watson, I.D., & Johnson, G.T. (1987). Graphical estimation of sky view-factors in urban environments. *International Journal of Climatology*, *7*, 193–197.

Wesely, M.L. (1989). Parameterization of surface resistances to gaseous dry deposition in regional-scale numerical models. *Atmospheric Environment*, *23*(6), 1293-1304.

Willmer, C., & Fricker, M. (1996). *Stomata* (2nd ed.). London: Chapman & Hall.

Zhao, M., Tabares-Velasco, P.C., Srebric, J., Komarneni, S., & Berghage, R. (2014). Effects of plant and substrate selection on thermal performance of green roofs during the summer. *Building and Environment*, *78*, 199-211.

Chapter 3: Empirical investigation of green roof energy performance in different climates

3.1 Introduction

As highlighted in Chapter 2, as living systems, plants introduce a tremendous amount of uncertainty in the prediction of green roofs' energy performance. Given the complexity of mechanistic models, a comprehensive knowledge of the plants, as well as the substrate, is required for computations to accurately reflect any given green roof system. Additionally, due to the numerous assumptions involved in these models, further research is required to explore the relationships between environmental and design parameters.

Extensive observations not only provide information to validate the theoretical relationships that form the foundation of numerical models, they also provide a means for predicting through empirical modelling. The most extensive empirical modelling study conducted on a vegetated building surface involved fitting an autoregressive model to data collected over a 3-year period from a green wall in Spain to estimate the vegetated surface's effect on indoor temperatures (Olivieri et al. 2014). Predicting the temperature difference between the exterior and interior spaces, their models provided a high degree of accuracy with the multiple *r*-squares around 0.85 with their standard error measures between 0.48-4.12 °C depending on the time of the day. However, as an inherit limitation of empirical models and as noted by the authors, the application of their model may only be suitable for

green walls located in a similar Mediterranean climate. Furthermore, with independent variables being the surface temperature of a metal sheet on the exterior and interior of the building and the air temperature near the ceiling and the floor of the interior space, this study provided no information on the transfer of heat and relationship between parameters within the green wall system. Given the greater depth of their substrate and vegetation layers, green roofs also ultimately have a more complex thermal effect on buildings.

The performance of the ecosystem services that green roofs provide have been found to be largely dependent on the local environment (Jim & Peng, 2012; Lin et al. 2013). For example, the hydrological performance of green roofs has been shown by simulations to vary between climates, with green roofs in warmer, drier climates have a greater retention performance compared to those in cooler, wetter climates (Stovin et al. 2013). Pertaining to the thermal benefits afforded by green roofs, numerical simulation studies have suggested that during summer periods, green roofs are most beneficial in warmer climates (Jaffal et al. 2012). Applying a numerical model based on the work of Sailor (2008) to data typical of the temperate oceanic climate of La Rochelle, France, the hot Mediterranean climate of Athens, Greece, and the cold climate of Stockholm, Sweden, Jaffal and colleagues' (2012) findings suggested indoor air temperatures would be most significantly reduced by the presence of a green roof in Athens. Mean indoor air temperature reductions of 2.6, 2.0 and 1.4 °C were found for Athens, La Rochelle and Stockholm, respectively.

However, as noted by the authors (Jaffal et al. 2012), the numerical model used in their study did not precisely consider the physiology or the growth of the vegetation. These parameters are important as they can have important impacts on the transfer of heat through green roofs by affecting the partitioning of available energy at the surface and the transmission of solar radiation through the vegetation layer. By assuming the different climates considered in their study had no effect on physiological model parameters such as the minimum stomatal resistance or growth factors such as the LAI, Jaffal and colleagues ignored the impact that the environment has on the functioning, and even the survival, of green roof vegetation.

These points highlight the current deficiencies limiting the ability of numerical models to accurately predict the likely benefits of green roof installations and maximize design options. In situ modelling studies like that of Olivieri et al. (2014) encompass all aspects of the vegetated surface's energy balance, including plant parameters, but the findings are likely to be site-specific limiting comparisons with sites in other climates. Additionally, the independent variables used in the study by Olivieri and colleagues had limited relevance to the parameters used in numerical modelling studies and therefore little could be gained as far as the refinement of numerical models. If empirical models are more closely related to their mechanistic counterparts, the relationships between parameters within a green roof system and between the system and its environment could be better

understood so that these models could be more accurately applied to buildings in a range of climatic conditions.

Given the need to develop more detailed green roof models, as suggested by Jaffal and colleagues (2012), and the lack of empirical studies comparing the thermal performance of green roofs in different climates, the current study aims to develop regression models that accurately predict the flux of heat through green roof substrates during summer. By installing identical green roofs, the effect of design parameters on thermal performance will be minimized so the effect of climate can be better observed and predicted. This will also facilitate the characterization of heat transfer through the substrate. Furthermore, a model should be validated using an extensive data set, an approach that has not been undertaken in the development of numerous mechanistic green roof models (Lazzarin et al. 2005; Alexandri & Jones, 2007). Therefore, the current study also aims to validate the regression models using extensive data collected during the summer period of different years.

3.2 Method

3.2.1 Study sites

In an effort to maximize the effect of climate on the performance of the green roof design, three Canadian cities located in different climate regions were chosen to conduct the study. As displayed in Fig 3.1, the selected cities of Calgary (Alberta), Halifax (Nova Scotia) and London (Ontario) differ significantly in their average annual precipitation. Each of the green roofs was installed in August, 2012. The rooftops on which the green roofs were located were three, four and five storeys above the ground surface in Calgary, London and Halifax, respectively.

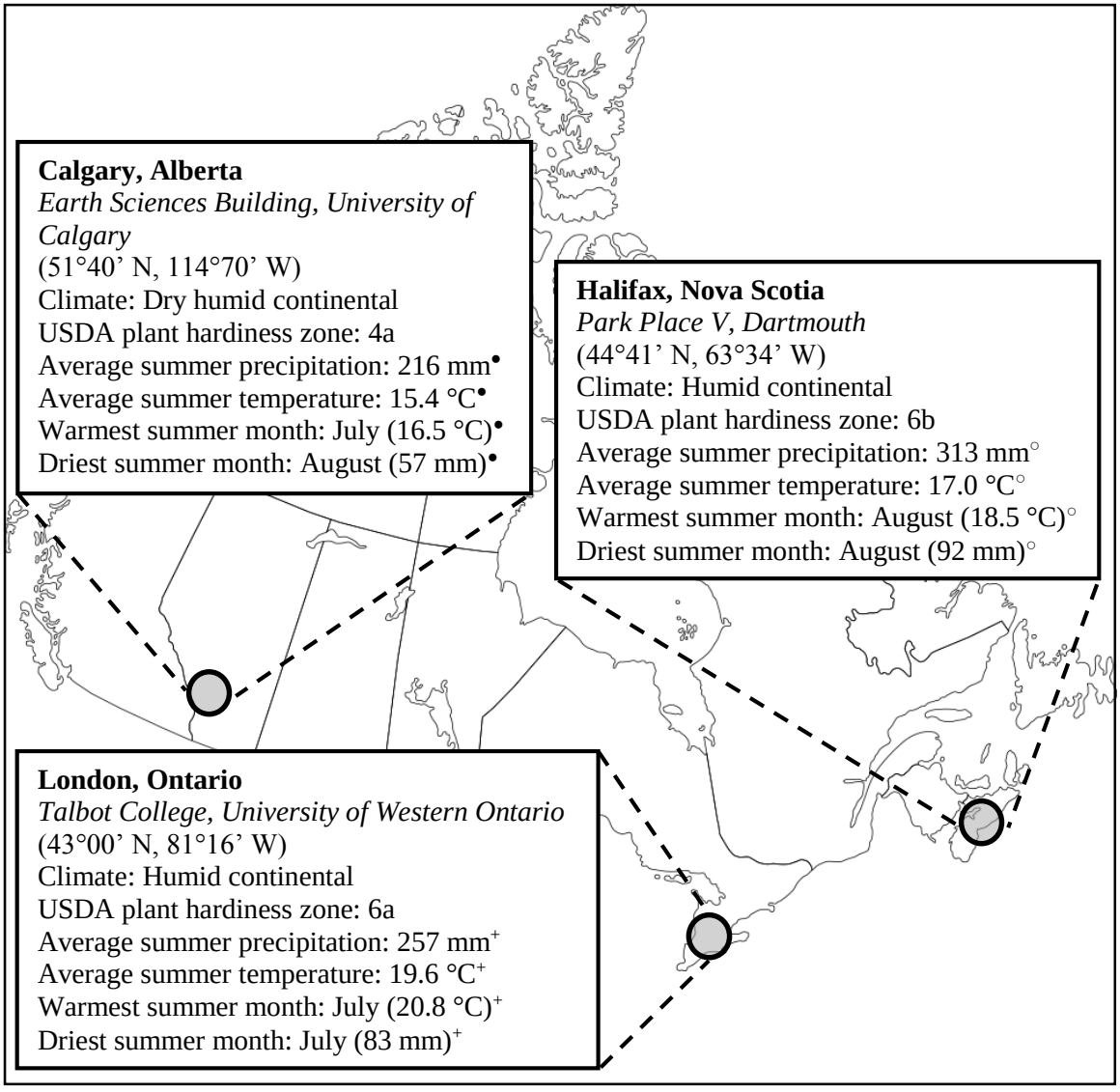

Fig 3.1 *Location of green roof sites used in study and their climate classification, USDA plant hardiness zone and climate averages*

● 1981-2010 average at Calgary International Airport weather station (51°06' N 114°01' W)
○ 1981-2010 average at Shearwater weather station (44°38', 63°30' W)
+ 1981-2010 average at London International Airport weather station (43°01' N, 81°09' W)

Climate data source: Environment Canada

3.2.2 Materials and data collection

Using a modular system, each of the extensive green roofs were almost identical in design, with the roofs consisting of 400, 395 and 514 1’ x 1’ modules in Calgary, Halifax and London, respectively. The green roofs were composed of a relatively large number of modules to minimize leading edge effects. The substrate in each module was either 10.2 or 15.2 cm in depth. The substrate used was a LiveRoof® engineered growing medium which was a blend of organic and inorganic materials. This lightweight substrate has a high porosity, giving the mixture a high water holding capacity.

The modules were planted as either monocultures containing one of the three major taxonomic and functional plant groups commonly used on green roofs; the forb *Aquilegia canadensis*, the succulent *Sedum spurium* or the grass *Sporobolus heterolepis*, or a mixture containing all three species. Approximately 50% of the modules of each green roof were *Sedum spurium* monocultures, with this species chosen for the current study as the monitoring equipment was installed exclusively on *Sedum spurium* monocultures at each study site.

As mentioned in Chapter 2, *Sedum spurium* was previously used in the validation study (Tabares-Velasco et al. 2012) for the green roof model of Tabares-Velasco and Srebric (2012) and is a popular choice for both extensive green roof research studies and industry designs. Displayed in Fig 3.2, previous research has shown this species can survive

long periods in the harsh environmental conditions that green roofs present (Rowe et al. 2012).

Given the importance of vegetation coverage to a green roofs energy balance, for descriptive purposes and assisting the interpretation of statistical analyses, the canopy density of each module was measured. The pin-frame technique was conducted once per month during the 2013 summer period and once per week during the 2014 summer at each of the sites. This technique involved placing 1’ x 1’ frame above each module which contained four pairs of strings across the frame, both vertically and horizontally, so as to provide 16 intersections between the pairs of strings. A pin was then lowered towards the substrate surface at each intersection and the number of leaves that touched the pin was recorded. This technique allowed an approximation of density that involved aspects of both LAI and vegetation fractional coverage. As this technique was only undertaken once per month during the 2013 study period, only one mid-month measurement was considered for the 2014 study period. Due to the poor temporal resolution of this technique, the canopy density data was not included in the statistical analyses as it was unable to provide a significant increase in models’ predictive power.

Fig 3.2 *Overhead view of the Sedum spurium canopy on the Halifax green roof in 2014*

To measure the transfer of heat through the green roofs and its relationship with environmental variables, micrometeorological monitoring equipment was installed at each of the sites. Shown in Table 3.1, the parameters measured by the monitoring instruments included a temperature profile spanning from above and within the green roof system, the amount of radiation entering the system, soil moisture and the wind speed. The data collected by these instruments was also used to calculate additional variables; the surface-to-air and canopy-to-air temperature differences as well as an estimate of the vapour pressure deficit (VPD) value for the within-canopy air. Positive values of the dependent variable meant the transfer of heat was downwards; towards the building, while negative values represented the transfer of heat upward; away from the building.

Table 3.1 *List of parameters measured and calculated for this study and accompanying notes on location of measurements or calculation methods*

Parameter	**Notes**
Dependent variable	
Substrate heat flux	Placed 7 cm deep in the heat flux module substrate
Independent variables	
Radiation:	
-Solar radiation	
-Net radiation	Measured approximately 40 cm above the substrate surface
Temperature:	
-Air temperature	Measured approximately 1.8 m above the roof surface
-Sub-canopy air temp	Measured approximately 5 cm above the substrate surface
-Surface temperature	Measured on a module neighbouring the heat flux module
-Soil temperature at 1''	Soil temperature in the heat flux module 1'' below the substrate surface
-Soil temperature at 4''	Soil temperature in the heat flux module 4'' below the substrate surface
Temperature difference:	Represents the gradient driving convective sensible heat fluxes
-Surface-to-air temp dif	Surface temperature minus air temperature
-Surf-canopy air temp dif	Surface temperature minus sub-canopy air temperature
Humidity:	Represents the gradient driving latent heat fluxes (except for the absolute measure of specific humidity which does not represent a gradient)
-Relative humidity	Measured approximately 1.8 m above the roof surface
-Specific humidity	Calculated using air temperature and RH data
-VPD_{canopy}	Calculated using canopy air temperature and RH data
Additional:	
-Soil moisture	Measured in the heat flux module at a depth of approximately 3'' below the substrate surface with the probe positioned horizontally within the substrate
-Wind speed	Measured approximately 1.8 m above the roof surface

Table 3.2 shows a list of the instruments used to measure these parameters. The net radiometer was placed above the module containing the heat flux plate, the soil temperature sensors and the soil moisture sensor, as shown in Fig 3.3. The sub-canopy air temperature sensors were located above another neighbouring module. All of these modules that either contained or were located below instruments were a part of a centre array containing 103 modules in Calgary and Halifax and 91 modules in London; each a *Sedum spurium* monoculture. The instruments were all connected to a CR3000 data logger (Campbell Scientific Inc., Logan, Utah, USA). The data were composed of five minute-averaged measurements for each variable.

Table 3.2 *List of instruments used in data collection and the manufacturers' reported accuracy*

Variable	Instrument	Accuracy
• Air temperature ◦ Relative humidity	RH and temperature probe (HC2-S3-L, Campbell Scientific Inc.)	• ±0.1 °C at 0 °C ◦ 0.8% at 23 °C
Net radiation	Net radiometer (Q-7.1, Campbell Scientific Inc.)	NA
Soil moisture	Soil moisture sensor (EC-5, Decagon Devices Inc., Pullman, Washington, USA)	±3%
Solar radiation	Pyranometer (TSP-400, Yankee Environmental Systems Inc., Turners Falls, Massachusetts, USA)	NA
Soil temperature (1'' & 4'')	Thermistor temperature sensor (ST-100, Apogee Instruments Inc., Logan, Utah, USA)	±0.2 °C at 0-70 °C
Sub-canopy air temperature	Thermistor temperature sensors (ST-200, Apogee Instruments Inc.)	±0.2 °C at 0-70 °C
Substrate heat flux	Soil heat flux plate (HFT3, Campbell Scientific Inc.)	<±5%
Surface temperature	Infrared radiometer (SI-100, Apogee Instruments Inc.)	±0.2 °C at -10-65 °C
Wind speed	Anemometer (03101, Campbell Scientific Inc.)	±0.5 m s^{-1}

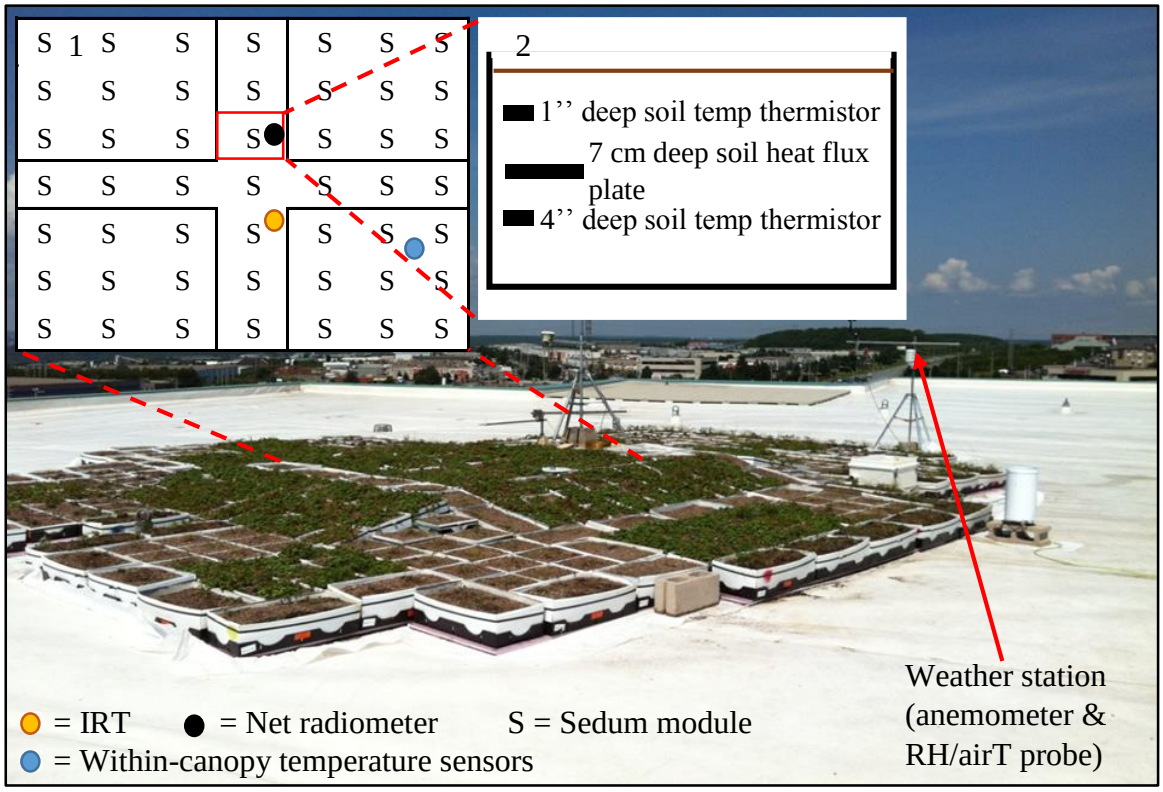

Fig 3.3 Photograph of Halifax green roof research site with inset of centre module array with inset: (1) overhead diagram of centre module array; and (2) side view-diagram of heat flux module

To correct for errors in the net radiometer measurements caused by convective cooling as air passes the sensors, the correction functions supplied by the manufacturer (s.campbellsci.com/documents/us/manuals/q-7-1.pdf) were applied to the data.

As atmospheric pressure (p, kPa) was not measured in the study, the ideal gas law could not be used to calculate the specific humidity (q, g kg^{-1}). As an alternative, the specific humidity was estimated using the approximation shown in Eq. 3.1. The

atmospheric pressure in Eq. 3.1 was kept constant at 101 kPa as hourly pressure measurements from the three weather stations mentioned in Fig 3.1 varied between approximately 1005 hPa and 1020 hPa during the study period. The saturation vapour pressure was calculated using Buck's (1981) version of the Tetens (1930) formula.

$$q = \frac{623\ e}{p - 0.377\ e} \tag{3.1}$$

Soil moisture was expressed as volumetric water content (VWC). To calculate the VWC from the EC-5 soil moisture sensors' data, Eqs. 3.2 and 3.3 from Sakaki et al. (2008) were employed. The saturated and dry substrate values as well as the porosity (ϕ) were obtained from previous research on the LiveRoof® growing medium (Perelli, 2014).

$$VWC = \frac{ADC^{\alpha} - {ADC_{dry}}^{\alpha}}{{ADC_{sat}}^{\alpha} - {ADC_{dry}}^{\alpha}}\,\phi \tag{3.2}$$

$$ADC = mV \times 1.3661 \tag{3.3}$$

The VPD_{canopy} was calculated from the sub-canopy air temperature and relative humidity data using Eq. 3.4 for the saturation vapour pressure (e_s), which is required for the calculation of VPD, as shown in Eq. 3.5 (Monteith, 1973).

$$e_s = 0.0611\, e\left(\frac{17.27\, T_a}{T_a + 237.3}\right) \quad (3.4)$$

$$VPD = e_s\left(1 - \frac{RH}{100}\right) \quad (3.5)$$

Data acquisition commenced in August 2012 and while still continuing in London, the data collection period concluded in Calgary in October 2014 and in Halifax in November 2014. This facilitated two full simultaneous summer periods of data collection across the sites. The meteorological summer; June, July and August, was chosen as the study period as it represents the period of peak incoming solar radiation, maximum heat flux through conventional roofing and the period when green roofs have shown to be most beneficial in reducing the heat flux through roofing membranes (Getter et al. 2011). It was also chosen because particular instruments, such as the thermistor temperature and soil moisture sensors, were recurrently inoperative during the fall, winter and early spring periods.

3.2.3 Data analysis

In order to model the time series data, multiple linear regression was employed. This approach allows for the examination of how much a particular set of independent variables can explain the variation in the substrate heat flux. During data preparation, data

points were removed based on missing variable(s) data and obvious instrument errors. The data points removed for each site based on these methods were also removed from the other sites' data sets so as to maintain an equal number of data points for each site. This was done to prevent skewing of the models' accuracy of estimates toward a particular site(s). Given large periods of data were missing at each site, the 2013 data collected in Calgary and London and the 2014 data collected in Halifax were used to formulate the models in order to maximize their respective data sets.

Multiple linear regression modelling relies on several assumptions for its results to be valid so the data were then examined to evaluate whether or not these assumptions were met prior to conducting the regression analysis. Firstly, the assumption of linearity contends that for a linear regression model to be appropriate for a particular data set, the independent variables should have a linear relationship with the dependent variable. This was tested visually by plotting each independent variable with the heat flux data. As each plot showed a linear relationship between the independent and dependent variables, linearity could be assumed (Stevens, 2009).

Multiple linear regression models also assume that the residuals (errors) of the dependent variable are normally distributed. A histogram and a normal probability plot of the standardized residuals were utilized (Keith, 2006; Stevens, 2009). As these plots provided no evidence to suggest the assumption of normality had been violated, no further testing was required for this assumption.

The data must also be homoscedastic, that is, the error in the predicted values is the same across the range of the dependent variable's values. To determine whether or not the data deviated considerably from homoscedasticity, a scatterplot of the predicted scores versus the residuals scores was used. The random distribution of data values in the scatterplot was sufficient evidence to suggest the assumption of homoscedasticity had not been violated.

The measurement of the variables must also be independent; a data value should provide no indication of subsequent data values. Conversely, for dependent (or autocorrelated) processes, the best predictor of the next data value is the previous observation(s). Autocorrelation is an inherent concern when using regression models for time series analysis. As such, both the Durban-Watson statistic and a plot of the unstandardized residuals versus time were used to test the assumption of independent observations. Given the Durban-Watson statistic did not exceed the critical value and the scatterplot had a random distribution, it was concluded that the data did not violate the assumption of independent observations.

It is also assumed for multiple linear regression models that the data contains no outliers as these data points can have a significant influence on the models' predictions. To define outliers in the data, the Mahalanobis and Cook's distances were computed. Although some of the data points exceeded the critical values for the Mahalanobis distance test, they were included in the final data set as they did not appear to be the result of instrument

errors. This decision was justified on account of none of the data points exceeding the critical Cook's distance value of 1, therefore suggesting that none of the outliers would have a significant influence on the model as a whole (Cook & Weisberg, 1982).

Finally, there should also be no multicollinearity between the independent variables in a multiple linear regression model. This refers to a high degree of linear dependency; correlation, between predictor variables that occurs as a result of multiple variables measuring the same phenomenon. The degree of multicollinearity was tested using multiple measures. As a preliminary investigation, a matrix of Pearson's Bivariate Correlation coefficients for the independent variables was used to identify closely related variables, with a Pearson Correlation of 0.9 used to identify cases of possible collinearity (Field, 2009). Next, the tolerance and its reciprocal; the variance inflation factor (VIF), were also used as additional evidence of multicollinearity. Both measures were considered given the debate over acceptable critical values. A tolerance value below 0.2, as suggested by Menard (1995), and a VIF value above 10, as suggested by Bowerman and O'Connell (1990) and Myers (1990), were considered critical for this study and were assumed to suggest multicollinearity. Using these measures of multicollinearity, there appeared to be within-parameter group collinearity.

With the dataset meeting the other assumptions, the multiple linear regression analysis was conducted using multiple combinations of independent variables. This approach allowed for the most accurate model that did not violate the assumption of little

or no multicollinearity to be determined. Once the regression model's predictor variables were determined for the entire data set (all sites), data transformations were performed to see if they elevated the accuracy of predictions. These included logarithmic transformations, squaring, one and three hour time lags as well as one, two and three hour moving averages for the dependent and/or independent variables.

With the model parameters finalised, multiple linear regression models were then formulated for the sites individually and for two-site combinations (Calgary-Halifax, Calgary-London and Halifax-London). A total of seven multiple linear regression models were thus developed in order to compare the importance of independent variables at different sites as well as compare the performance of models developed from different data sets. The r-square and normalized root mean square error (NRMSE) values were used to assess and compare the predictive power of the regression models. Given the models were formulated using different data sets, the NRMSE was used rather than the root mean square error (RMSE) as some of the data sets had different ranges of values for the dependent variable. Using the NRMSE allowed for a comparison of the models' standard error because, unlike the RMSE, it is a non-dimensional measure of a model's predictive power that is solved by dividing the standard error by the range of observed measures. The RMSE and NRMSE statistics were chosen as they, unlike the mean absolute error, amplify large errors.

To validate the developed models, data for the independent variables collected during contiguous years (Calgary and London, 2014; Halifax, 2013) were used to compute estimates of the substrate heat flux. These estimates were compared to the heat flux measurements collected during these years using the r-square, RMSE and NRMSE values. A validation period of 25 days for each site was used as this was the maximum number of days that data was available for each of the independent variables and the dependent variable at the Halifax site for 2013. The 25 day period was also employed in the validation of the models in Calgary and London in order to obtain an equal validation between the sites.

All statistical analyses were performed using IBM SPSS Version 21.

3.3 Results

As a general overview of the data, the descriptive statistics of means and standard deviations for each of the independent variables and the dependent variable are displayed in Table 3.3. These figures highlight some key differences between the study sites. Of particular interest is the dependent variable; the substrate heat flux, which showed much greater variability in Halifax compared to the other sites. Interestingly however, the incoming and available energy (solar and net radiation, respectively); the radiation parameters, were similar between the three sites. The temperature parameter averages were

all highest in London and lowest in Calgary while the other independent variables were generally fairly similar between the study sites.

Table 3.3 *Means, with standard deviations in parenthesis, for the measured and calculated variables at each study site*

	Heat flux	Solar rad	Net rad	Air temp	Sub can T	Surface T
Calgary	0.9 (5.1)	221 (291)	108 (211)	16.0 (5.2)	17.4 (5.9)	17.4 (7.6)
Halifax	2.2 (15.2)	223 (293)	119 (207)	18.1 (4.0)	18.6 (4.6)	19.5 (6.2)
London	0.5 (8.4)	221 (291)	120 (185)	19.9 (5.1)	20.5 (6.3)	20.6 (7.1)

(*cont.*)

	Soil T 1''	Soil T 4''	S-A T diff	S-C T diff	Rel hum	Spec hum
Calgary	16.5 (4.3)	16.3 (4.0)	1.4 (3.7)	0.0 (2.9)	65 (18)	7.1 (1.8)
Halifax	19.5 (4.0)	19.3 (3.6)	1.3 (3.2)	0.9 (2.4)	74 (19)	9.5 (2.5)
London	20.4 (4.0)	20.4 (3.8)	0.8 (3.3)	0.1 (3.0)	71 (17)	10.2 (2.8)

(*cont.*)

	VPD_{can}	Soil Moist	Wind Spd
Calgary	1.3 (1.0)	0.17 (0.03)	1.6 (1.4)
Halifax	1.3 (1.0)	0.27 (0.03)	1.6 (1.4)
London	1.3 (1.0)	0.24 (0.03)	1.6 (1.4)

As indicated by the standard deviation, the substrate heat flux exhibited more dynamic variation in Halifax compared to Calgary, as highlighted by the week shown in Fig 3.4. The heat flow through the substrate in Halifax exhibited higher maximum (towards the building) and lower minimum (away from the building) values compared to Calgary. On the other hand, London's heat flux values were intermediate, occasionally exceeding the extremes of Halifax while at other times showing less fluctuation than Calgary.

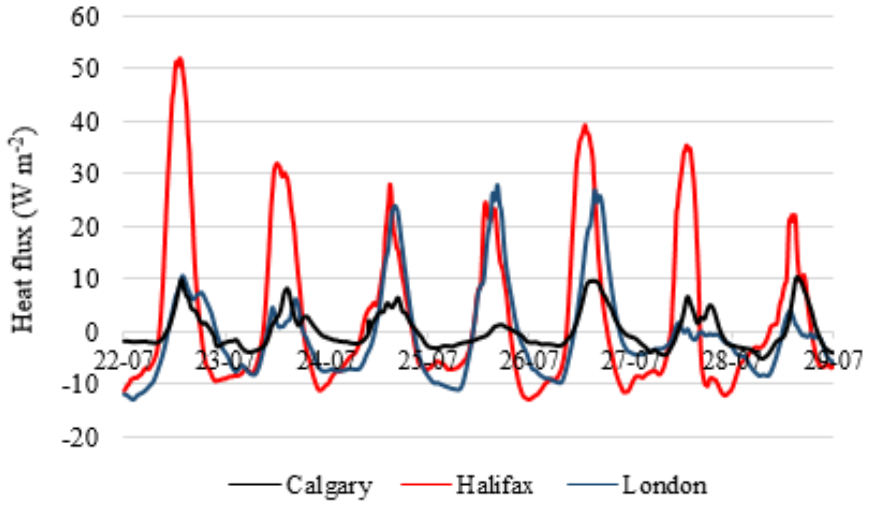

Fig 3.4 *Heat flux measurements during 22/7-28/7 in Halifax, London and Calgary*

The available energy at the surface; the net radiation, is shown in Fig 3.5 for the same period. Unlike the heat flux data, the three sites were more comparable in the amount of energy available at their surfaces for non-radiative processes. There also appears to be considerable variation in net radiation between the days at each site, with the highest net radiation values occurring at different sites on different days. During this particular week, London's daily maximum values varied markedly between days which correspond with the heat flux data.

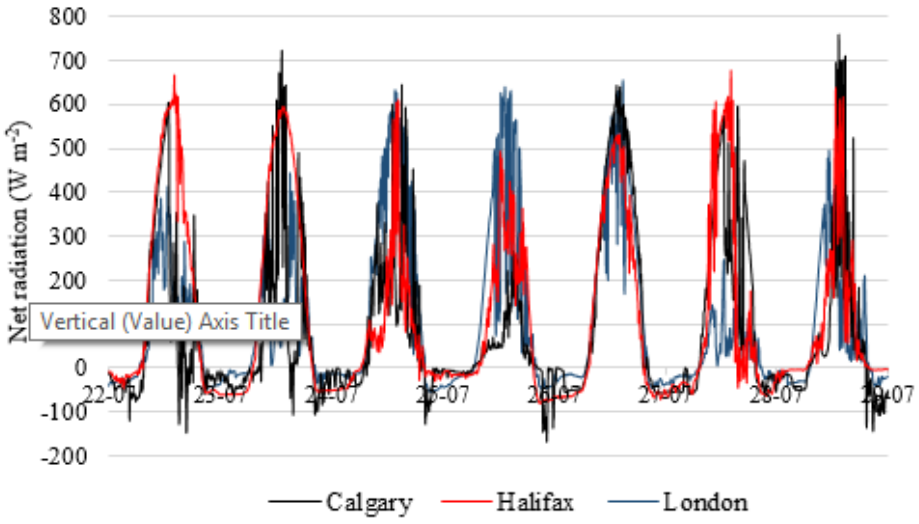

Fig 3.5 *Net radiation measurements during 22/7-28/7 in Calgary, Halifax and London*

Under normal circumstances during diurnal periods, the majority of the available energy that is absorbed by the surface but not conducted downward through the substrate constituting the ground heat flux, is dissipated through sensible and latent heat mechanisms. The gradient forces that result in these processes are that of vapour pressure for latent heat processes and temperature for sensible heat dissipation. Fig 3.6 shows the relationship between these two drivers of heat dissipation at the surface over the same period at each site as represented by the relative humidity and the surface-to-air temperature difference. The two variables generally showed an inverse pattern with each other at each of the sites

with the surface-to-air temperature difference peaking during diurnal periods and the relative humidity peaking during nocturnal periods. This is to be expected as an increase in evapotranspiration will result in a decrease in surface temperatures. Noticeable and almost immediate increases in the relative humidity followed the rain events that exceeded 27 mm, while delayed decreases in the temperature difference followed these events. The highest surface-to-air temperature differences featured in Fig 3.6 at each of the sites occurred during days when there were no rain events exceeding 27 mm. Of particular note is London, which showed the highest temperature differences of above 15 °C for the three days 24/7-26/7 but then following rain the daily peaks were less than 6 °C for the following two days.

a) Calgary

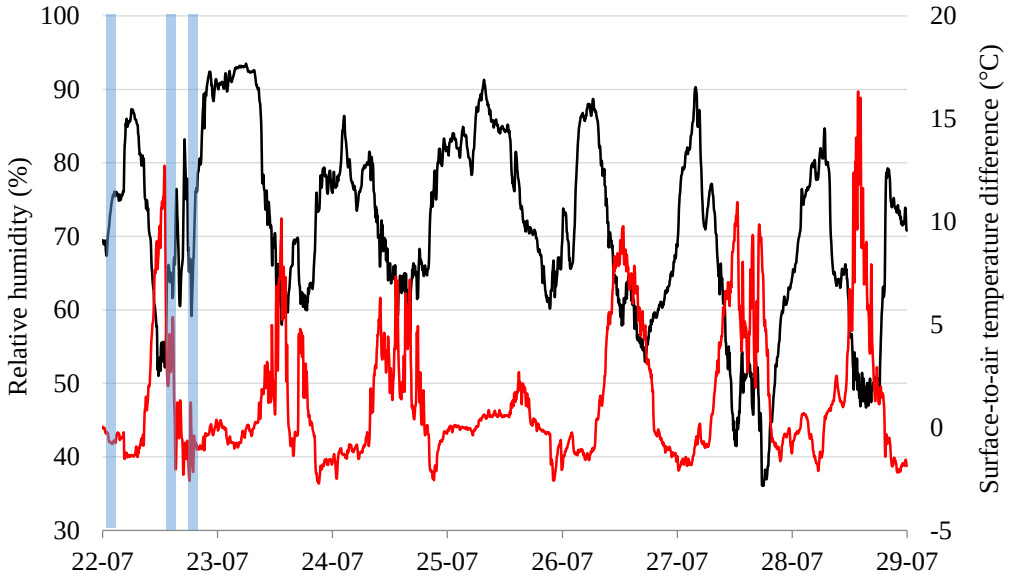

b) Halifax

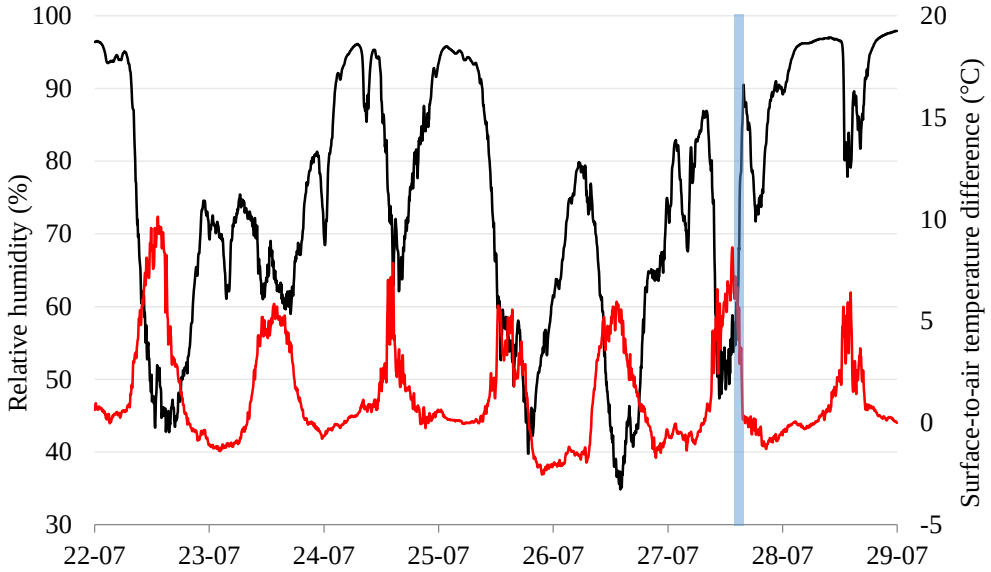
100
90
80
70
60
50
40
30
Relative humidity (%)
20
15
10
5
0
-5
Surface-to-air temperature difference (°C)
22-07
23-07
24-07
25-07
26-07
27-07
28-07
29-07

c) London

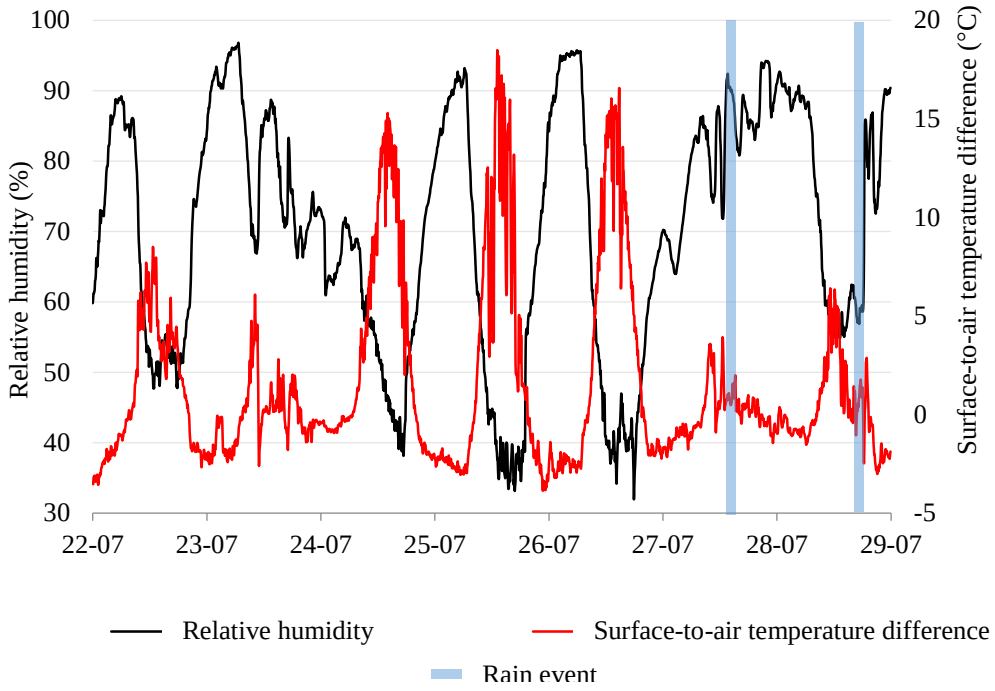

Fig 3.6 *Relative humidity and surface-air temperature difference from 22/7-28/7 in a) Calgary; b) Halifax; and c) London, featuring rain events where the rainfall was above 27 mm*

Given the important role of hydrology on the energy balance, as suggested by Fig 3.6, the volumetric water content (VWC) of the substrate is shown in Fig 3.7 for the entire study period. The plot shows a marked difference between the sites, with Halifax generally having the highest VWC and Calgary having the lowest. Calgary had a period of particularly low VWC during August. Each site also appeared to receive fairly large rainfall events following extended dry periods.

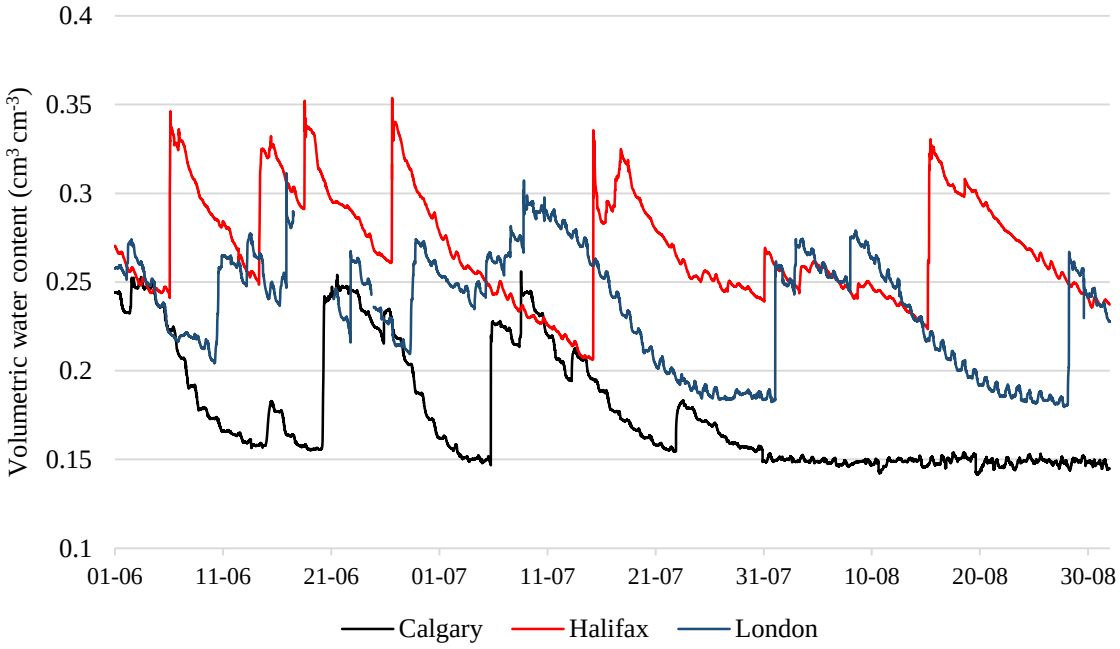

Fig 3.7 *Soil moisture in Calgary, Halifax and London for the duration of the study period (01/06-31/08)*

3.3.1 Regression analysis

Besides characterizing the conditions at each of the study sites, these variables were also measured with the aim of developing multiple regression models for predicting the substrate heat flux. As mentioned in the Methods section, multicollinearity occurred between parameters within the same parameter group; radiation, temperature, temperature difference and humidity. Nevertheless, as seen in Table 3.4, comparing between the models containing related parameters shows little difference in terms of model performance and were all statistically significant (p<.001). While the combinations of parameters shown in

the table is not as extensive as those trialled, it features the highest and lowest coefficient of determination values obtained and allows for a comparison between the variables within parameter groups. It also does not include models that featured independent variables that were collinear.

Table 3.4 *Selected combinations of different model parameters with respective r-squared and p values for entire data set (all sites)*

Parameter	Parameter group								
	Radiation			Temperature			Temp diff	Hum	
Solar radiation	•								
Net radiation		•	•	•	•	•	•	•	•
Air T			•						
Sub canopy T				•		•			
Surface T					•				
Soil T 1''	•	•					•	•	•
Soil T 4''						•			
S-A Temp diff	•	•	•	•	•	•		•	•
S-C Temp diff							•		
Relative hum	•	•	•	•	•	•	•		
Specific hum								•	
VPD can									•
Soil moisture	•	•	•	•	•	•	•	•	•
Wind speed	•	•	•	•	•	•	•	•	•
r^2	.604	.614	.610	.611	.610	.609	.609	604	.609
p	<.001	<.001	<.001	<.001	<.001	<.001	<.001	<.001	<.001

Greater variability between regression results was found when data transformations were considered. The Pearson Correlation coefficient matrix displayed in Table 3.5 shows

the relationships between the substrate heat flux and the independent variables that were found to provide the most accurate predictions in the regression analysis. Except for a few results showing weak or no correlation between variables, all of the correlations were statistically significant (p<0.01, 2-tailed). Strong correlations were generally found between the dependent variable and the net radiation with a one hour moving average, the relative humidity with a one hour moving average and the surface-to-air temperature difference with a one hour moving average.

Table 3.5 *Pearson correlation coefficient matrix for the dependent (heat flux) and independent variables of the multiple linear regression models at each of the study sites*

	Net $rad_{1\ hr}$			R $hum_{1\ hr}$			Soil moist			Soil temp 1			S-A T $dif_{1\ hr}$			Wind speed		
	C	H	L	C	H	L	C	H	L	C	H	L	C	H	L	C	H	L
Heat flux	.79	.93	.83	-.77	-.50	-.70	.11	.07	.08	.33	.46	.34	.70	.85	.72	-.04	.00	.01
Net rad				-.64	-.56	-.64	.06	.04	.10	.22	.50	.20	.86	.86	.86	-.01	-.03	.01
Rel hum							-.05	-.01	.06	-.38	-.39	-32	-.46	-.37	-.49	.06	.07	-.01
Soil M										-.51	-.30	.07	-.08	-.03	.03	-.22	-.12	-.07
Soil T 1													.25	.51	.14	.16	.20	.14
S-A TD																.04	.04	.05

Underlined = non-significant (p > 0.01, 2-tailed)
C = Calgary H = Halifax L = London
Note: the Pearson correlation coefficients for a particular column (variable/study site) are calculated with data collected at the same site for the other variable (row)

The coefficients and performance statistics for the multiple linear regression models developed for all of the sites, each site individually and for the two-site combinations are shown in Table 3.6. The Halifax and Halifax-London models were the most accurate while all sites model was least accurate by linear dependence (r^2) and the Calgary model was the least accurate according to the normalized standard error. The models involving Halifax data tended to be the most accurate while the models developed using Calgary data were generally the least accurate. As noted below the table, all of the models were statistically significant (p<.001).

Table 3.6 *Regression model results for all sites, each individual site and two-site combinations*

	Unstandardized coefficients									
	Constant	Net rad 1 hour avg	R hum 1 hr avg	Soil Moist	Soil temp 1''	S-A T dif 1 hr avg	Wind speed	*F*	r^2	NRMSE
All sites•	-5.333	0.033	-0.060	10.528	0.217	0.455	-0.073	16371	.67	0.076
Calgary○	0.177	0.007	-0.122	27.548	0.157	0.443	-0.016	9377	.78	0.092
Halifax○	-10.905	0.056	-0.003	23.251	-0.065	1.104	0.201	19028	.88	0.067
London○	-2.008	0.025	-0.126	9.913	0.288	0.324	-0.134	8285	.75	0.086
Calgary-Halifax+	-7.650	0.035	-0.034	12.889	0.235	0.535	-0.072	10641	.66	0.083
Calgary-London+	4.466	0.013	-0.142	8.031	0.122	0.467	-0.068	12099	.69	0.080
Halifax-London+	-15.665	0.047	-0.023	26.674	0.295	0.424	-0.046	18758	.78	0.073

Note: Each model is significant (p<.001)

$r^2_{adjusted} = r^2$ for each model

● df = 6, 48791

○ df = 6, 16259

\+ df = 6, 32525

When comparing the standardized regression coefficients in Table 3.7, which are measured in standard deviation units so are directly comparable, there are marked differences between the models as to the relative importance of certain variables. Of particular note, Calgary data lowered the net radiation and increased the relative humidity coefficients while Halifax data tended to increase the net radiation and reduce the effect of relative humidity. Interestingly, the Halifax model was the only analysis to feature a negative soil temperature 1'' and positive wind speed standardized coefficient.

Table 3.7 *Standardized coefficients of regression models*

	Standardized coefficients					
	Net rad 1 hour avg	R Hum 1 hr avg	VWC	Soil temp 1''	S-A T dif 1 hr avg	Wind speed
All sites•	0.607	-0.104	0.048	0.091	0.125	-0.010
Calgary°	0.263	-0.427	0.162	0.133	0.255	-0.005
Halifax°	0.755	-0.004	0.043	-0.017	0.208	0.019
London°	0.543	-0.252	0.034	0.136	0.111	-0.023
Calgary-Halifax+	0.620	-0.057	0.062	0.091	0.136	-0.009
Calgary-London+	0.366	-0.359	0.050	0.080	0.195	-0.014
Halifax-London+	0.730	-0.034	0.069	0.096	0.099	-0.005

3.3.2 Model validation

The results of the validation were generally similar to those obtained during the development of the models. As seen in Table 3.8, the models involving Halifax tended to be amongst the most accurate and Calgary models were generally the weakest. The Halifax-London model was even slightly more accurate at predicting the London heat flux during the 2014 period than the London model that was developed with 2013 data. It also more accurately predicted the 2013 Halifax heat flux than the 2014 Halifax model. Although it was poor at predicting the heat flux with the combined data set, the All sites regression model generally performed well. The model even provided more accurate estimates of the Halifax and London heat fluxes than the models developed exclusively with data from those sites.

Table 3.8 *Regression model validation performance for each model and green roof site*

	Model											
	All sites			Calgary			Halifax			London		
Site(s)	r^2	RMSE	NRMSE	r^2	RMSE	NRMSE	r^2	RMSE	NRMSE	r^2	RMSE	NRMSE
All sites	.50	7.13	0.102									
Calgary	.65	1.79	0.094	.68	1.71	0.090						
Halifax	.87	4.60	0.066				.86	4.87	0.070			
London	.91	3.33	0.067							.89	3.61	0.072

(*cont.*)

	Model								
	Calgary-Halifax			Calgary-London			Halifax-London		
Site(s)	r^2	RMSE	NRMSE	r^2	RMSE	NRMSE	r^2	RMSE	NRMSE
Calgary	.65	1.78	0.094	.68	1.71	0.090			
Halifax	.88	4.49	0.064				.88	4.40	0.063
London				.87	3.95	0.079	.90	3.52	0.071

As highlighted graphically in Fig 3.8, except for the Calgary model which was reasonably accurate, the regression models tended to overestimate Calgary's diurnal heat flux. During the nocturnal periods, the All sites and Calgary-Halifax generally overestimated the flow of heat toward the substrate surface while the Calgary and Calgary-London models either underestimated the upward flow of heat (negative) or predicted a downward (positive) flux of heat, such as 28/07. Generally the greater the fluctuation in the heat flux measurements, the more inaccurate the models' predicted values.

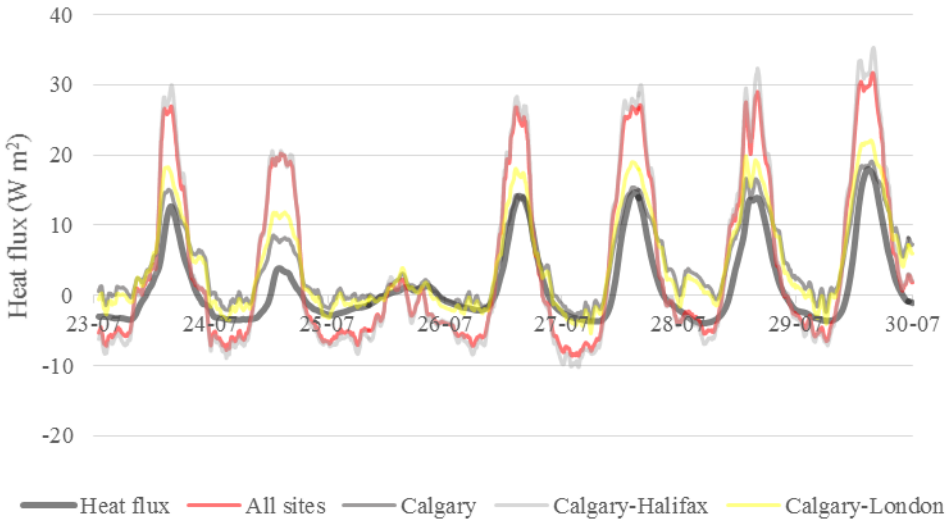

Fig 3.8 *Heat flux measured in Calgary for period 23/07/14-29/07/14 and model predictions*

Conversely, aside from the Halifax model, the models tended to underestimate the diurnal peaks in the Halifax heat flux when it rose above 20 W m^{-2}, as shown in Fig 3.9. However, during days when the substrate heat flux did not rise above 10 W m^{-2}, the models' predictions were fairly accurate. During nocturnal periods, besides the All sites model generally underestimating the magnitude of the upward (negative) heat flux, the models tended to be fairly accurate.

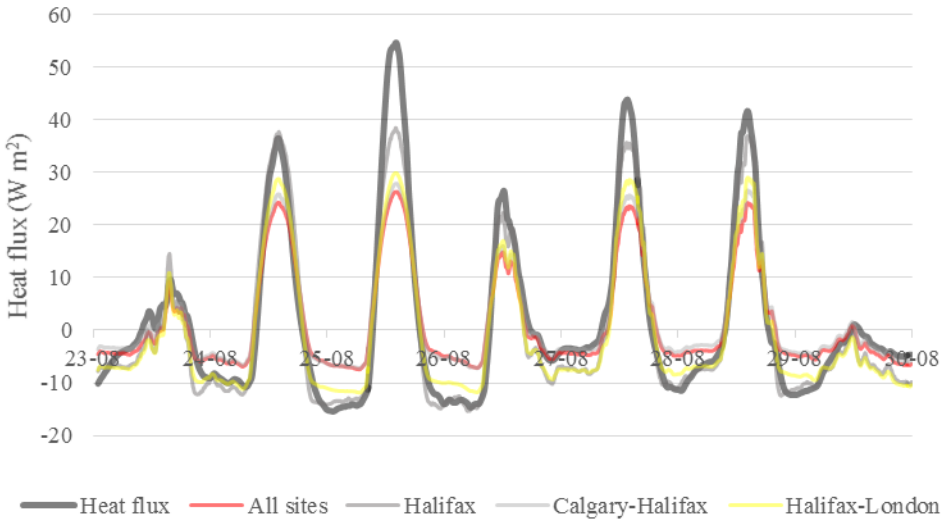

Fig 3.9 *Heat flux measured in Halifax for period 23/08/13-29/08/13 and model predictions*

During the diurnal periods in London, the models tended to coalesce more in London than the other sites, as highlighted by Fig 3.10. While they were fairly accurate during the day, they generally tended to underestimate the heat flow away from the building during the night. Despite a tendency to overestimate the most during diurnal periods, the Halifax-London model was regularly the most accurate during the validation study.

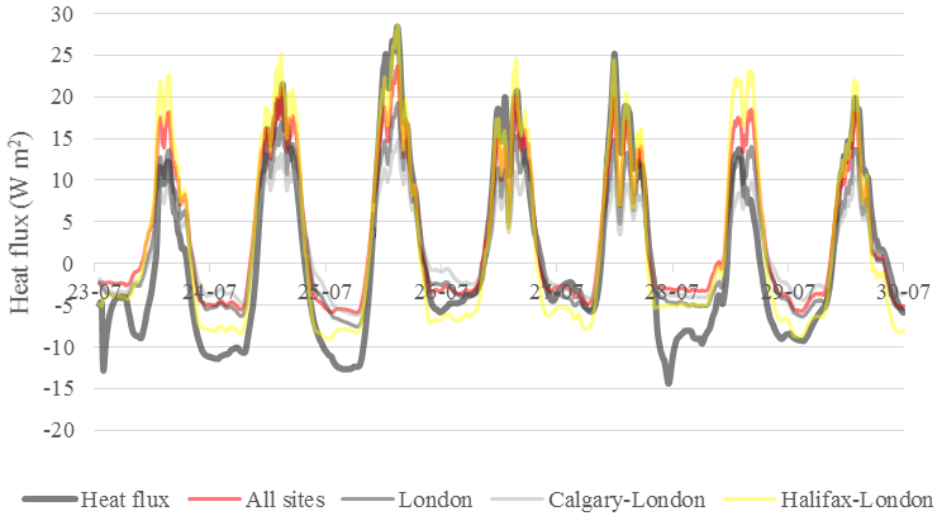

Fig 3.10 *Heat flux measured in London for period 23/07/14-29/07/14 and model predictions*

3.3.3 Supplementary substrate heat flux data analysis

Given the considerable differences in the pattern of substrate heat flux between the three sites, further analysis was performed. As the temperature gradient force in the substrate results in the conduction of heat through the substrate layer, a comparison of the difference between soil temperatures recorded at 1'' and 4'' were compared to the heat flux data. The relationship between the soil temperature difference and the heat flux is shown in Table 3.9.

Table 3.9 *Statistics for the relationship between the measured substrate heat flux and the soil temperature difference between the depths of 1'' and 4''*

	r^2	RMSE	NRMSE	Min °C (W m^{-2})	Max °C (W m^{-2})
Calgary	.95	0.47	0.053	-2.41 (-7.89)	6.30 (18.19)
Halifax	.84	0.83	0.056	-6.75 (-21.48)	6.95 (58.39)
London	.97	0.25	0.041	-2.06 (-12.96)	3.98 (35.48)

Note: the minimum and maximum values for the entire time series are the soil temperature differences with the minimum and maximum heat flux values in parenthesis

Although Halifax was the weakest, each of the sites' data showed a strong relationship between the substrate heat flux and the soil temperature gradient. Halifax recorded the lowest and highest temperature difference and heat flux values. London recorded the highest minimum and lowest maximum temperature difference values of any site while its heat flux minimum and maximum values were intermediate.

3.3.4 Canopy density

Lastly, the pin-frame data showed discernible differences between the heat flux module's vegetation coverage in the Halifax compared to those in Calgary and London. Presented in Table 3.10, the Halifax canopy density was approximately half that of the other sites. The heat flux modules in Calgary and Halifax did show a decreasing trend in measurements, with a small decrease in canopy density between June and July and then a larger decrease between July and August. Vegetation fractional coverage data in London echoed the small decrease between June and July and then comparing measurements taken

early-August with those recorded mid-August, London also has a significant reduction in canopy density between July and August.

Table 3.10 *Heat flux module canopy density during the study period at each of the sites*

	# of hits		
Site	June	July	August
$Calgary_{2013}$	65	62	46
$Halifax_{2014}$	32	31	23
$London_{2013}$	80*	75*	44

***** = pin-frame data was not collected in London during this period so values were estimated according to vegetation fractional coverage estimates and data collected early in August, 2013

3.4 Discussion

The goal of this study was to characterize the heat transfer through green roof substrate in three climates during the summer period and develop empirical models for the purposes of predicting the substrate heat flux. This is the first empirical study to compare the thermal performance of green roofs in different climates. Using identical green roof designs at each of the three sites aided the comparison of the environment's relationship with the transfer of heat through the green roof substrate between the sites by minimizing the influence of design parameters. The results provided an unprecedented opportunity to validate numerical energy balance models and the theoretical framework from which they are derived.

Congruent with previous simulation studies (Jaffal et al. 2012; Zhao et al. 2014), the heat transfer in green roofs was found to vary between climates. Halifax had the greatest fluctuation in its substrate heat flux while Calgary generally had the lowest variability. The micrometeorological results of this study suggest that these differences in the ground heat flux were likely the result of variations in the partitioning of energy at the surface of the green roofs and the soil moisture content. Regression modelling highlighted the importance of net radiation, humidity and leaf-air temperature differences, which are related to available energy, latent heat and sensible heat dissipation, respectively, for predicting the variability in the substrate heat flux.

The multiple linear regression models developed in this study were validated using data collected during the summer period of other years. This validation showed that the models generally predicted the substrate heat flux accurately, although they tended to overestimate the heat transfers when the fluxes were minimal, like those in Calgary, and underestimate them when the fluxes are high, like in Halifax. The heat flux model that was developed using data from all of the sites was fairly accurate compared to the other models, particularly for the Halifax and London green roofs.

The almost identical solar radiation average values suggest that, on average, the same amount of energy was entering each of the green roof system. However, differences in the net radiation averages and standard deviations suggest that the partitioning of this incoming energy at the surface varied between the three sites. The finding that the net

radiation was the strongest predictor of variability in the heat flux is understandable as it indicates that the amount of energy available at the surface of the green roof system is related to the variability in the heat transferred through the substrate.

3.4.1 Calgary

The driving forces of the sensible and latent heat fluxes, namely the canopy-air temperature differences and the vapour pressure gradient, respectively, were generally greatest in Calgary. Calgary tended to have the greatest atmospheric demand for evapotranspiration, particularly during diurnal periods when the available energy for heat dissipation is greatest. However, while this atmospheric demand alone would account for a greater latent heat flux through the evaporation of soil moisture and intercepted rainfall by the canopy, the transpiration rates of the *Sedum* may have been reduced in Calgary as a result of the higher VPD, lower volumetric water content and surface (foliage) temperatures. As mentioned in Chapter 2 (section 2.2.3), higher soil moisture content and higher foliage temperatures (usually peaking at around 30-35 °C) support stomatal aperture and therefore result in greater transpiration (Willmer & Fricker, 1996).

VWC was found by Tabares-Velasco & Srebric (2011) to be the dominant parameter limiting latent heat losses in their sample of *Delosperma nubigenum* and *Sedum spurium*. Soil moisture deficits likely caused reductions in the transpiration rate in Calgary

during several periods during the summer, particularly throughout August when the volumetric soil water content was at its minimum. Even more important to latent heat dissipation though is the effect lower VWC would have had on evaporation. The lower soil moisture content in Calgary would have minimized soil evaporation, thus limiting latent heat dissipation during periods of dry substrate, such as August.

A suppression of transpiration in the *Sedum spurium* in Calgary explains its comparatively high average surface-to-air temperature difference. As seen in Fig 3.5, the lower the relative humidity, the greater the surface-to-air temperature. An increase in the surface (leaf) temperature would have occurred as transpiration acts as a cooling mechanism for the leaves by releasing water vapour through the stomata, reducing heat stress in the foliage in the process. Djedjig and colleagues (2012) observed in their green roof study that a dry substrate reduced evapotranspiration to a minimum with almost all of the radiation absorbed by the leaves being dissipated as sensible heat. Therefore, it is likely that during much of the study period, energy was predominately dissipated through sensible heat mechanisms at the surface in Calgary while drying rates following precipitation events were likely higher than at the other sites.

The generally low volumetric water content in Calgary also would have minimized the thermal diffusivity of the substrate in Calgary relative to the other sites. Comparing the thermal conductivity of five different substrate types at particular percentages of their respective maximum water contents, Ouldboukhitine and colleagues (2012) found the

difference in thermal conductivity between the dry and saturated substrates was significant. The Siplast® substrate had the greatest difference, with the saturated sample having a thermal conductivity 12 times greater than that of the dry sample. As air is a better insulator than water, the generally lower water content in the Calgary substrate would have reduced thermal fluctuations in the ground heat flux. Given the Calgary green roof showed the highest thermal resistance, these findings support those of Zinzi and Agnoli (2012) who suggested that for the purposes of thermal insulation and the reduction of building energy costs, green roofs are most beneficial in drier climates.

3.4.2 Halifax

Conversely, the comparatively higher volumetric water content in Halifax is likely an important factor explaining the more dynamic pattern of ground heat flux seen in Halifax compared to Calgary. The combination of more rainfall and less atmospheric evaporative demand in Halifax facilitates, on average, an increased diffusivity of heat through the substrate. In line with this finding, using thermal simulations Alcazar and Bass (2005) suggested that the heat transfer coefficient (*U*-value) of a modelled green roof would have increased by 26% when the moisture content of the substrate was increased from 0% to 80%, leading to greater thermal diffusivity in the substrate layer.

Like Calgary however, a higher average surface-to-air temperature difference was recorded, suggesting more heat dissipated by sensible mechanisms at the surface compared to London. This process was again likely the result of a decreased transpiration rate causing less cooling of the leaf surface. However, unlike the low soil moisture and high atmospheric evaporative demand found in Calgary, the suppression of evapotranspiration in Halifax was likely caused by a lower VPD. Essentially, although the stomata of the *Sedum spurium* would not have generally been closed in Halifax due to hydrological stress stemming from low VWC like in Calgary, a lower vapour pressure gradient would have resulted in a lower evapotranspiration rate. This is suggested by Halifax having the lowest correlation between relative humidity and substrate heat flux. This is congruent with the findings of Jim and Peng (2012) who observed that during periods of high relative humidity, lower evapotranspiration rates were caused by the low vapour pressure gradient. While transpiration was likely suppressed generally during the summer study period in Calgary and Halifax, unlike Calgary the reduced vapour pressure gradient would have also lowered evaporation rates in Halifax. Like Calgary, lower transpiration rates would have increased the dissipation of energy at the surface by sensible heat. Although the diurnal surface-to-air temperature difference was not particularly high during the week plotted in Fig 3.5b, Halifax's average surface-to-air temperature difference was similar to that in Calgary.

Important to consider though is the lower canopy density measured in Halifax. This may have been the result of a reduced growth rate following winter injury after a prolonged

2013-2014 winter period or due to physical injury sustained during data collection periods. This could have had important implications on the thermal performance of the green roof in Halifax and may explain the greater fluctuation observed in the substrate heat flux. Lower canopy density in Halifax would have resulted in greater transmittance of shortwave radiation through the vegetation layer, increasing substrate surface temperatures, as well as the substrate temperature at 1'', and the heat flux during the day. As a result of the Halifax substrate layer absorbing more shortwave radiation during the day, there would have been increased heat loss during the evening by means of longwave emission. As evident in Chapter 2, the related plant canopy parameter of leaf area index has been repeatedly shown in numerical studies to affect the heat flux through green roofs, with higher values of vegetation coverage resulted in lower substrate surface temperatures and therefore heat transfer through the soil (Del Barrio, 1998; Kumar & Kaushik, 2005; Sailor, 2008; Jaffal et al. 2012). Together, the lower canopy density of the heat flux module in Halifax combined with the higher volumetric water content likely explain the more dynamic pattern observed in the Halifax substrate heat flux data compared to the other sites.

However, the combined Halifax models (Calgary-Halifax and Halifax-London) performed particularly well with predicting not only the Halifax heat flux but also Calgary and London relative to the other models. This suggests that although Halifax's lower canopy density may have affected the magnitude of the heat flux, it did not greatly affect

the predictive power of the regression models. However, the underestimation of diurnal extremes like 25/08 in Fig 3.8 may be attributable to a decreased canopy density in August.

3.4.3 London

The substrate heat flux, as well as the data of some important predictor variables, in London generally showed an intermediate pattern between the extremes of Calgary and Halifax. While the hydrometeorological conditions in Calgary and Halifax tended to suppress latent heat dissipation and increase sensible heat losses, these conditions were not replicated in London where generally high VWC and moderate humidity would have promoted evapotranspiration. This is reflected in London generally having the lowest surface-to-air temperature difference of any site suggesting the availability of moisture assisted transpiration. The site also had the strongest Pearson correlation coefficient between heat flux and relative humidity, likely resulting from London generally having high soil moisture complemented by a moderate atmospheric evaporative demand. The variation in this atmospheric demand was likely the dominant factor affecting the latent heat flux in London. London's regression model also has the lowest standardized coefficient for surface-to-air temperature difference, suggesting sensible heat dissipation had a weaker relationship with the ground heat flux in London. All this considered, unlike

Calgary and Halifax, latent heat was likely the predominant mechanism of heat dissipation of net radiation in London.

Like Halifax, the thermal conductivity of the London substrate was likely increased by the relatively high soil moisture compared to Calgary. This is consistent with the previously mentioned findings of Ouldboukhitine et al. (2012) whose thermal conductivity study showed a linear relationship between increasing soil moisture and increased conductivity in green roof substrates. Considering the thermal conductivity of the substrate alongside the differences in the canopy density between the heat flux modules at each of the sites, London's higher canopy density would have likely increased the dissipation of net radiation at the surface relative to Halifax, while the generally higher soil moisture content in Halifax would have increased the thermal conductivity of the substrate relative to London. These two mechanisms combined are probably the major reasons behind the differences seen in the substrate heat fluxes at each of the sites.

3.4.4 Regression modelling

Most of the models appeared to have a reasonable ability to predict the substrate heat flux when their standard error measures were considered with the observations from which they were developed as well as when the models were applied to data collected during other years. Given the respective performance of each of the models as measured

by normalized standard error, it would appear from the within-model data that the models formulated using Halifax data (Halifax, Calgary-Halifax and Halifax-London) generally were the most accurate while those formulated using data collected in Calgary (Calgary, Calgary-Halifax and Calgary-London) tended to be the least accurate. When validated against data collected from either the previous or following year, the order of predictive power did not change with the Halifax models remaining the most accurate.

However, although the Halifax models are the most accurate according to the normalized standard error, given the greater range of substrate heat flux values measured in Halifax, their predictions are also the most inaccurate when considered by standard error. When considering the daily patterns of estimations in Halifax shown in Fig 3.8, the underestimation of extreme heat flux maximums like 25/08 sees the most accurate model underestimating the daily maximum by over 15 W m^{-2}. This is a considerable amount given the substrate heat flux in Calgary rarely reached 15 W m^{-2} during the study period. The lower the fluctuation, like that seen on 23/08 in Halifax, the more accurate the predictions. This highlights the relative importance of the RMSE, as opposed to the NRMSE, for evaluating the performance of the models. From a relative perspective, for an uninsulated roof, 15 W m^{-2} may have significant implications for the thermal comfort of the indoor space below. On the contrary, the most accurate model for Calgary had a maximum absolute error of roughly 5 W m^{-2} during the same period. This highlights the difficulty of predicting greater thermal fluctuations like that observed in Halifax. Ideally, it is these

larger substrate heat flux values that should be most accurately predicted by a model given this is when the thermal insulation effect of green roofs is most beneficial. Therefore, relatively the Halifax models were the most accurate, whereas from an absolute perspective, the Calgary models were the most accurate.

Nevertheless, the error of the current study's empirical models' estimations was comparable to those of numerical models. The range of NRMSE for the current study's models' ranged from 0.07-0.09 for the data from which they were derived and 0.6-1.0 when validated with data from previous or following years while Tabares-Velasco and Srebric's (2012) numerical model's substrate temperature estimates yielded an NRMSE of 0.07 (Tabares-Velasco & Srebric, 2011) and 0.06 (Tabares-Velasco & Srebric, 2012) when validated against data collected in an experimental laboratory apparatus. Noteworthy however is that the predictive power of the empirical models developed in the current study includes precipitation events whereas the numerical model of Tabares-Velasco and Srebric (2012) did not consider the thermal response of the green roof system during rain events. This is an important consideration as Jim and He (2010) observed that sensible heat fluxes were reduced by 20-75% following rain events during diurnal periods. The transitional period between these conditions; during the rain event, would then likely be a source of error for models, particularly for extended rain events. It is important for numerical models to include these events as they may be an important period for the substrate moisture content and evapotranspiration which greatly affect the energy balance of green roofs.

The relative importance of net radiation, relative humidity and the surface-to-air temperature difference in the regression models is consistent with the findings that the phenomena underlying these variables is closely related to the substrate heat flux (Ayata et al. 2011; Tabares-Velasco et al. 2012). This is understandable because if metabolic and thermal storages as well as advective heat fluxes are ignored, the net radiation minus the latent heat flux, related to the relative humidity, minus the sensible heat flux, associated with the surface-to-air temperature difference, equals the ground (substrate) heat flux. The increase in model predictive power gained by using a moving average for these three parameters is likely attributed to the heat capacity of the vegetation and substrate layers as well as delays in stomatal response. Model errors may have arisen as a result of the time period of the moving average being kept constant rather than varying. This could explain the general inability of the models to underestimate maximum and minimum values in Halifax and overestimate maximum and minimum values in Calgary as they could have suffered from resulted from longer or shorter than average periods of heat absorption and emission, respectively. A more accurate moving average would require the inclusion of properties relating to the thermal regime, including site latitude and longitude values. The fact that the wind speed was generally the least important parameter in the model was likely a result of *Sedum spurium*'s low stature. This would affect the influence of the wind speed parameter as, according to the wind profile discussed in in Section 2.2.2, the wind speed is expected to extrapolate to zero at the substrate surface, meaning wind will have less effect

on turbulent transfers for shorter vegetation (Hungate & Koch, 2014). The suggested importance of soil moisture in explaining the differences between the heat fluxes at the three sites is not evident by its apparent lack of importance in the regression models. However, as the variables were measured and estimated according to a five-minute time step, variations in the soil moisture were likely to be on a much larger time scale than the variations in the heat flux. This would have limited soil moisture's importance in the regression models.

Interestingly, the relative humidity provided a more useful measure of the vapour pressure gradient than the VPD_{canopy}. The measurement of the relative humidity was above and beside the green roof rather than the VPD_{canopy} which involved using the sub-canopy temperature. Although the VPD_{canopy} would be expected to provide a more accurate estimate of the driving force behind the latent heat flux as it includes a temperature measure closer to the leaf-air interface, it likely provided less predictive power as the sub-canopy air temperature sensor involved the use of an exposed thermistor. This was likely disadvantageous as temperature sensors are susceptible to a range of errors, the most significant of which is caused by heating of the thermistor by solar radiation; radiative error, which can exceed several degrees Celsius (Nakamura & Mahrt, 2005; Huwald et al. 2009). In the case of radiation errors, the sensor would be detecting its own temperature increase by absorption of solar radiation rather than the increase in the canopy air temperature. This would likely have caused errors during diurnal periods which would have perturbed

statistical analyses. The relative humidity-temperature probe on the other hand was protected from direct and reflected solar radiation exposure by a stacked multi-plate shield. Furthermore, the VPD_{canopy} measure was not ideal as there was no monitoring of the within-canopy air vapour pressure, with the relative humidity measured outside of the green roof system used as a proxy.

As the vapour pressure gradient is largely dependent on air temperature, the relationship observed may have been a result of the relationship between the substrate heat flux and air temperature rather than the relative humidity. For this reason, specific humidity was included in the analysis as it is an absolute measure of humidity; it specifies the mass of water vapour present in a mass of air. The relative humidity essentially incorporates both the air temperature by means of the saturation vapour pressure and the specific humidity by way of the actual vapour pressure. Although the model that included the relative humidity provided better predictive power than that of the model that employed the specific humidity measure, this superior performance may have been due to the added effect of the air temperature. Nevertheless, for the purposes of validating and assisting the formulation of green roof energy balance models, a measure of the vapour pressure gradient is of more use than that of an absolute humidity measurement as it is this gradient force that drives evapotranspiration.

As shown in Chapter 2, the vegetation layer plays a very important role in determining the flow of energy within the green roof system. As greater canopy density

increases the surface area of the atmosphere interface, it will also increase the amount of energy that can be exchanged between the masses. Furthermore, as detailed in the modelling study by Zhao et al. (2014), the substrate has a very different surface energy balance than vegetation. In Halifax where the canopy density was lower, the vegetation fractional coverage was also likely reduced resulting in more of the substrate surface being exposed to direct solar radiation compared to the other green roofs. By increasing the surface temperature of the substrate, the additional absorption of solar radiation in Halifax would have increased the substrate's temperature gradient thus increasing the transfer of heat. The sites differing in this key parameter may have compromised comparisons between the green roofs' results although the differences in canopy density did not appear to have greatly affected the performance of the regression models. However, the canopy density values in the validation data years were similar. Although there were no June or July canopy density recordings for London in 2013, they could be assumed high based on vegetation fractional coverage estimates and canopy density estimates taken in early August. A parametric study by Jaffal and colleagues (2012) found that increasing the LAI value reduced simulated summer indoor air temperature but the impact of increasing this parameter reduced at higher LAI values. From this finding, it can be assumed that canopy density differences measured between the Calgary and London heat flux modules can be assumed negligible given their high values. Nevertheless, it is recommended that future

research applies these models using green roof arrays that feature a range of canopy densities.

The multicollinearity between variables within the same parameter group could be a useful finding for both green roof research and industry empirical evaluations. This finding suggests, from a predictive perspective, that the specific parameter chosen for measurement may not have a significant effect on the accuracy of the model's output. It also highlights the closely related nature within these parameter groups. With regard to the temperature profile, the multicollinearity between these variables and the finding that time lags did not enhance the predictive power of the models suggests that there was limited temporal variation within the temperature profile. Zhao and colleagues (2014) found a time lag of approximately six hours between the substrate heat flux and net radiation due to the thermal mass of the substrate in their simulation study. The inability of time lag transformations to increase the predictive power of the regression models in the current study is likely explained by the use of a soil temperature measurement only one inch deep into the substrate. At this shallow depth, there will be much less of a time lag between the surface and atmospheric conditions and the substrate. Alternatively, it may be the result of the thermal properties of the *Sedum spurium* canopy and the LiveRoof substrate, which through different mechanisms increased thermal conductivity relative to the green roof array used in the study by Zhao et al.

It was suspected that errors may have occurred in the measurement of the heat fluxes due to the placement of the heat flux plates. When dismantling the green roofs, it was observed that the substrate was more heterogeneous than expected. The heterogeneity observed was either the result of introduced soil from when the plants were transplanted or a product of the soil's manufacturing process. Nevertheless, this could have had important implications on the diffusivity of heat through the substrate as well as its measurement. If the heat flux plate at one or each of the sites was placed in soil with different properties to the other sites, particularly with respect to density and porosity, this could have significantly affected the results. Given this uncertainty, the supplementary analysis was performed in an attempt to verify the heat flux data. There were strong correlations between the heat flux and the temperature gradient at each of the sites, albeit the relationship in Halifax was noticeably weaker. This may have occurred because the VWC was generally highest in Halifax with the increased thermal conductivity resulting in heat fluxes that were higher relative to the temperature gradient. Furthermore, given the heterogeneity of the substrate, the temperature sensors in Halifax may also have been placed in soil with different thermal properties. While the results of this supplementary analysis were inconclusive and although the general differences between the three sites are explainable within the theoretical framework of heat transfer, the magnitude of these differences may have still of been exaggerated in the current study due to the inhomogeneity of the soil.

Although the models developed in the current study showed similar levels of accuracy to numerical models reported in the literature, the assumption of empirical models that multivariate correlations remain consistent in different conditions to those observed may limit their application. As mentioned in Chapter 2, substrate types and plant species other than those used in this study may have markedly different thermal properties that will likely limit the predictive power of these models. Therefore, it is recommended that future studies apply the models devised in this study using green roof arrays that feature other species in monocultures and diverse plantings, different substrate types and depths as well as in other climates. The performance of the All sites regression model was fairly strong across the three sites, which is promising, but further applications are needed to confirm the robustness of these models.

3.5 Conclusion

New empirical green roof models were proposed and validated using data collected during summer periods at three sites in an attempt to predict substrate heat fluxes. The analysis was performed using multiple linear regression with the validation being carried out with root mean square deviation and the coefficient of determination. The monitoring results showed that while each green roof greatly reduced the radiation that reached the building membrane, the green roof in the driest climate of Calgary was the most effective

in providing thermal insulation while the least effective was in the wettest climate of Halifax. The regression models highlighted the importance of the variability in the net radiation at the surface of the green roof and the dissipation of this energy by latent and sensible heat gradients for predicting the variability in the heat transferred through the substrate.

Green roofs are very difficult systems to model numerically given the high number of parameters that affect heat transfer mechanisms and the limited amount of information pertaining to the input data, such as plant properties, required for these models. Employing an empirical method in this study allowed the performance of the system to be modelled without requiring an in-depth knowledge of the heat transfer mechanisms involved. Meanwhile, it also provided validating evidence for the results of numerical simulation studies that have found similar differences in performance between green roofs located in different climates.

However, the variability of green roofs in terms of design and components' thermal characteristics means that further analysis involving different arrays is required. Nevertheless, the findings of the present study highlight the important relationship between heat transfer in the substrate and the water content of the system as well as the impact that canopy density and meteorological conditions have on the surface energy balance.

References

Alcazar, S., & Bass, B. (2005). Energy performance of green roofs in a multi storey residential building in Madrid. Proceedings from *Greening Rooftops for Sustainable Communities* (pp. 569-582). Washington, D.C.

Alexandri, E., & Jones, P. (2007). Developing a one-dimensional heat and mass transfer algorithm for describing the effect of green roofs on the built environment: Comparison with experimental results. *Building and Environment*, *42*(8), 2835-2849.

Ayata, T., Tabares-Velasco, P.C., & Srebric, J. (2011). An investigation of sensible heat fluxes at a green roof in a laboratory setup. *Building and Environment*, *46*(9), 1851-1861.

Bowerman, B.L., & O'Connell, R.T. (1990). *Linear statistical models: An applied approach* (2nd ed.). Belmont: Duxbury.

Buck, A.L. (1981). New equations for computing vapor pressure and enhancement factor. *Journal of Applied Meteorology*, *20*(12), 1527-1532.

Cook, R.D., & Weisberg, S. (1982). *Residuals and influence in regression*. New York: Chapman & Hall.

Del Barrio, E.P. (1998). Analysis of the green roofs cooling potential in buildings. *Energy and Buildings*, *27*(2), 179-193.

Djedjig, R., Ouldboukhitine, S.E., Belarbi, R., & Bozonnet, E. (2012). Development and validation of a coupled heat and mass transfer model for green roofs. *International Communications in Heat and Mass Transfer*, *39*(6), 752-761.

Field, A. (2009). *Discovering statistics using SPSS* (3rd ed.). London: SAGE Publications.

Getter, K.L., Rowe, D.B., Andresen, J.A., & Wichman, I.S. (2011). Seasonal heat flux properties of an extensive green roof in a Midwestern US climate. *Energy and Buildings*, *43*(12), 3548-3557.

Hungate, B.A., & Koch, G.W. (2014). Biospheric impacts and feedbacks. In G.R. North, J.A. Pyle, & F. Zhang (ed.), *Encyclopedia of atmospheric sciences, volumes 1-6* (2nd ed., pp.132-140). London: Academic Press.

Huwald, H., Higgins, C.W., Boldi, M.O., Bou-Zeid, E., Lehning, M., & Parlange, M.B. (2009). Albedo effect on radiative errors in air temperature measurements. *Water Resources Research*, *45*(8).

Jaffal, I., Ouldboukhitine, S.E., & Belarbi, R. (2012). A comprehensive study of the impact of green roofs on building energy performance. *Renewable Energy, 43*, 157-164.

Jim, C.Y., & Peng, L.L. (2012). Weather effect on thermal and energy performance of an extensive tropical green roof. *Urban Forestry & Urban Greening*, *11*(1), 73-85.

Keith, T. (2006). *Multiple regression and beyond*. New York: Pearson.

Kumar, R., & Kaushik, S.C. (2005). Performance evaluation of green roof and shading for thermal protection of buildings. *Building and Environment, 40*(11), 1505-1511.

Lazzarin, R.M., Castellotti, F., & Busato, F. (2005). Experimental measurements and numerical modelling of a green roof. *Energy and Buildings, 37*(12), 1260-1267.

Lin, B.S., Yu, C.C., Su, A.T., & Lin, Y.J. (2013). Impact of climatic conditions on the thermal effectiveness of an extensive green roof. *Building and Environment, 67*, 26-33.

Menard, S. (1995). *Applied logistic regression analysis*. Sage university paper series on quantitative applications in social sciences, 07-106. Thousand Oaks: Sage.

Monteith, J.L. (1973). *Principles of environmental physics*. London: Edward Arnold.

Myers, R. (1990). *Classical and modern regression with applications* (2nd ed.). Boston: Duxbury.

Nakamura, R., & Mahrt, L. (2005). Air temperature measurement errors in naturally ventilated radiation shields. *Journal of Atmospheric and Oceanic Technology, 22*(7), 1046-1058.

Olivieri, F., Redondas, D., Olivieri, L., & Neila, J. (2014). Experimental characterization and implementation of an integrated autoregressive model to predict the thermal performance of vegetal facades. *Energy and Buildings, 72*, 309-321.

Ouldboukhitine, S.E., Belarbi, R., & Djedjig, R. (2012). Characterization of green roof components: Measurements of thermal and hydrological properties. *Building and Environment, 56,* 78-85.

Perelli, G.A. (2014). Characterization of the green roof growth media. Retrieved from *University of Western Ontario – Electronic Thesis and Dissertation Repository.* Paper 2205.

Rowe, D.B., Getter, K.L., & Durhman, A.K. (2012). Effect of green roof media depth on Crassulacean plant succession over seven years. *Landscape and Urban Planning, 104*(3), 310-319.

Sailor, D.J. (2008). A green roof model for building energy simulation programs. *Energy and Buildings, 40*(8), 1466-1478.

Sakaki, T., Limsuwat, A., Smits, K.M., & Illangasekare, T.H. (2008). Empirical two-point α-mixing model for calibrating the ECH_2O EC-5 soil moisture sensor in sands. *Water Resources Research, 44*(4), W00D08, doi:10.1029/2008WR006870.

Stevens, J.P. (2009). *Applied multivariate statistics for the social sciences* (5th ed.). New York: Routledge.

Stovin, V., Poë, S., & Berretta, C. (2013). A modelling study of long term green roof retention performance. *Journal of Environmental Management, 131,* 206-215.

Tabares-Velasco, P.C., & Srebric, J. (2011). Experimental quantification of heat and mass transfer process through vegetated roof samples in a new laboratory setup. *International Journal of Heat and Mass Transfer, 54*(25), 5149-5162.

Tabares-Velasco, P.C., & Srebric, J. (2012). A heat transfer model for assessment of plant based roofing systems in summer conditions. *Building and Environment, 49,* 310-323.

Tabares-Velasco, P.C., Zhao, M., Peterson, N., Srebric, J., & Berghage, R. (2012). Validation of predictive heat and mass transfer green roof model with extensive green roof field data. *Ecological Engineering, 47,* 165-173.

Tetens, O. (1930). Uber einige meteorologische Begriffe. *Zeitschrift für Geophysik, 6,* 297-309.

Willmer, C., & Fricker, M. (1996). *Stomata* (2nd ed.). London: Chapman & Hall.

Zhao, M., Tabares-Velasco, P.C., Srebric, J., Komarneni, S., & Berghage, R. (2014). Effects of plant and substrate selection on thermal performance of green roofs during the summer. *Building and Environment*, *78*, 199-211.

Zinzi, M., & Agnoli, S. (2012). Cool and green roofs. An energy and comfort comparison between passive cooling and mitigation urban heat island techniques for residential buildings in the Mediterranean region. *Energy and Buildings*, *55*, 66-76

Chapter 4: Conclusion

Given concerns over climate change adaptation and reducing building energy demand, in recent years there has been a significant effort towards predicting the passive cooling and building energy savings when a green roof is installed. These research efforts have generally focussed on predicting the thermal insulation supplied by green roofs using mechanistic models. Given the complex nature of this approach of modelling with respect to vegetation, green roof energy balance models have involved numerous assumptions related to the structure and physiology of green roof plants.

Upon review of the energy balance modelling literature in Chapter 2, it was noted that these models tend to consider the thermal and metabolic storage of energy, as well as advective heat transfers, as negligible to the energy balance of a green roof. These assumptions are despite limited empirical investigation of the transfer and storage of heat within a rooftop environment. There is also limited research to support the adoption of single source models in the vegetation layer of green roof energy balance models. There has been insufficient investigation of the composition and uniformity (or non-uniformity) of parameters within green roof canopies for the use of averaged input parameters to be considered a practical representation.

While these assumptions have not appeared to be particularly restraining for the predictive power of these models, their outputs have generally only been compared to the measured results obtained from a single green roof during a temporally narrow validation study. These assumptions may therefore be to the models' detriment when they are applied

to green roofs in other climates or containing other plant species. Prior to this study, there had been no direct comparison of the energy performance of green roofs located in different climates. As a green roof is a living system, their functioning and survival is directly influenced by the climate, as the results of this study showed. The findings of Chapter 3 highlighted the importance of soil moisture, humidity and canopy density in predicting the transfer of heat through a green roof's substrate layer. These findings suggest that green roofs are most beneficial for reducing building energy demand in drier climates as the substrate provides more thermal insulation.

The validation of multiple linear regression analyses suggested that empirical models can be fairly accurate when applied to different climates, although the model developed using a particular site's data was generally the most accurate for that green roof. The underestimation of substrate heat flux extremes suggests that further research is necessary to predict thermal performance in these conditions. This is important given climate extremes correspond with peak electricity demand and deficits in heavily air conditioned cities (Miller et al. 2008). The accuracy of these regression models' was similar, and at times better, than the accuracy of numerical models found in the literature.

4.1 Future research recommendations

The long term goal of this research, and that of similar studies, is to be able to predict building energy savings when a green roof is installed. The present research made significant progress to this end by providing the first empirical study comparing the thermal performance of a green roof design in different climates. Data from this study have shown that the insulation provided by green roofs varies significantly depending on climate.

The dataset collected in this study provides an unprecedented resource for the validation of green roof energy balance models. As mentioned in Chapter 2, these models have only previously been validated using data collected from one green roof. By using an identical design, the three green roofs used in this study allow numerical models to be tested across different climates. The dataset also provides an opportunity to validate urban climate models which are increasingly integrating green roofs into their surface schemes in order to assess climatic effects of widespread green roof installations.

New empirical models were also validated during this study. Further research is required to examine the accuracy of these models using different green roof design parameters, particularly for different plant species and substrate types and depths, and in climates other than those used in the current study. Regarding plant species, there is an increasing list of species that are being recommended for green roofs (Dvorak & Volder, 2010; MacIvor & Lundholm, 2011; Van Mechelen et al. 2014). Those with markedly

different water use and architecture to the *Sedum spurium* used in the present study may yield significantly different results, thus likely adversely affecting the accuracy of the current regression models. While the current study provided data for the validation of numerical models across different climates, this future research would facilitate better validation of design parameters' representation in numerical models.

The current study also only considered the summer period. Further research is also needed to investigate the influence of green roofs on energy transfer during other periods of the year in different climates, particularly in winter. While this study examined the performance of green roofs during the peak HVAC cooling period, green roofs can also provide energy savings in cold climates where there is significant energy use during winter for heating. Changes in season will also see significant changes in the green roof canopy related to plant phenology which will likely have important implications on the transfer of heat through the green roof. This may require different empirical models to be developed for different periods of the year.

If one or more of the models in their current form, or with further refinement, show good predicative power across multiple green roof designs and climates, empirical models may be a satisfactory option for predicting the thermal performance of green roofs. As mechanistic models attempt to predict the influence of some factors for which there are no first principles, such as transpiration and the wind field, they too must rely on empirical and semi-empirical methods as well as a multitude of other assumptions that attempt to

simplify a complex system. Multiple linear regression may ultimately provide a method more accurate than current numerical simulations while also not requiring extensive input parameter data for the green roof canopy. With further validation and refinement of these models and using some aspects of mechanistic models, the empirical models developed in this study may be able to provide accurate heat flux forecasts for prospective green roofs based solely on local climate data. For instance, the soil moisture parameter can be estimated using a water balance model in conjunction with information on the properties of the substrate. This approach may provide the opportunity to accurately estimate the thermal benefits a prospective green roof could offer prior to its construction.

References

Dvorak, B., & Volder, A. (2010). Green roof vegetation for North American ecoregions: A literature review. *Landscape and Urban Planning*, *96*(4), 197-213.

MacIvor, J. S., & Lundholm, J. (2011). Performance evaluation of native plants suited to extensive green roof conditions in a maritime climate. *Ecological Engineering*, *37*(3), 407-417.

Miller, N.L., Hayhoe, K., Jin, J., & Auffhammer, M. (2008). Climate, extreme heat, and electricity demand in California. *Journal of Applied Meteorology and Climatology*, *47*(6), 1834-1844.

Van Mechelen, C., Dutoit, T., Kattge, J., & Hermy, M. (2014). Plant trait analysis delivers an extensive list of potential green roof species for Mediterranean France. *Ecological Engineering*, *67*, 48-59.

Appendix

Dependent and independent variable time series for study period

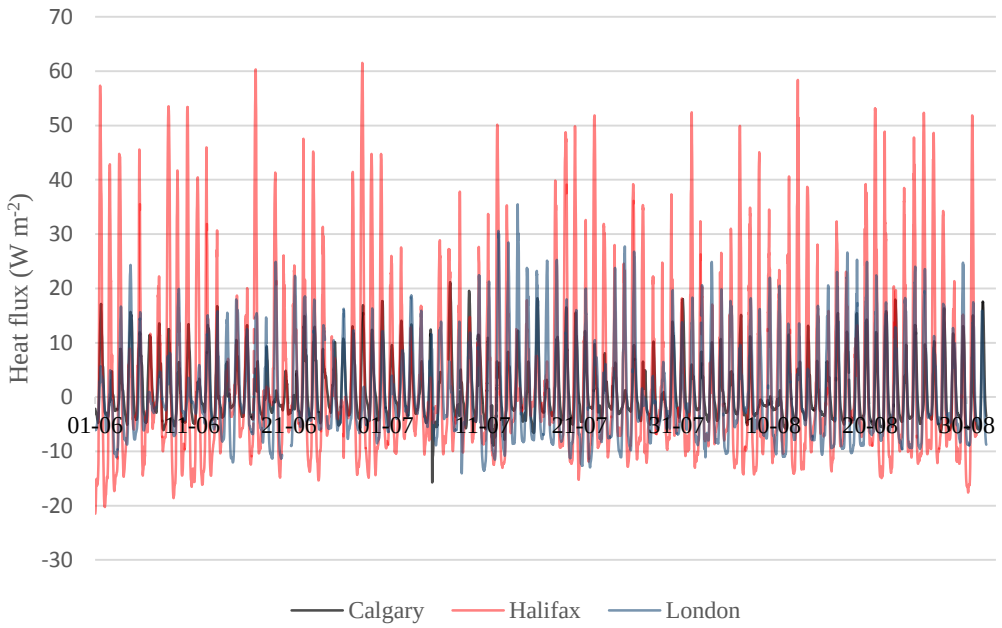

Fig A.1 *Heat flux in Calgary, Halifax and London for the duration of the study period (01/06-31/08)*

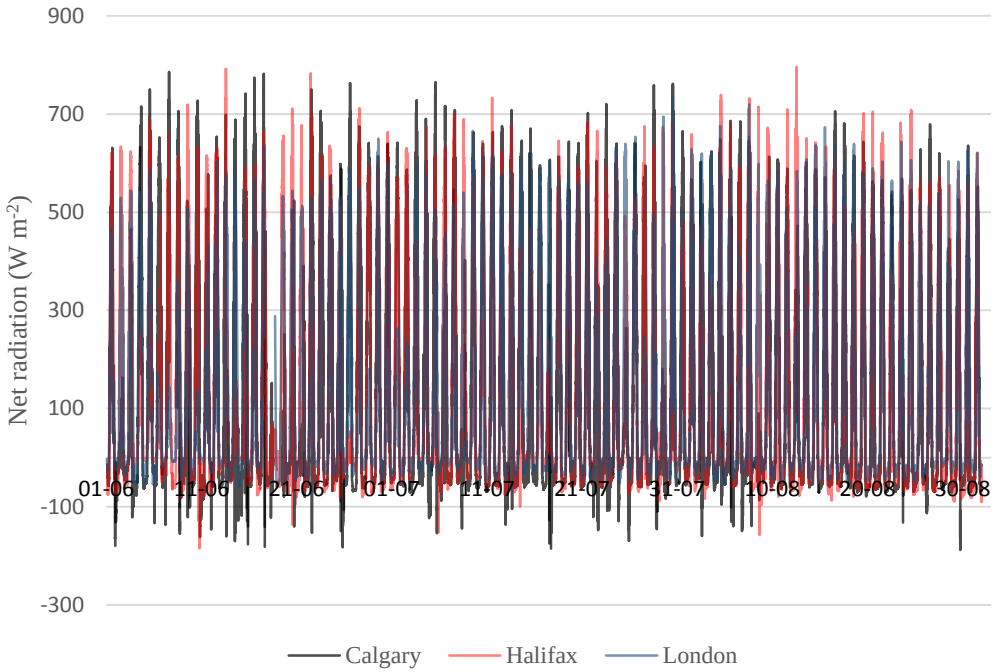

Fig A.2 *Net radiation in Calgary, Halifax and London for the duration of the study period (01/06-31/08)*

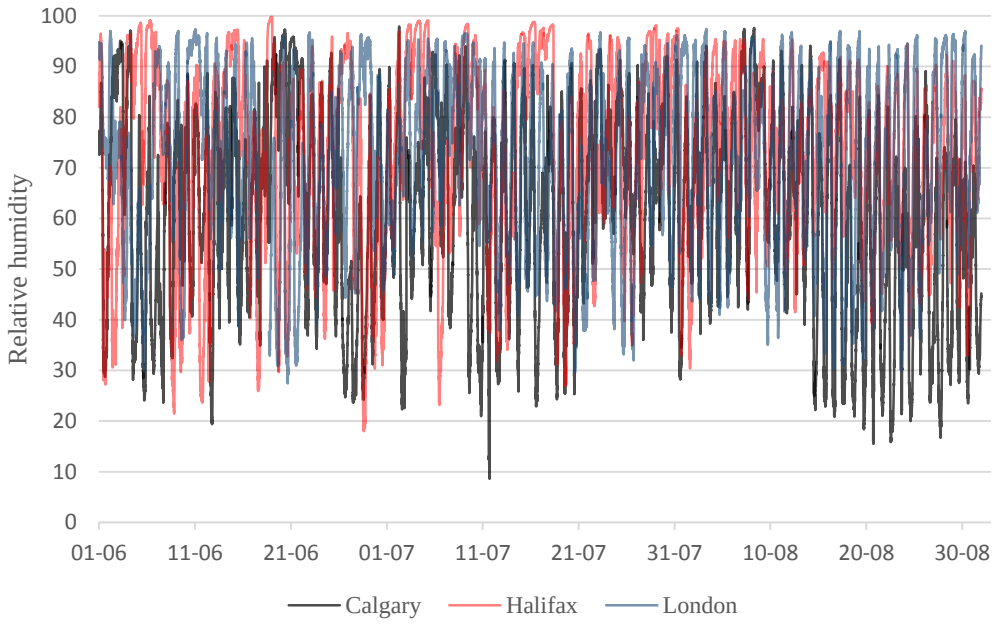

Fig A.3 *Relative humidity in Calgary, Halifax and London for the duration of the study period (01/06-31/08)*

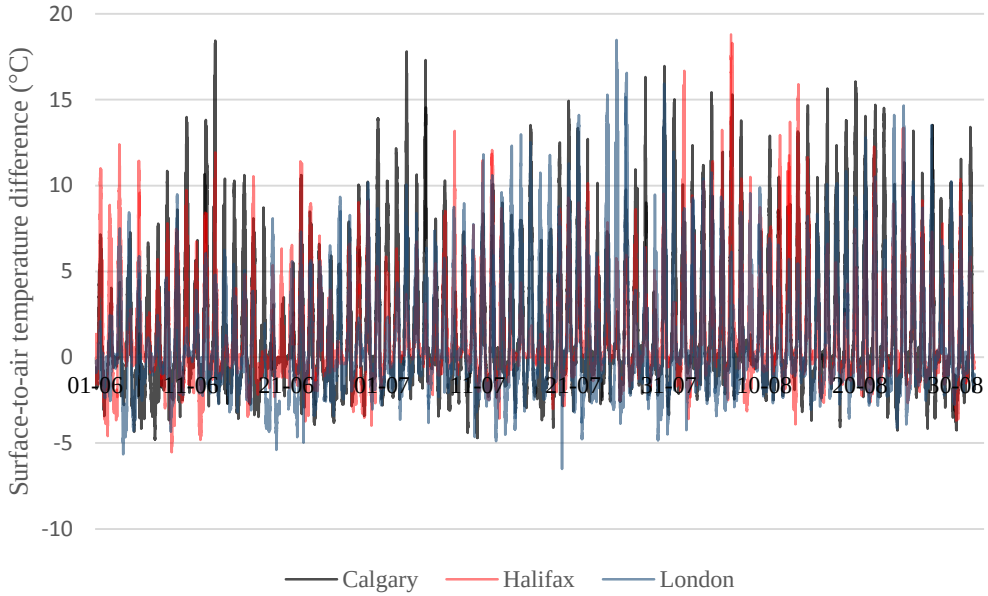

Fig A.4 *Surface-to-air temperature difference in Calgary, Halifax and London for the duration of the study period (01/06-31/08)*